Environmental isotopes in the hydrological cycle

Principles and applications

Edited by W.G. Mook

Volume II

Atmospheric water

International Hydrological Programme

IHP-V | Technical Documents in Hydrology | No. 39, Vol. II

INTERNATIONAL HYDROLOGICAL PROGRAMME

Environmental isotopes in the hydrological cycle

Principles and applications

Edited by
W.G. Mook

Volume II

Atmospheric water

by
Joel R. Gat
Weizmann Institute, Rehovot, Israel
Willem G. Mook and Harro A.J. Meijer
Centre for Isotope Research, Groningen, The Netherlands

IHP-V | Technical Documents in Hydrology | No. 39, Vol. II
UNESCO, Paris, 2001

United Nations Educational,
Scientific and Cultural Organization

International Atomic Energy Agency

UNESCO/IAEA Series on

Environmental Isotopes in the Hydrological Cycle
Principles and Applications

÷

Volume I	**Introduction: Theory, Methods, Review**
Volume II	**Atmospheric Water**
Volume III	**Surface Water**
Volume IV	**Groundwater: Saturated and Unsaturated Zone**
Volume V	**Man's Impact on Groundwater Systems**
Volume VI	**Modelling**

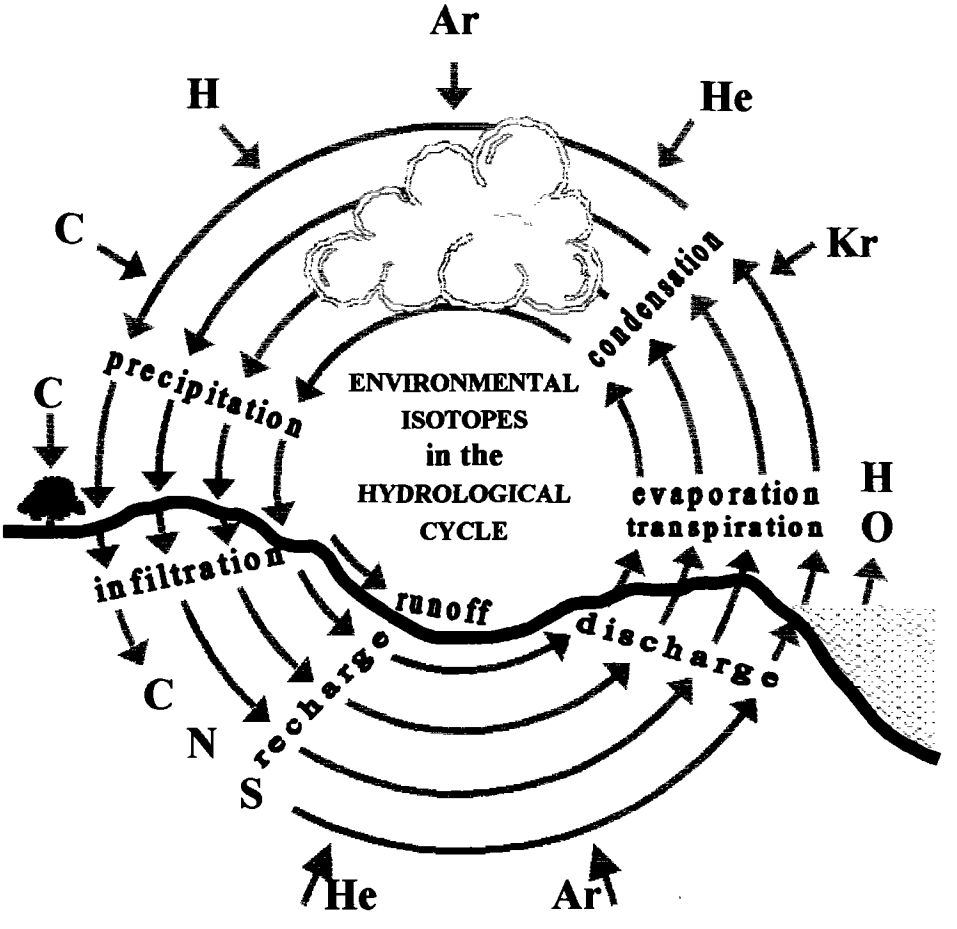

PREFACE

The availability of freshwater is one of the great issues facing mankind today - in some ways the greatest, because problems associated with it affect the lives of many millions of people. It has consequently attracted a wide scale international attention of UN Agencies and related international/regional governmental and non-governmental organisations. The rapid growth of population coupled to steady increase in water requirements for agricultural and industrial development have imposed severe stress on the available freshwater resources in terms of both the quantity and quality, requiring consistent and careful assessment and management of water resources for their sustainable development.

More and better water can not be acquired without the continuation and extension of hydrological research. In this respect has the development and practical implementation of isotope methodologies in water resources assessment and management been part of the IAEA's programme in nuclear applications over the last four decades. Isotope studies applied to a wide spectrum of hydrological problems related to both surface and groundwater resources as well as environmental studies in hydro-ecological systems are presently an established scientific discipline, often referred to as "Isotope Hydrology". The IAEA contributed to this development through direct support to research and training, and to the verification of isotope methodologies through field projects implemented in Member States.

The world-wide programme of the International Hydrological Decade (1965-1974) and the subsequent long-term International Hydrological Programme (IHP) of UNESCO have been an essential part of the well recognised international frameworks for scientific research, education and training in the field of hydrology. The International Atomic Energy Agency (IAEA) and UNESCO have established a close co-operation within the framework of both the earlier IHD and the ongoing IHP in the specific aspects of scientific and methodological developments related to water resources that are of mutual interest to the programmes of both organisations.

The first benchmark publication on isotope hydrology entitled "Guidebook on Nuclear Techniques in Hydrology" was realised in 1983 through the activity of the joint IAEA/UNESCO Working Group on Nuclear Techniques established within the framework of IHP, and it has been widely used as practical guidance material in this specific field.

In view of the fact that the IHP's objectives include also a multi-disciplinary approach to the assessment and rational management of water resources and taking note of the advances made in isotope hydrology, the IAEA and UNESCO have initiated a joint activity in preparation of

a series of six up-to-date textbooks, covering the entire field of hydrological applications of natural isotopes (environmental isotopes) to the overall domain of water resources and related environmental studies.

The main aim of this series is to provide a comprehensive review of basic theoretical concepts and principles of isotope hydrology methodologies and their practical applications with some illustrative examples. The volumes are designed to be self-sufficient reference material for scientists and engineers involved in research and/or practical applications of isotope hydrology as an integral part of the investigations related to water resources assessment, development and management. Furthermore, they are also expected to serve as "Teaching Material" or text books to be used in universities and teaching institutions for incorporating the study of "isotopes in water" in general into the curriculum of the earth sciences. Additionally the contents can fulfil the need for basic knowledge in other disciplines of the Earth Sciences dealing with water in general.

These six volumes have been prepared through efforts and contributions of a number of scientists involved in this specific field as cited in each volume, under the guidance and co-ordination of the main author/co-ordinating editor designated for each volume. W.G.Mook (Netherlands), J.Gat (Israel), K.Rozanski (Poland), M.Geyh (Germany), K.P.Seiler (Germany) and Y.Yurtsever (IAEA, Vienna) were involved as the main author/co-ordinating editors in preparation of these six volumes, respectively. Final editorial work on all volumes aiming to achieve consistency in the contents and layout throughout the whole series was undertaken by W.G.Mook (Netherlands).

Mr.Y.Yurtsever, Staff Member of the Isotope Hydrology Section of the IAEA; and Mrs. A.Aureli, Programme Specialist, Division of Water Sciences of UNESCO, were the Scientific Officers in charge of co-ordination and providing scientific secretariat to the various meetings and activities that were undertaken throughout the preparation of these publications.

The IAEA and UNESCO thank all those who have contributed to the preparation of these volumes and fully acknowledge the efforts and achievements of the main authors and co-ordinating editors.

It is hoped that these six volumes will contribute to wider scale applications of isotope methodologies for improved assessment and management of water resources, facilitate incorporation of isotope hydrology into the curricula of teaching and education in water sciences and also foster further developments in this specific field.

Paris / Vienna, March 2000

PREFACE TO VOLUME II

The changes in the isotopic composition of water in the water cycle occur primarily during the passage of water into and through the atmosphere. The specific isotopic signatures engendered by these processes are then imprinted on the terrestrial water bodies, forming the basis for the many applications of isotopes in hydrological studies. A detailed understanding of the complex and changing processes involved is thus a necessary pre-condition for the use of this tool in studies of present and past climatic systems.

However, considering the variability and changeability of the atmosphere, the data base for describing the atmospheric isotopic composition is very limited, being based mainly on long-term precipitation samples. Our concepts thus have to rely to a large degree on the physical models of the atmosphere and the anticipated isotope fractionation related to the atmospheric processes.

This volume will present both the theoretical and the empirical aspects of the atmospheric part of the water cycle. It is hoped that the readers will be able to identify gaps in our knowledge of the system and incorporate steps in their respective projects to narrow down these gaps by judiciously designed measurements and observations.

It is only proper to acknowledge the contribution of the pioneers of isotope hydrology, who provided the elements of our understanding of the atmospheric system, often on the basis of very sketchy and scattered evidence. Among these, the names of H.Craig, W.Dansgaard, S.Epstein, E.Eriksson, I.Friedman, W.F.Libby, K.O.Münnich, E.Tongiorgi and J.C.Vogel come to mind immediately. An important part of the entire structure of "isotopes in precipitation" comprises the GNIP sampling programme, the IAEA/WMO Global Network of Isotopes in Precipitation, established by the IAEA, Vienna, Section of Isotope Hydrology. This data base is nowadays accessible through Internet and has extensively been used in this volume.

Rehovot, March 2001

Joel R.Gat

CONTENTS

1 THE ATMOSPHERE

1.1 ATMOSPHERIC CONSTITUTION

The gaseous envelope of planet Earth, the environment in which life subsists, is the most dynamic and changeable of the "spheres" of this planet. The medium controls the energy distribution over the Earth's surface and many of the chemical transformations, especially photochemically induced, occur within it. Furthermore, it is the "port" through which the exchange of matter (and energy) with the rest of the solar system and with space in general takes place. On the other hand, it is in intimate contact with the oceans, the terrestrial biosphere and the lithosphere, functioning as the transfer medium for the material from one sphere to another.

Table 1.1 Composition of the atmosphere at ground level (based on Junge, 1963; Andrews et al., 1966; IPCC report 2001).

Gas	Concentration % or ppm	Residence time
Nitrogen (N_2)	78.084%	–
Oxygen (O_2)	20.946%	–
Argon (Ar)	0.934%	–
Water (H_2O)	(0.4 to 400) x 10^2 ppm	10 days
Carbon dioxide (CO_2)	370 ppm (280 ppm)*	4 yrs
Neon (Ne)	18.18 ppm	–
Helium (He)	5.24 ppm	~$2 \cdot 10^6$ yrs
Methane (CH_4)	1.75 ppm (0.7 ppm)**	~10 yrs
Krypton (Kr)	1.14 ppm	–
Hydrogen (H_2)	0.4 to 1.0 ppm (??)	–
Xenon (Xe)	0.087 ppm	–

* Value at 01/01/2001 (pre-industrial value in parenthesis)

** Value at 01/01/2001 (pre-industrial value in parenthesis)

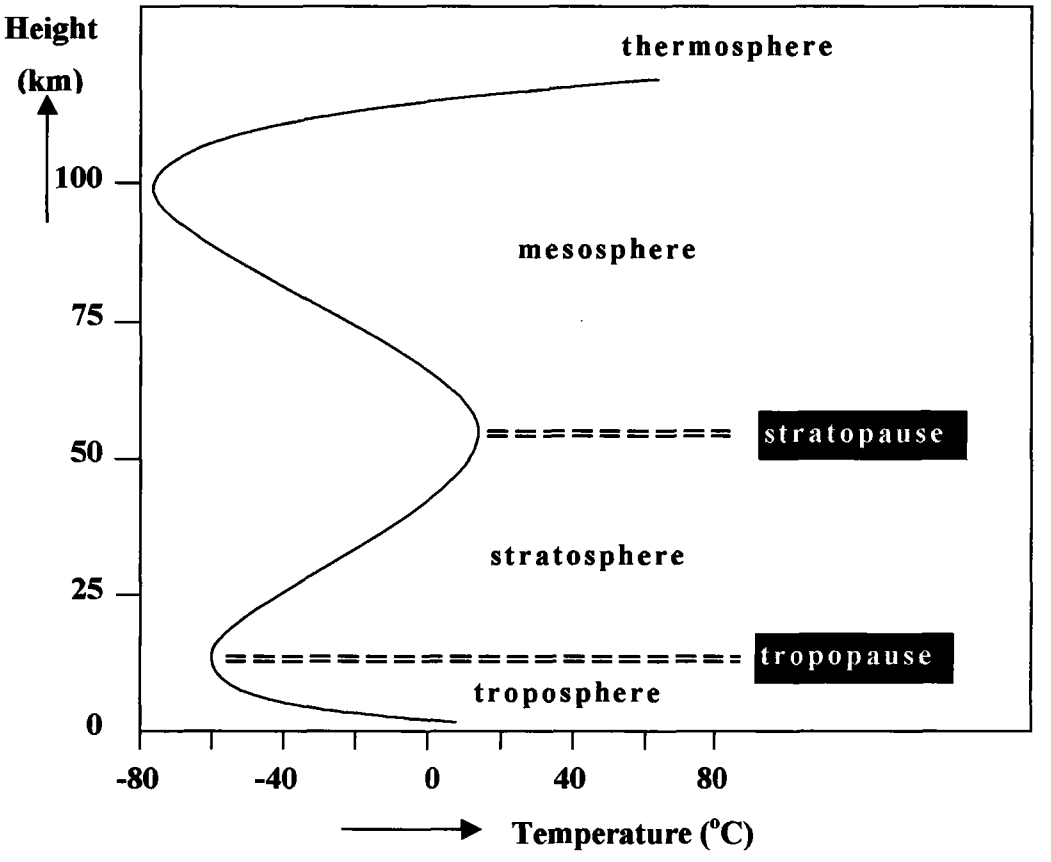

Fig.1.1 The vertical temperature profile in the atmosphere, delineating the extent of the troposphere, stratosphere and mesosphere. An average profile is shown. Actual data at specific locations differ slightly, spatially as well as seasonally.

The composition of the atmosphere is shown in Table 1.1. Nitrogen, oxygen and argon make up the bulk of the atmosphere. The percentages of these gases are constant throughout the atmosphere up to a height of close to 100 km. However, on a geological timescale the amount of oxygen has not been constant, O_2 being involved in the life processes and other chemical interactions.

Of the less abundant gases, the noble gases Ne, He, Kr and Xe also occur at well defined abundances. Other minor gases, the most prominent of which are carbon dioxide, water, methane, dinitrogen (or nitrous) oxide and hydrogen, show a variable concentration both in space and time. Water is the extreme example, with a concentration range spanning three orders of magnitude.

Variability is an indication of a short residence time of a constituent in the atmosphere as a result of the preponderance of source (and sink) terms relative to the accumulated amounts in the atmosphere and to the transport and mixing rates (Junge, 1963).

Sources and sinks of most gaseous components are situated at the land or sea surface, often by mediation of the biosphere and biological activity. This is true for the case of carbon dioxide, oxygen and water, as well as for most anthropogenic gases and greenhouse gases such as methane (CH_4). However, water stands out as the only one whose phase transition occurs in the temperature range of the (lower) atmosphere itself, resulting in a sink by condensation within the air column and a residence time which is short relative to the mixing and transport rates within the atmosphere.

The vertical distribution of mass in the atmosphere is basically controlled by gravity and described by $p_z = p_o \exp(-z/H)$ where p_o and p_z are the pressures at groundlevel and at altitude z, respectively; H is the scale height, about 8.4 km in the lower troposphere. The vertical temperature distribution shown in Fig.1.1 controls the vertical motions and also the partitioning of the atmosphere into discrete spheres.

In the lower atmosphere, the *troposphere*, a noticeable convection driven by the heating of the Earth's surface by absorption of solar radiation results in mixing of the air column. The thermally driven convection is dampened at a height of about 8 to 15 km, where the temperature lapse rate is reduced, a region called the *tropopause*. At a height of about 15 to 25 km, the atmosphere is further heated by absorption of UV radiation. The resulting rise in temperature with height imparts stability to this part of the atmosphere, *the stratosphere*, against vertical motions.

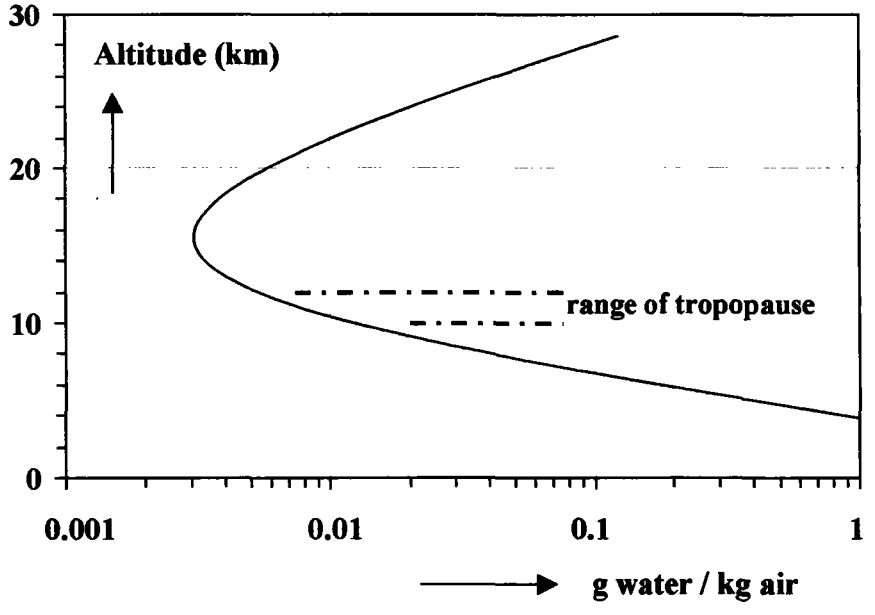

Fig.1.2 Vertical profile of humidity, expressed as the mixing ratio of water vapour in the atmosphere as a function of altitude. An average profile is shown, based on Junge (1963).

The vertical distribution of the water vapour content in the atmosphere (Fig.1.2) is also primarily controlled by temperature. However, since both sources and sinks of water reside in the troposphere and its lower boundary, and as the residence time of water is short compared to the air mixing rates, there is a large variability in the amount of water in the lower atmosphere in both space and time.

Horizontal motion in the atmosphere results primarily from the revolution of the earth and proceeds along bands of latitude. However it is modified by the differential pressure fields which respond to the unequal heating of the surface and the resultant convective motions.

Characteristic residence times in the atmosphere are given in Table 1.1. These are turbulent systems where molecular diffusion is not the dominant process, except in the upper atmosphere, the *exosphere*, where the atmosphere is rarefied and at the lower boundary near the ground surface where the turbulent motion is suppressed. This has far reaching consequences regarding the source term of the gases above the sea.

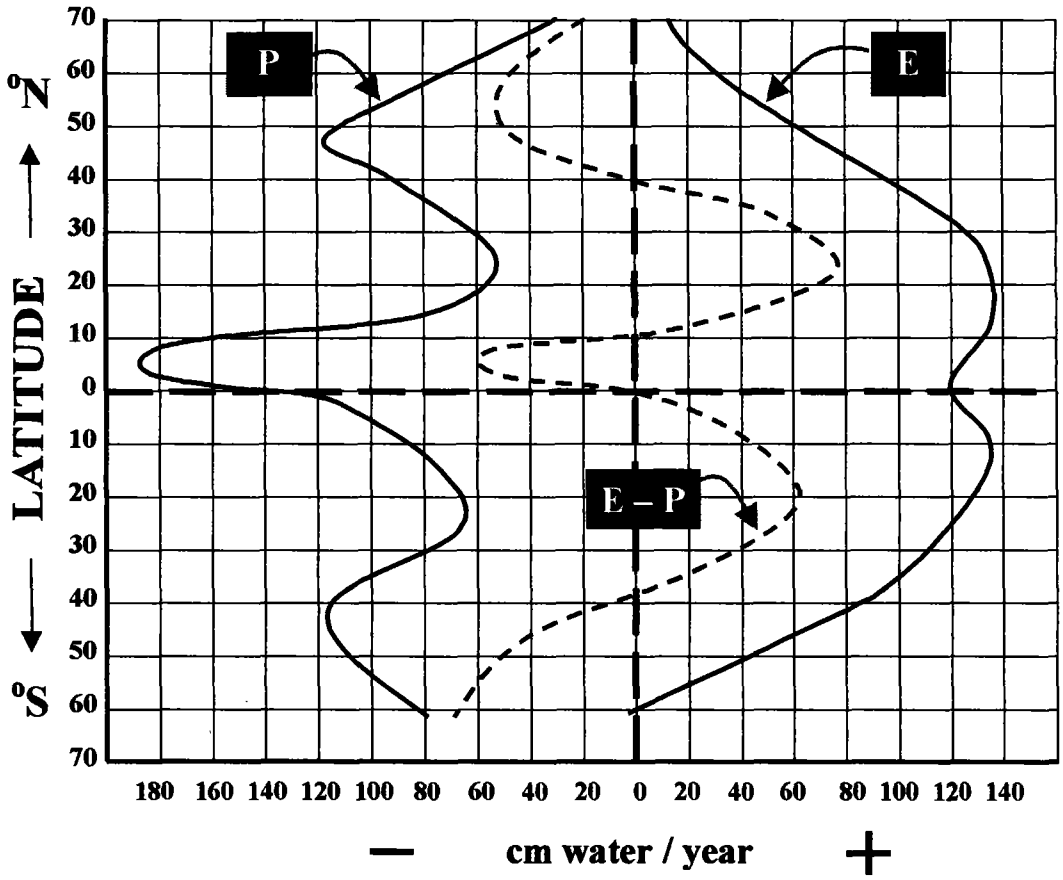

Fig.1.3 Geographic distribution of the evaporation/precipitation balance.

1.2 ATMOSPHERIC MOISTURE

Atmospheric moisture constitutes only about 10^{-5} of the ocean water mass, the latter being close to the total amount of water on the surface of the earth (see Volume I, Chapter 1). The amount of water in different parts of the atmosphere is controlled primarily by the temperature of the atmosphere, as was shown above. However, the annual flux through the atmosphere is about 40 times as large as the total atmospheric inventory. This explains the prominent role of the atmosphere in the water cycle, even though the amount of water contained in it at any time is small. The residence time of water in the atmosphere of about 10 days is short relative to the mixing times in the atmosphere (Table 1.1), so that there is large variability in the amount of water in the lower atmosphere in both space and time. To a first approximation the ratio of evaporation over precipitation (E/P) is close to the value of 1 on a latitudinal averaged basis. The geographic distribution of this parameters (Fig.1.3) highlights the oceanic source regions with E/P>1 and the continental sinks where E/P<<1 on an annual basis. However, a closer look on the continental water balance, for example by Benton and Estoque (1954) over the North-American continent, shows a slight excess of E over P in summer, based obviously on water stored in the soil during the cooler months.

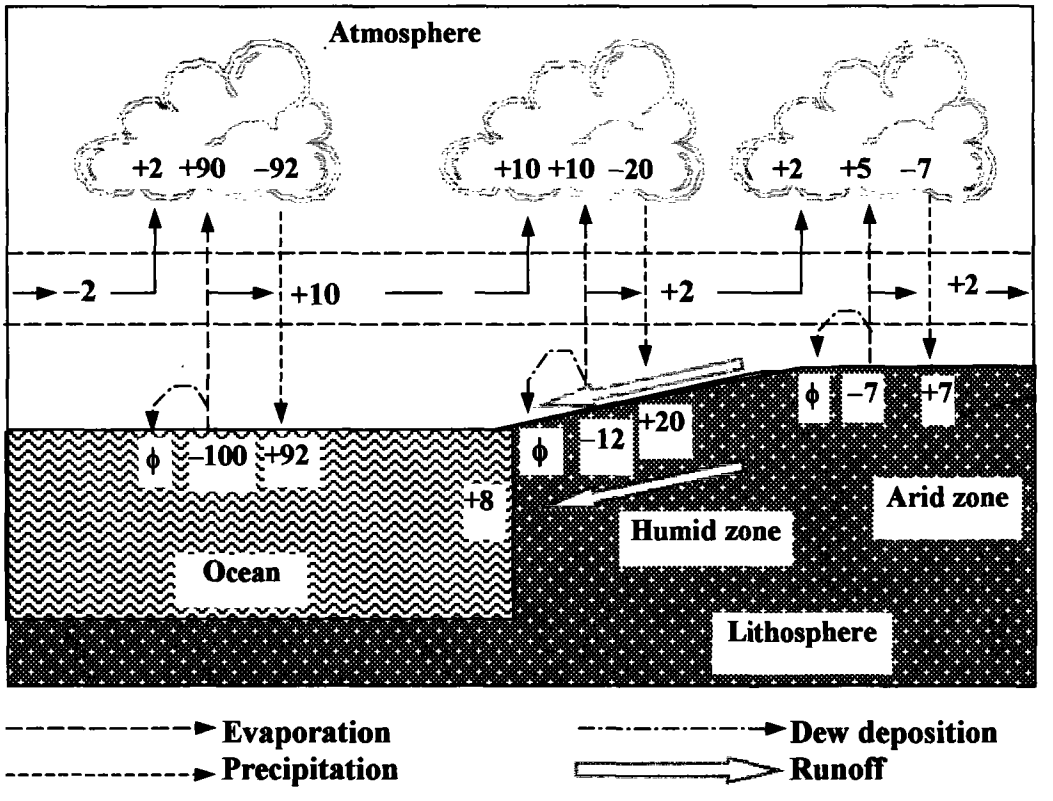

Fig.1.4 The atmospheric part of the hydrological cycle. Units are relative fluxes with respect to the evaporation rate from the ocean, which is arbitrarily set at 100 flux units; ϕ is a small fraction of the flux (adapted from Chow, 1964).

On a world-wide average, the annual evaporation is about 1 m/a, with an evaporation rate of 1250 mm/a in oceanic and 410 mm/a in continental regions (Budyko, 1962). A schematic representation of the atmospheric part of the water cycle is shown in Fig.1.4.

2 ISOTOPE METHODOLOGY

2.1 ISOTOPE ABUNDANCE

(see for details Volume I)

Both hydrogen and oxygen consist of a number of isotopes, whose variations in natural water are the basis for applying the isotope methodology in hydrology. Isotopes of the elements carbon, nitrogen, sulphur and chlorine also play a role in the geochemistry of water resources (Table 2.1).

Table 2.1 Stable isotopes of some light elements.

Element	Z	N	A	Abundance (%)	Symbol
Hydrogen	1	0	1	99.985	^{1}H
	1	1	2	0.0155	^{2}H, D
Carbon	6	6	12	98.892	^{12}C
	6	7	13	1.108	^{13}C
Nitrogen	7	7	14	99.635	^{14}N
	7	8	15	0.365	^{15}N
Oxygen	8	8	16	99.759	^{16}O
	8	9	17	0.037	^{17}O
	8	10	18	0.204	^{18}O
Sulphur	16	16	32	95	^{32}S
	16	17	33	0.75	^{33}S
	16	18	34	4.21	^{34}S
	16	20	36	0.02	^{36}S
Chlorine	17	18	35	~75.7	^{35}Cl
	17	20	37	~24.3	^{37}Cl

Hydrogen, whose major isotope of mass 1 (^{1}H) occurs in the hydrosphere at a mass abundance of 99.985%, is accompanied by 0.015% of the heavy isotope, ^{2}H or *deuterium*. An even heavier isotope of mass 3, ^{3}H or *tritium*, is unstable to β decay with a half-life of 12.32

years. As this half-life is compatible with the hold-up time in many subsurface reservoirs, it is also widely used in hydrological studies. This is also true for the radioactive isotope of carbon, ^{14}C, with a half-life of 5730 years (see Volumes I and IV).

The radioactive oxygen isotopes ^{14}O, ^{15}O, ^{19}O and ^{20}O all have half-lives of seconds only and thus are too short-lived to be of significance in the study of the hydrologic cycle. However, of the two stable heavy isotopes of oxygen, ^{17}O and ^{18}O, whose abundances are 0.037% and 0.20% respectively, the latter figures prominently in isotope hydrology.

Even though these isotopes are stable and not subject to radioactive decay, they can be products or reactants in nuclear reactions initiated by natural radioactivity or by cosmic radiations. Moreover hydrogen is accreted from the solar wind with isotopic abundances that are very much different from the terrestrial. However, such interactions are only of minor consequence for the average terrestrial abundance. To a good approximation, the latter can be considered invariant on the timescale relevant to hydrological systems.

Isotopic abundances may be given by their isotopic abundance ratios, for instance $^{2}H/^{1}H$ or $^{18}O/^{16}O$. For practical reasons, instead of using the *isotope ratio* R, isotopic compositions are generally given as δ values, the relative deviations with respect to a standard value, as defined by:

$$\delta = \frac{R_{sample}}{R_{standard}} - 1 \qquad \textbf{(2.1)}$$

The accepted standard for the isotopes in water is VSMOW (Vienna Standard Mean Ocean Water), which is close to the original standard of SMOW as defined by Craig (1961b).

Signifying R as the abundance ratio of the isotopic species, i.e. $^{2}H/^{1}H$ or $^{18}O/^{16}O$, respectively, then

$$^{2}R_{VSMOW} = (155.75 \pm 0.05) \times 10^{-6}$$

$$^{18}R_{VSMOW} = (2005.20 \pm 0.45) \times 10^{-6}$$

($^{2}H/^{1}H$: Hagemann et al., 1970; De Wit et al., 1980; Tse et al., 1980; $^{18}O/^{16}O$: Baertschi, 1976) (for details see Volume I).

These abundances are the values reported for the reference standard VSMOW, defining the value of $\delta = 0$ on the VSMOW scale. The δ values of water samples are then given as:

$$\delta_{VSMOW} = \frac{R_{sample}}{R_{VSMOW}} - 1 \qquad \textbf{(2.2)}$$

Since δ is usually a small number, δ is given in ‰ (permil, equivalent to 10^{-3}).

Applied to the deuterium-hydrogen, (^{2}H-^{1}H), system we use $^{2}\delta$ or $\delta^{2}H$; for the ^{18}O isotope the notation is $^{18}\delta$ or $\delta^{18}O$.

In water of the hydrological cycle, the variability ranges of $^2H/^1H$ and $^{18}O/^{16}O$ are:

$$-450‰ < {}^2\delta < \text{ to } +100‰$$

$$-50‰ < {}^{18}\delta < \text{ to } +50‰$$

The estimated isotopic composition of primordial water (juvenile) is:

$${}^2\delta_{VSMOW} = \sim -60‰$$

$${}^{18}\delta_{VSMOW} = \sim +5‰$$

These differ from the values of the present hydrosphere, due to the preferential loss of ^1H relative to ^2H in the outer atmosphere over the geological time span, on the one hand, and to the removal of enriched oxygen into the sedimentary column, in particular in carbonates, on the other.

Typical measurement precisions for $^2\delta$ and $^{18}\delta$ are:

$$\sigma({}^2\delta) = \pm 1.0‰ \quad (0.3‰ \text{ best})$$

$$\sigma({}^{18}\delta) = \pm 0.1‰ \quad (0.03‰ \text{ best})$$

2.2 ISOTOPE FRACTIONATION

Isotope fractionation is defined as the phenomenon that the isotopic composition of an element in a certain compound changes by the transition of the compound from one physical state or chemical composition to another. One distinguishes three **mass-dependent** isotope fractionation processes, namely *thermodynamic* (in physical or chemical equilibrium systems), *kinetic* (in one-way (bio)chemical reactions) and *transport fractionation* during diffusive processes.

Within the hydrologic cycle the variability in the isotope composition results primarily from mass-dependent isotope fractionation accompanying the phase transitions and transport processes in the cycle. A special case of **mass-independent** fractionation is the phenomenon that $^{17}O^{16}O$ in the atmospheric oxygen is affected by collisions of atmospheric gases with cosmic particles and photochemical reactions in the higher atmosphere.

2.2.1 EQUILIBRIUM ISOTOPE FRACTIONATION

The *thermodynamic or equilibrium isotope effect* between molecules (with a common element) or between coexisting phases at equilibrium can be described by an exchange reaction, where X^0 and X^1 are two isotopic species of the element X.

$$AX^0 + BX^1 \Leftrightarrow BX^0 + AX^1 \qquad \textbf{(2.3)}$$

The (equilibrium) isotope fractionation factor α is defined by the (equilibrium) constant K_X of this exchange reaction:

$$K_X(T) = \frac{[AX^1][BX^0]}{[AX^0][BX^1]} = \frac{R_{AX}}{R_{BX}} \equiv \alpha_{AX/BX}(T) \qquad \textbf{(2.4)}$$

The equilibrium isotope effect is temperature (T) dependent. In this equation, R obviously is the ratio of the abundance of the respective isotopic species. The subscript AX/BX stands for AX relative to BX.

For phase equilibria (e.g. between vapour and liquid) the equivalent expression is

$$\frac{R_{(\text{phase 1})}}{R_{(\text{phase 2})}} = \alpha_{1/2}(T) \qquad \textbf{(2.5)}$$

According to Eq.2.1 the relationship $\alpha_{1/2} = R_1/R_2$ is also given by:

$$\alpha_{1/2} = \frac{1+\delta_1}{1+\delta_2} \qquad \textbf{(2.6)}$$

In Rayleigh processes, to be discussed later (Sect.2.3 and Sect.3.1.5.), the fractionation is given as $\alpha - 1$, also designated by ε:

$$\varepsilon = \alpha - 1 \qquad \textbf{(2.7)}$$

As with the δ values, ε is usually a small number and therefore also given in ‰, equivalent to 10^{-3}.

In δ nomenclature this is then expressed as follows:

$$\alpha_{1/2} - 1 \equiv \varepsilon_{1/2} = \frac{\delta_1 - \delta_2}{1+\delta_2} \qquad \textbf{(2.8)}$$

which can be approximated to $\delta_1 = \delta_2 + \varepsilon$.

The most relevant fractionation phenomenon in this volume is that for the equilibrium exchange reaction between liquid water and vapour. This isotope exchange process is written as:

$$H_2O_L + H_2O^*_V \leftrightarrow H_2O^*_L + H_2O_V \qquad \textbf{(2.9)}$$

where * stands for the rare isotopic species containing ^2H or ^{18}O. For oxygen isotopes, the expression equivalent to Eq.2.4 is:

$$^{18}\alpha_{L/V} = \frac{[H_2{}^{18}O]_L\,[H_2{}^{16}O]_V}{[H_2{}^{16}O]_L\,[H_2{}^{18}O]_V} = \frac{^{18}R_L}{^{18}R_V} \qquad \textbf{(2.10)}$$

where ^{18}R is the isotope ratio for oxygen in the water molecule; molecular symbols in square brackets denote the respective concentrations; $\alpha_{L/V}$ is the fractionation factor for the liquid-

vapour equilibrium (liquid relative to vapour), $\alpha_{V/L}$ is the reverse factor (vapour relative to liquid).

Specific values for oxygen and hydrogen isotopes, respectively, are given by Majoube (1971), as a function of the temperature:

$$\ln^{18}\alpha_{L/V} = -\ln^{18}\alpha_{V/L} = 1.137\times10^3/T^2 - 0.4156/T - 2.0667\times10^{-3} \quad \textbf{(2.11a)}$$

$$\ln^{2}\alpha_{L/V} = -\ln^{2}\alpha_{V/L} = 24.844\times10^3/T^2 - 76.248/T + 52.612\times10^{-3} \quad \textbf{(2.11b)}$$

This then yields values of $^{18}\alpha_{L/V} = +11.72‰$ and $^{2}\alpha_{L/V} = +112.3‰$ at 0°C, decreasing to $^{18}\alpha_{L/V} = +9.79‰$ and $^{2}\alpha_{L/V} = +85.0‰$ at 20°C (see for more details Volume I).

The presence of dissolved salts not only decreases the overall vapour pressure, but also changes the isotope fractionation in the water–vapour equilibrium, due to an isotope effect in the binding of water in the hydration sphere of the ions. Both enhancing and diminishing effects on the fractionation are found.

The isotope fractionation factor of the liquid-vapour exchange over a brine (α_b) is related to that over freshwater (α) according to:

$$\alpha_b(S,T) = \Gamma(S).\alpha(T) \quad \textbf{(2.12)}$$

In the case of ^{18}O the effect of anions is insignificant and that of the cations dominates, especially of the divalent, Ca^{2+} and Mg^{2+}. The effect of K^+ is opposite to that of the divalent ions, whereas that of Na^+ is very small. This is consistent with Craig's observation that NaCl does not affect the results of ^{18}O analyses up to marine concentrations. In the case of ^{2}H the value of Γ was for a long time in disagreement between different sets of measurements, but following the application of the H_2–H_2O equilibration technique (Horita, 1988), most disagreements appear to be resolved. To a first approximation, the effect of the different ions in a multi-component brine are additive. Some synergistic effects, however, occur at very high ionic strength, due to the competition for free water between different ions.

The following difference between the isotopic composition of vapour in isotopic equilibrium with a brine and with freshwater, respectively, appears to be reasonably correct for chloride solutions:

$$\Delta^{18}\delta = 1.11M_{CaCl_2} + 0.47M_{MgCl_2} - 0.16M_{KCl} \quad \text{(Sofer and Gat, 1972)}$$

$$\Delta^{2}\delta = 6.1M_{CaCl_2} + 5.1M_{MgCl_2} + 2.4M_{KCl} + 2.4M_{NaCl} \quad \text{(Horita and Gat, 1989)}$$

2.2.2 KINETIC ISOTOPE FRACTIONATION

The isotope fractionation factor in one-way or irreversible chemical or biochemical reactions is designated as α_{ki}. In literature it is often referred to as *kinetic fractionation*, to distinguish it

from *thermodynamic or equilibrium* fractionation. Generally the isotope fractionation factor is defined as the ratio between the new and the old isotope ratio **(new relative to old)**:

$$\alpha_{kin} = \frac{R_{\text{new compound or phase}}}{R_{\text{original compound or phase}}} \qquad \textbf{(2.13)}$$

According to this definition $\alpha_{kin} < 1$ (and ε_{kin} negative) if the actual process causes a *depletion*, $\alpha_{kin} > 1$ (ε_{kin} positive) in case of an *enrichment* of the rare isotopes. The kinetic isotope effects are generally larger than the equilibrium isotope effects. The reason for this is that in principle an equilibrium process consists of two opposite one-directional processes. Consequently the equilibrium fractionation factor is the ratio of two kinetic fractionation factors (Volume I, Sect.3.3). Similar to the equilibrium effects, they diminish exponentially with increasing temperature (Melander, 1960).

2.2.3 TRANSPORT ISOTOPE FRACTIONATION

A special case of isotope fractionation occurs due to the different mobilities of the isotopic species of water, such as $^1H_2{}^{16}O$, $^1H^2H^{16}O$ and $^1H_2{}^{18}O$. The transport isotope fractionation factors must be distinguished from the kinetic isotope fractionation factors described above in a number of respects. With transport isotope fractionation

1) the mass difference between the isotopic **molecules** shown above comes into play (namely 18:19:20), rather than the atomic mass differences (1:2 and 16:18 respectively, for the hydrogen and oxygen), the effect of both hydrogen and oxygen substitution is rather similar for the transport process, slightly larger for the oxygen isotope, whereas the kinetic effects, involving the breakage of intramolecular bonds, are almost an order of magnitude larger for the hydrogen isotopes
2) a gas kinetic process is involved, as given in Eq.2.14, the temperature effect is small and positive, increasing with $\sqrt{T}$.

The molecular diffusivities of gas A through gas B (e.g. of water vapour through air), whose molecular masses are M_A and M_B respectively, are given by the expression:

$$D_{A,B} = C\frac{(1/M_A + 1/M_B)T^3}{P \cdot \sigma_{A,B}^2 \cdot \Omega_{A,B}} \qquad \textbf{(2.14)}$$

(M = molecular mass, T = absolute temperature, P = total pressure, C = a constant, $\sigma_{A,B}$ = sum of atomic radii, $\Omega_{A,B}$ = an interactive correction term) (Chapman and Couling, 1951).

The measured ratio of diffusivities of isotopic water molecules through air are reported by Merlivat (1978) as:

$$D_{^1H^2HO}/D_{^1H_2O} = 0.9755 \pm 0.0009 \qquad \textbf{(2.15a)}$$

$$D_{H_2{}^{18}O} / D_{H_2{}^{16}O} = 0.9723 \pm 0.0007 \qquad \textbf{(2.15b)}$$

where H and O without a mass assignment signify the element at its natural (average) abundance.

The measured values which are rather similar for both the ^2H and ^{18}O substituted water molecules, in spite of their mass difference, show that the parameter Ω differs considerably for the ^2H substituted relative to the ^{18}O containing water molecule, due to some hydrogen-bonding in the gas phase.

From the inverse values, namely:

$$D_{^1H_2O} / D_{^1H^2HO} = 1.02512$$

and $$D_{H_2{}^{16}O} / D_{H_2{}^{18}O} = 1.02849$$

one obtains the values of

$$(^1D/^2D)^{0.5} = 1.01248 \quad \text{and} \quad (^{16}D/^{18}D)^{0.5} = 1.01414$$

equivalent to $^2C_m = +12.5‰$ and $^{18}C_m = +14.1‰$, the superscripts referring to the molecules containing ^1H, ^2H, ^{16}O and ^{18}O, respectively (see Sect.3.2).

2.3 ISOTOPIC ENRICHMENT AND DEPLETION BY THE RAYLEIGH PROCESS

In literature the removal from a mixed reservoir of material in momentary isotopic equilibrium with the reservoir material itself (Fig.2.1) is mathematically described by two different approaches.

A) The isotopic composition of the compound in the original reservoir is:

$$R_r = \frac{N_i}{N}$$

where the respective rare and abundant isotopic species dN_i and dN with an isotopic composition

$$R_e = \frac{dN_i}{dN}$$

are being removed under the fractionation condition

$$\left(\frac{dN_i}{dN}\right) / \left(\frac{N_i}{N}\right) = \alpha_{e/r} .$$

$$\frac{dR_r}{dN} = \frac{d(N_i / N)}{dN} = \frac{1}{N}\left(\frac{dN_i}{dN} - \frac{N_i}{N}\right) = \frac{R_r}{N}(\alpha_{e/r} - 1) \qquad \textbf{(2.16)}$$

with e/r denoting effluent relative to reservoir, and

$$\frac{d\ln R}{d\ln N} = (\alpha_{e/r} - 1) \qquad (2.17)$$

which can be positive or negative depending on whether $\alpha_{e/r} \gtrless 1$.

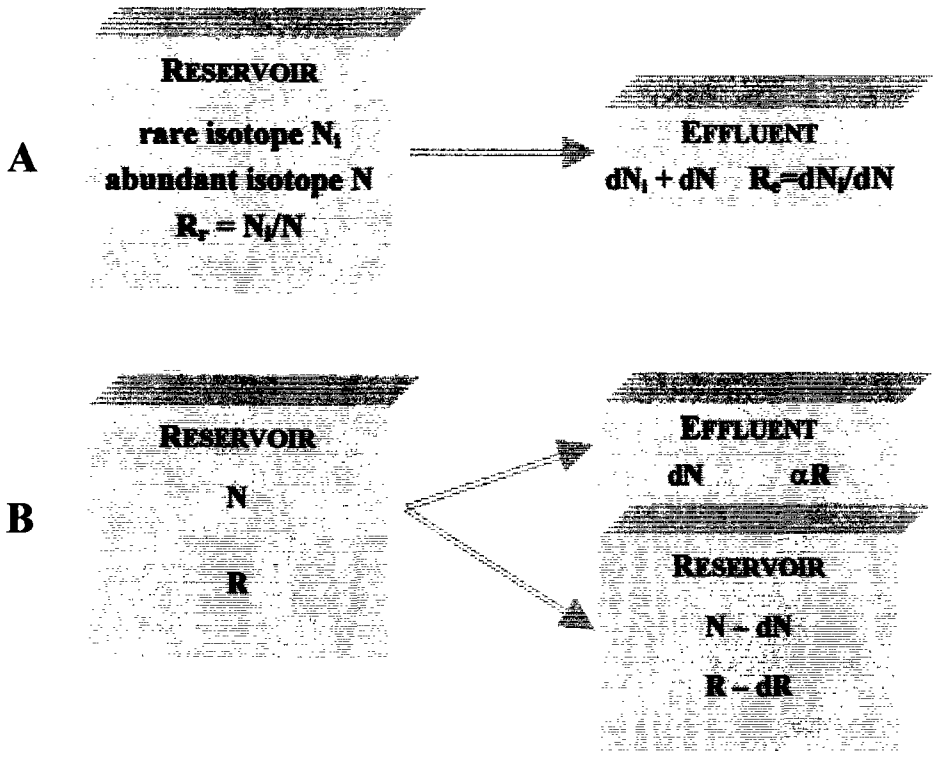

Fig.2.1 Schematic representation of two mathematical approaches of the Rayleigh model.

A. from a reservoir containing N isotopically abundant molecules (such as $^1H_2{}^{16}O$) and N_i molecules of the rare isotopic species ($^2H^1H^{16}O$ or $^1H_2{}^{18}O$) small amounts of both species, dN and dN_i respectively, are being removed under equilibrium isotope fractionation conditions: $R_e = \alpha_{e/r}R_r$

B. the changing isotopic composition of the reservoir is calculated from a mass balance consideration for the rare isotopic species: $RN = (R - dR)(N - dN) + RdN$.

The fraction of the compound remaining in the reservoir is:

$$f = \frac{N + N_i}{N_0 + N_{i,0}}$$

but $N >> N_i$ so that $d(N+N_i) \approx dN$

The differential form is: $$\frac{d\ln R}{d\ln f} = (\alpha_{e/r} - 1) \quad \textbf{(2.18)}$$

the integral form (for constant $\alpha_{e/r}$) is: $$R = R_0 \times f^{(\alpha_{e/r}-1)} \quad \textbf{(2.19)}$$

If written as δ values, since

$$\frac{R}{R_{std}} = 1 + \delta \rightarrow d\ln R = d\ln(1+\delta) = \frac{d\delta}{1+\delta}$$

$$d\delta = (\alpha_{e/r} - 1)(1+\delta)\cdot d\ln f \quad \textbf{(2.20)}$$

For small values of δ this results in

or: $d\delta = \varepsilon_{e/r}.d\ln f$ (differential form) **(2.21)**

or: $\delta \cong \delta_o - \varepsilon_{e/r} \ln f$ (integral form) **(2.22)**

B) In the mass balance approach of the Rayleigh model application the amounts of rare isotopic species before and after the removal of dN abundant isotopic species have to balance:

$$RN = (R - dR)(N - dN) + \alpha R \cdot dN$$

from which we have (products of differentials are to be neglected):

$$N \cdot dR = (\alpha - 1)R \cdot dN$$

resulting in the differential equation:

$$\frac{dR}{R} = (\alpha - 1)\frac{dN}{N}$$

with the solution:

$$\ln R = (\alpha - 1)\ln N$$

Applying the boundary condition that before the removal started $R = R_0$ and $N = N_0$:

$$\frac{R}{R_0} = \left(\frac{N}{N_0}\right)^{\alpha-1} \quad \textbf{(2.23)}$$

and in δ notation (by dividing both sides by R_{VSMOW}):

$$\delta = (1 + \delta_0)(N/N_0)^{\alpha - 1} - 1 \quad \textbf{(2.24)}$$

The result of Eq.2.24 is essentially equal to that of Eq.2.22, although slightly more exact. Eq.2.24 can be written as:

$$(1 + \delta)/(1 + \delta_0) \approx \delta - \delta_0 = (\alpha - 1)\ln(N/N_0) = \varepsilon \ln f$$

It is assumed that ε (and $\varepsilon_{e/r}$ under **A**) has a constant value. However, often $\varepsilon_{e/r}$ changes from the initial to final state with a change in temperature. This has been applied in the Rayleigh model calculation of Sect.3.5.1.

Although the Rayleigh equation was originally derived for the situation where the effluent is in instantaneous isotopic equilibrium with the material in the reservoir, similar equations will apply also in other cases, e.g. for kinetic or diffusive processes. In those cases, obviously, the appropriate fractionation factors need to be introduced instead of the thermodynamic (equilibrium) fractionation factors.

3 STABLE ISOTOPE PROCESSES IN THE WATER CYCLE

In this section we will discuss the isotopic composition of the various elements in the global water cycle in a kind of natural order. Water is evaporating from the sea. The marine vapour for a large part precipitates over the oceans, as it is transported to higher latitudes and altitudes, where the vapour cools down and condenses. Part of the vapour is brought to the continents where it precipitates and forms different modes of surface- and groundwater. The "last" marine vapour is precipitated as ice over the Arctic and the Antarctic.

Compared to the waters of the ocean, the *meteoric waters* (i.e. the atmospheric moisture, the precipitation and the ground- and surface waters derived from them) are mostly depleted in the heavy isotopic species: ^{18}O, ^{17}O and ^{2}H. This observation is explained by the fact that the (kinetic) isotope fractionation during evaporation of seawater is larger than the reverse (equilibrium) fractionation during the condensation process to precipitation (see Volume I). The average ocean composition is accepted as the reference standard for these isotopes (Sect.2.1) so that $\delta_{SMOW} = 0‰$ by definition (Craig, 1961b).

All $^{2}\delta$ and $^{18}\delta$ values of water are given relative to the VSMOW standard.

The δ values of the meteoric waters are thus negative numbers. An extreme value is the composition of Antarctic ice with $^{18}\delta = -50‰$ (Epstein et al., 1965). The weighted mean $^{18}\delta$ of all water in the hydrosphere can be estimated to be about –0.64‰, assuming $^{18}\delta \sim -30‰$ as the average of ice accumulation (Craig and Gordon, 1965) and $^{18}\delta = -7‰$ as the average value of groundwater. Melting of the ice-caps would change the ocean water isotopic composition to an average of $^{18}\delta = -0.6‰$. On the other hand, at the maximum extent of glaciation at the peak of the last ice age the mean ocean water composition was estimated to have been $^{18}\delta = +1‰$, thus making the total "glacial increment" about 1.6‰. This number is of great interest for the palaeo-temperature effect in deep-sea carbonate cores.

Our picture about the global distribution of isotopes in meteoric waters is derived from the data of GNIP (the Global Network of Isotopes in Precipitation) established by the IAEA in co-operation with WMO in 1961 (see Box). In this program, monthly pooled samples of precipitation are collected world-wide and then analysed for their ^{18}O, ^{2}H and ^{3}H content. The annually averaged $^{18}\delta$ values are shown in Fig.3.1 (Dansgaard, 1964; Rozanski et al., 1993). The degree of depletion is related phenomenologically to geographic parameters such as latitude, altitude and distance from the coast and to the fraction precipitated from a vapour mass content, each of which is discussed in more detail in Chapter 4.

The Global Network of Isotopes in Precipitation, GNIP

In the early 1960ies a precipitation sampling network was established by the International Atomic Energy Agency (IAEA) in Vienna and the World Meteorological Organisation in Geneva with the view of documenting the isotopic parameters, $^{2}H/^{1}H$, $^{18}O/^{16}O$ and ^{3}H, together with some meteorological parameters of the input into the hydrological systems. The network consisted of about 100 sampling sites world-wide, including marine, coastal and inland stations. Samples are still being collected monthly and analysed, although the network has been slightly reduced and modified over the years. Also some local and regional networks and stations were added over shorter periods of time.

Results have been evaluated by Dansgaard (1964), Yurtsever (1975) and Rozanski et al. (1993). The available data have been published regularly in the Technical Report Series of the IAEA, but have lately become available on Internet (look at www.iaea.org for *GNIP Data*; it is advised to download per WMO Region).

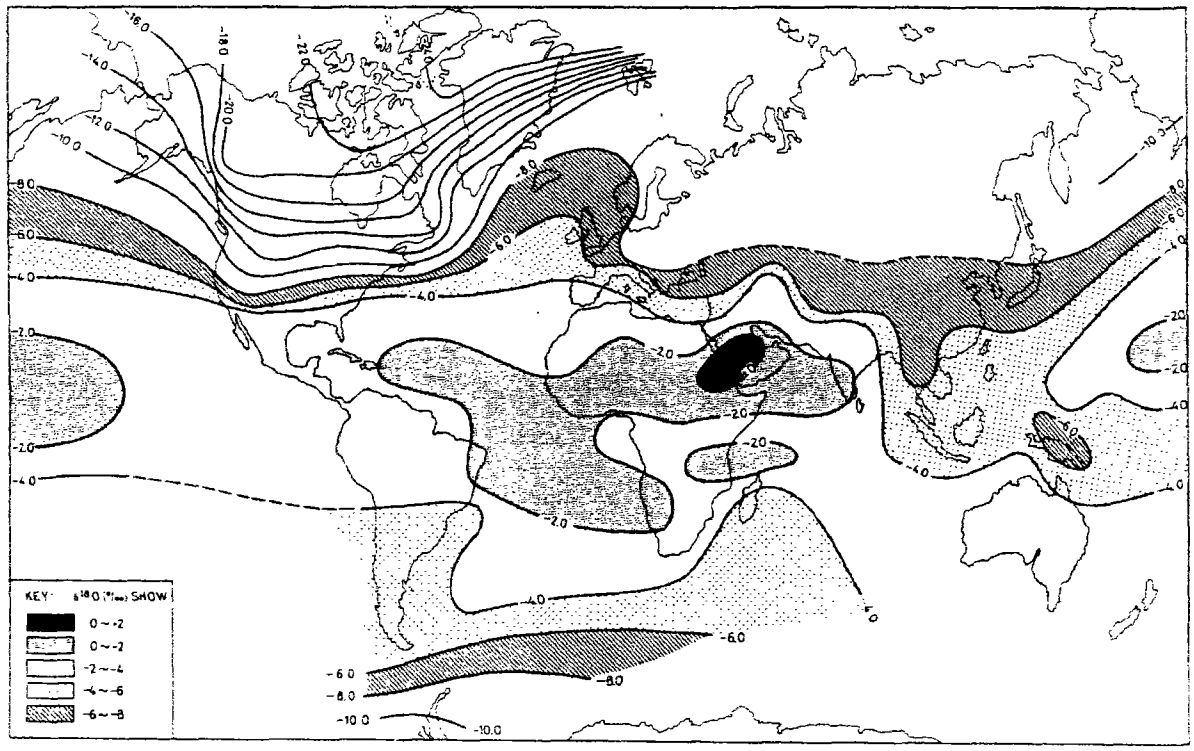

Fig.3.1 World-wide distribution of the annual mean of $^{18}\delta$ in precipitation, based on the GNIP data set (Yurtsever and Gat, 1981).

While the monthly sampling regime can serve the purposes of specifying the inputs into larger hydrological systems, more detailed sampling may be required for regional water studies. Furthermore, more detailed data on precipitation and atmospheric moisture will be necessary in order to understand the effect of changes in climate and of the surface/atmosphere interaction pattern on the isotopic signal of these lumped monthly data.

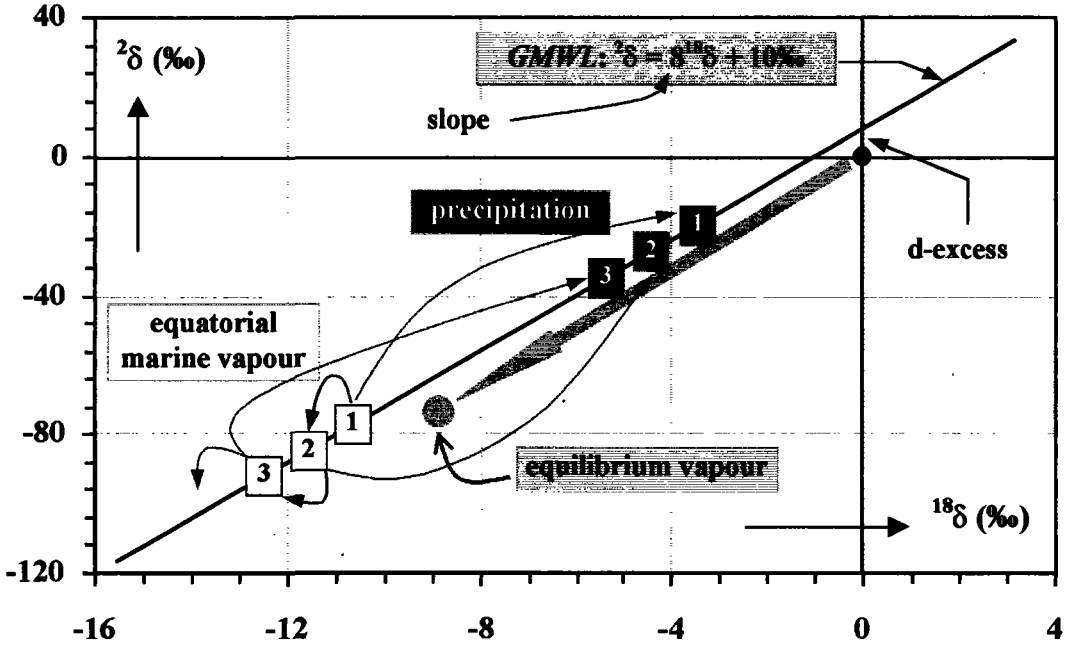

Fig.3.2 Schematic representation of the isotopic consequences of (non-equilibrium) evaporation from the oceans (black slice at (0,0)) forming the marine atmospheric vapour (white squares). Hypothetical equilibrium fractionation (grey arrow) would have resulted in a smaller fractionation (grey slice). The figure furthermore shows the progressive depletion of the vapour mass and thus of the precipitation (stippled squares) by the (here stepwise) condensation process, preferentially removing the ^{18}O and ^2H isotopes from the vapour (in the ($^{18}\delta$,$^2\delta$) plot the $^2\delta$ axis is usually compressed by a factor of 10, due to the larger variations).

The GNIP data pertain to precipitation samples. The atmospheric vapour is always much more depleted in the heavy isotopic species, by close to 10‰ in $^{18}\delta$ on the average. In a continental setting, in the temperate and humid regions, the air moisture and precipitation are found to be close to isotopic equilibrium with each other at the prevailing temperature. This is not strictly true close to the vapour source, i.e. in a maritime or coastal setting (Matsui et al., 1983; Tzur, 1971), nor under dry conditions when the droplets below the cloud base are subject to evaporation, as will be discussed below.

3.1 RELATION BETWEEN $^{18}O/^{16}O$ AND $^{2}H/^{1}H$ IN NATURAL WATERS

The changes of ^{18}O and ^{2}H concentrations in meteoric waters were shown to be fairly well correlated (Friedman, 1953; Craig, 1961a; Dansgaard, 1964; Yurtsever, 1975) so that in the ($^{2}\delta$,$^{18}\delta$) graph the isotopic compositions of precipitation are aligned along what is referred to as a *Meteoric Water Line* (MWL) for which a global average is $^{2}\delta = 8 \cdot {}^{18}\delta + 10‰$ (then called the *GMWL*).

The variations in $^{18}\delta$ and $^{2}\delta$ can be better understood if we consider the two main processes in the global water cycle:

1) evaporation of surface ocean water, and
2) the progressive raining out of the vapour masses as they move towards regions with lower temperatures, i.e. higher latitudes and altitudes.

These processes and the resulting isotope effects are (irrealistically) visualised stepwise in Fig.3.2. The evaporation of seawater is in part a non-equilibrium process. This results from the fact that the air above the sea surface is under-saturated with respect to water vapour, and that the rate-determining step is one of diffusion from the surface to the marine air. If it were saturated, the isotopic composition ($^{18}\delta$, $^{2}\delta$) would move along the grey arrow, as determined by the equilibrium fractionations for ^{18}O and ^{2}H (Table 3.1).

Table 3.1 Hydrogen and oxygen isotope fractionation in the equilibrium system liquid water (l) and water vapour (v); $\varepsilon_{v/l}$ represents the fractionation of v relative to l (details in Volume I).

t (°C)	$^{2}\varepsilon_{v/l}$ (‰)	$^{18}\varepsilon_{v/l}$ (‰)	$^{2}\varepsilon_{v/l} / {}^{18}\varepsilon_{v/l}$
0	−101.0	−11.55	8.7
5	− 94.8	−11.07	8.5[5]
10	− 89.0	−10.60	8.4
15	− 83.5	−10.15	8.2[5]
20	− 78.4	− 9.71	8.1
25	− 73.5	− 9.29	7.9
30	− 68.9	− 8.89	7.7[5]
35	− 64.6	− 8.49	7.6
40	− 60.6	− 8.11	7.4

Once the (non-isotopic-equilibrium) vapour has been formed (open square numbered 1), the rainout process proceeds in isotopic equilibrium, as the vapour is then saturated. Removing the "first" rain (black square nr.1) causes the remaining vapour (nr.2) to be depleted in both

isotopes. This process continues: vapour and condensate (= rain) become progressively depleted, the isotopic compositions "move" along a meteoric water line (black line in Fig.3.2), of which the slope is given by the ratio of $^{2}\varepsilon_{v/l}$ / $^{18}\varepsilon_{v/l}$ (see also Sect.3.6.1).

In (surface) water subject to evaporation the conditions concerning the ($^{18}\delta$, $^{2}\delta$) relation are such that the slopes of the evaporation lines are generally different from 8. A schematic view is given in Fig.3.3 and will be discussed in the next section.

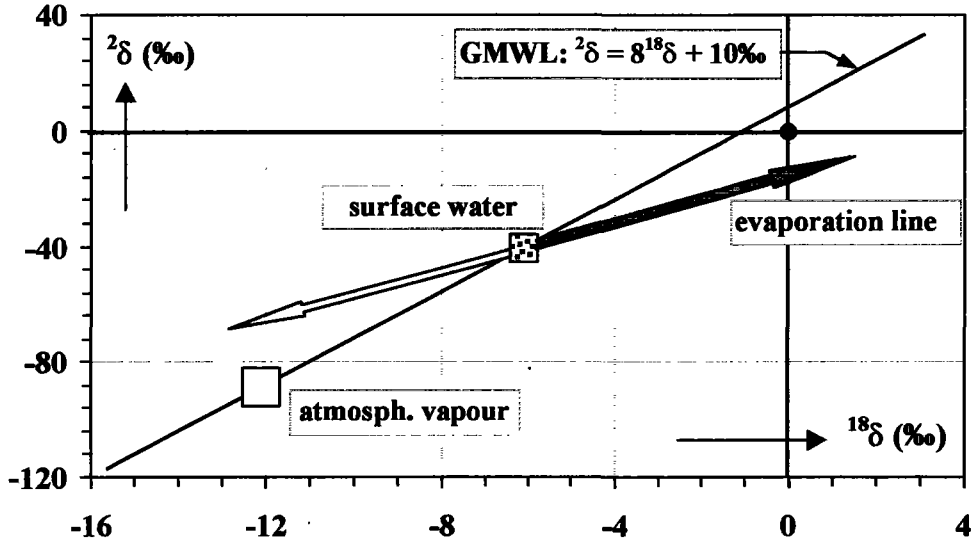

Fig.3.3 Relation between the ($^{18}\delta$, $^{2}\delta$) values of meteoric water which undergoes evaporation, the vapour leaving the water and the residual water following evaporation, described by the *evaporation line*, compared with the relationship between atmospheric water and precipitation described by the meteoric water line (cf. Fig.3.2). The relatively "light" (depleted) water vapour leaves the water reservoir (open arrow) causing the residual water to become enriched (grey arrow).

3.2 EVAPORATION

3.2.1 THE CASE OF COMPLETE MIXING OF THE LIQUID RESERVOIR

The source of water in the atmosphere is the evaporation of water on the surface of the Earth, foremost from the oceans and open water bodies. To a lesser extent, evaporation from the plants (referred to as transpiration) and from the soil adds to the evaporation flux into the atmosphere. The isotope fractionation which accompanies the evaporation process is one important factor in the variability of isotopic composition within the water cycle.

Evaporation into the (under-saturated) air above the water is rate-limited by the transport of vapour from the air layer near the surface into the ambient atmosphere (Brutsaert, 1965). Compared to this, the establishment of liquid-vapour equilibrium at the water-air interface is rapid; isotopic equilibrium between the surface waters (L) and the saturated vapour (V) can

thus be assumed at the interface, i.e. $\delta_V = \delta_L + \varepsilon_{V/L}$ where the equilibrium isotopic fractionation term depends only on the temperature and salinity of the water (Sect.2.2.1).

The mechanism and rate of transport from the saturated "layer" at the interface into the ambient atmosphere depends on the structure of the air boundary layer and the airflow pattern. For the simple case of a stagnant air layer (as applies for evaporation from within the soil as well as for the case of water loss from plants through the stomata openings), where the transport is by molecular diffusion, a fixed (linear) concentration profile is established. The flux of water and its isotopic species is then determined by their respective diffusion coefficients through air, D_m, as given in Sect.2.2.3.

On the other hand, for an open interface under strong wind conditions most of the transport is by turbulent diffusion and molecular diffusion through a non-steady variable air layer plays a role only close to the surface. The transient-eddy model of Brutsaert (1965) is then be applied, where the diffusion flux is proportioned to $D_m^{-1/2}$. At more moderate wind speeds a transition from the proportionality of $D_m^{-2/3}$ to $D_m^{-1/2}$ is to be expected (Merlivat and Contiac, 1975).

Craig and Gordon (1965) suggested a model for the isotope fractionation during evaporation as shown in Fig.3.4 (see also Volume III). The model is based on the Langmuir linear-resistance model (Sverdrup, 1951), and in addition to the assumption of an equilibrium condition at the air/water interface, it is assumed that there is no divergence or convergence in the vertical air column and no isotopic fractionation during a fully turbulent transport. In the model the vapour flux is described in terms equivalent to an Ohmian law so that the vapour flux equals the quotient of the concentration difference (expressed as the humidity difference) and the transport resistance.

The appropriate flux equations for the water substance (E) and isotopic molecules (E_i, either for $^1H^2H^{16}O$ or $^1H_2{}^{18}O$) are then:

$$E = (1 - h_N)/\rho \quad \text{with } \rho = \rho_M + \rho_T \tag{3.1}$$

and

$$E_i = (\alpha_{V/L} R_L - h_N R_A)/\rho_i \qquad \text{with } \rho_i = \rho_{Mi} + \rho_{Ti} \tag{3.2}$$

The ρ terms are the appropriate resistances as shown in Fig.3.4. Subscripts M and T signify the *diffusive* and *turbulent* sub-layers, respectively. Subscript A refers to a free atmosphere far above the evaporating surface and subscript L to the liquid (surface). $R = N_i/N$ is the isotope ratio (N_i and N being number of the isotopic species, N_i representing the less abundant isotope; for the light elements hydrogen, nitrogen, carbon and oxygen: $N >> N_i$); h_N is the relative humidity, normalised with respect to the saturated vapour pressure for the temperature and salinity conditions at the surface.

The isotopic composition of the evaporation flux is now:

$$R_E = E_i / E = \frac{(\alpha_{V/L} R_L - h_N R_A)}{(1 - h_N)\rho_i / \rho} \tag{3.3}$$

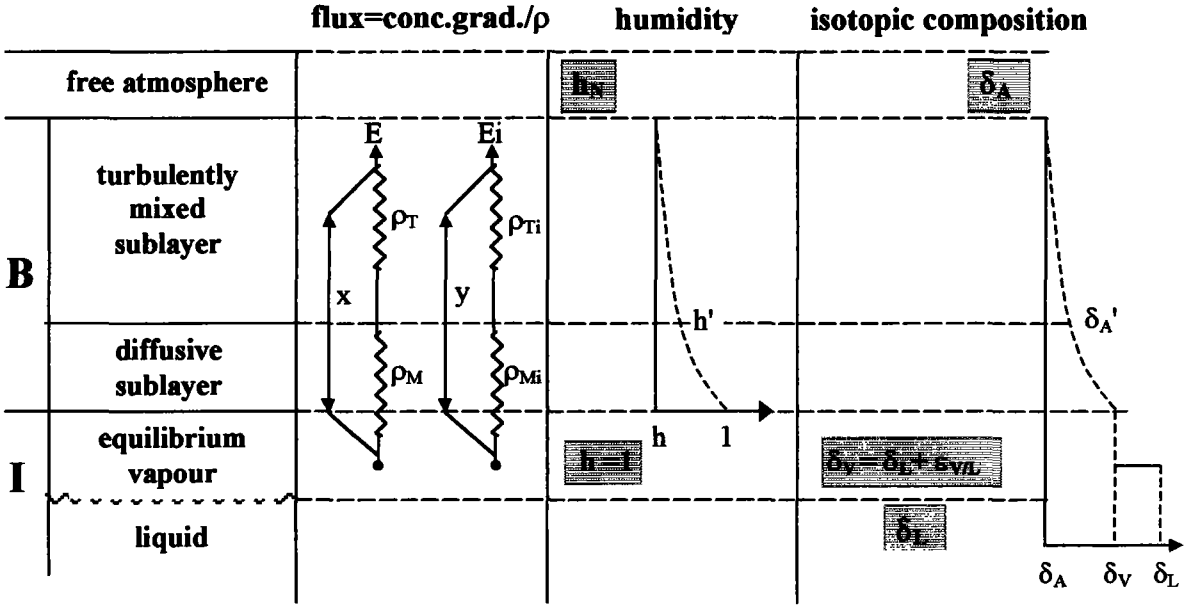

Fig.3.4 The Craig-Gordon isotopic evaporation model. I and B signify the surface inter-phase zone and the atmospheric boundary layer, respectively; $x = 1 - h_N$, and $y = \alpha_{V/L}R_L - h_N R_A$, where h_N is the relative humidity normalised to the saturated vapour pressure at the temperature and salinity conditions of the water surface; δ_A' is the isotopic composition of the air moisture at the boundary of the diffusive sublayer and h_N' is the corresponding relative humidity.

Written in δ values (by substituting each R by the respective (1 + δ):

$$\delta_E = \frac{\alpha_{V/L}\delta_L - h_N\delta_A + \varepsilon_{V/L} + \varepsilon_{diff}}{(1 - h_N) - \varepsilon_{diff}} \tag{3.4}$$

and approximately

$$\delta_E \approx \frac{\delta_L - h_N\delta_A + \varepsilon_{V/L} + \varepsilon_{diff}}{1 - h_N} \tag{3.5}$$

where

$$\varepsilon_{diff} \equiv (1 - h_N)\left(1 - \frac{\rho_i}{\rho}\right) \tag{3.6}$$

(cf. $\varepsilon_{diff} \equiv -\Delta\varepsilon$ as used by Craig and Gordon, 1965).

The total fractionation consists of two steps, as shown in Fig.3.4:

$$\varepsilon_{tot} = \varepsilon_{V/L} + \varepsilon_{diff} \qquad \textbf{(3.7)}$$

Each ε is < 0: the overall process results in an isotopic depletion, for ^{18}O as well as for ^{2}H.
(on the contrary, Craig and Gordon defined ε values such that they are always positive).

In the linear resistance model $\rho_i = \rho_{Mi} + \rho_{Ti}$ and $\rho = \rho_M + \rho_T$. Thus:

$$\frac{\rho_i}{\rho} = \frac{\rho_{Mi} + \rho_{Ti}}{\rho_M + \rho_T} = \frac{\rho_M}{\rho} \cdot \frac{\rho_{Mi}}{\rho_M} + \frac{\rho_T}{\rho} \cdot \frac{\rho_{Ti}}{\rho_T}$$

The term $(1 - \rho_i/\rho)$ can thus be written as:

$$1 - \frac{\rho_i}{\rho} = \frac{\rho_M}{\rho}\left(1 - \frac{\rho_{Mi}}{\rho_M}\right) + \frac{\rho_T}{\rho}\left(1 - \frac{\rho_{Ti}}{\rho_T}\right)$$

The second term on the right-hand side can be eliminated on the assumption that $\rho_{Ti} = \rho_T$, so that substitution into the expression for ε_{diff} results in:

$$\varepsilon_{diff} = (1 - h_N)\left[\frac{\rho_M}{\rho}\left(1 - \frac{\rho_{Mi}}{\rho_M}\right)\right]$$

As discussed before $\varrho_M \propto D_m^{-1}$ for a stagnant air layer, where D_m is the molecular diffusivity of water in air. For a rough interface under strong (turbulent) wind conditions, $\rho_M \propto D_m^{-1/2}$ and at more moderate wind speed a transition from the proportionality of $D^{-1/3}$ to $D^{-2/2}$ can be expected. Accordingly $\left(1 - \frac{\rho_{Mi}}{\rho_M}\right)$ can be written as $\left(1 - \frac{D_m^n}{D_{mi}^n}\right)$, where $1/2 < n \leq 1$. Since $\left(1 - \frac{D_m}{D_{mi}}\right) = \Delta_{diff}$ is a very small number:

$$\left(1 - \frac{D_m^n}{D_{mi}^n}\right) \approx n\left(1 - \frac{D_m}{D_{mi}}\right) = n\,\Delta_{diff}$$

(cf. Craig and Gordon (1965): $C_m = D_{mi}/D_m - 1$, so that: $\Delta_{diff} \equiv 1/(1+1/C_m)$; $C_m > 0$, whereas here $\Delta_{diff} < 0$, consistent with $\varepsilon_{diff} < 0$).

Furthermore, by defining $\frac{\rho_M}{\rho} \equiv \Theta$ the diffusional fractionation ε_{diff} is expressed as:

$$\varepsilon_{diff} = n\,\Theta(1 - h_N)\,\Delta_{diff} \qquad \textbf{(3.8)}$$

(Because the diffusion coefficient of the light/abundant molecule is the largest, $\varepsilon_{diff} < 0$, as mentioned above).

The weighting term, which according to Fig.3.4 is given by $\Theta = (1 - h_N')/(1 - h_N)$, can be assumed equal to 1 for a small water body whose evaporation flux does not perturb the ambient moisture significantly (Gat, 1995). However, Θ has been shown to have a value of 0.88 for the North American Great Lakes (Gat et al., 1994) and a value of close to 0.5 for evaporation in the eastern Mediterranean Sea (Gat et al., 1996). This value of $\Theta = 0.5$ appears to be the limiting value for large water bodies.

For an open water body under natural conditions, a value of n = 1/2 seems appropriate. In contrast, in the case of evaporation of water through a stagnant air layer, such as from the soils (Barnes and Allison, 1988) or leaves (Allison et al. 1985), a value of $n \sim 1$ fits the data well. The ratio of the molecular diffusivities in air, of the pairs $H_2{}^{18}O/H_2{}^{16}O$ and $^1H^2HO/^1H_2O$, has been determined by Merlivat (1978) as $(D_i/D)_m = 0.9723$ and 0.9755, respectively (Sect.2.2.3), so that for ^{18}O: $^{18}\Delta_{diff} = -28.5‰$ and for ^2H: $^2\Delta_{diff} = -25.1‰$.

Fig.3.3 shows in a schematic manner the $(^{18}\delta,^2\delta)$ relationships in this process. δ_E and δ_L define a line called the *evaporation line* (EL) of which the slope is given by:

$$S_E = \frac{h_N(^2\delta_A - {}^2\delta_L) - {}^2\varepsilon_{tot}}{h_N(^{18}\delta_A - {}^{18}\delta_L) - {}^{18}\varepsilon_{tot}} \qquad \textbf{(3.9)}$$

As shown in Fig.3.3, the initial water composition, the evaporated moisture and the isotopic composition of the remnant liquid (such as lake waters, surface ocean water, or soil waters) all lie on this line, as is obvious from material balance considerations.

The humidity, the isotopic composition of the air vapour, and the fractionations $\varepsilon_{L/V}$ and ε_{diff} - which in turn depend on temperature and mechanism, respectively- determine the slope, as shown in Fig.3.5.. A special case is presented when δ_L and δ_A are in isotopic equilibrium with each other for both the hydrogen and oxygen isotope, in which case, S_E is independent of h_N:

$$S_E^* = \left(^2\varepsilon_{V/L} + n\Theta\,{}^2\Delta_{diff}\right)/\left(^{18}\varepsilon_{V/L} + n\Theta\,{}^{18}\Delta_{diff}\right) \qquad \textbf{(3.10)}$$

This slope is $S_E^* = 3.82$ when $\Theta = 1$, n = 0.5 and $\varepsilon_{V/L}$ is given in Table 3.1. It is lower for the case of the stagnant boundary layer; when n = 1 the equilibrium slope can be calculated to be $S_E^* = 2.72$. If $\Theta < 1$ the slope of the relevant evaporation line will be increased, as is the case where

$$\delta_L - \delta_A > \varepsilon_{L/V}$$

The Craig-Gordon model does not account for the case where evaporation of droplets and spray contribute to the evaporation flux.

δ_E is the (isotopic) source term for the atmospheric moisture. It is only under very unusual conditions, namely if $\delta_A = \delta_L + \varepsilon_{V/L} + \varepsilon_{diff}$, that $\delta_E = \delta_A$. More commonly, as shown in

Fig.3.3, the evaporate differs from the isotopic composition of the ambient air so that its admixture changes the isotopic composition of the atmospheric moisture, usually increasing the d-excess value. At the same time the isotopic composition of the evaporating waters also changes, increasing the content of the heavy isotopes in the residual liquid. The degree of such an enrichment depends on the relative magnitude of the evaporation flux to the amount of water in the evaporating water pool and whether the system is open or closed (see further Volume III on Surface Waters).

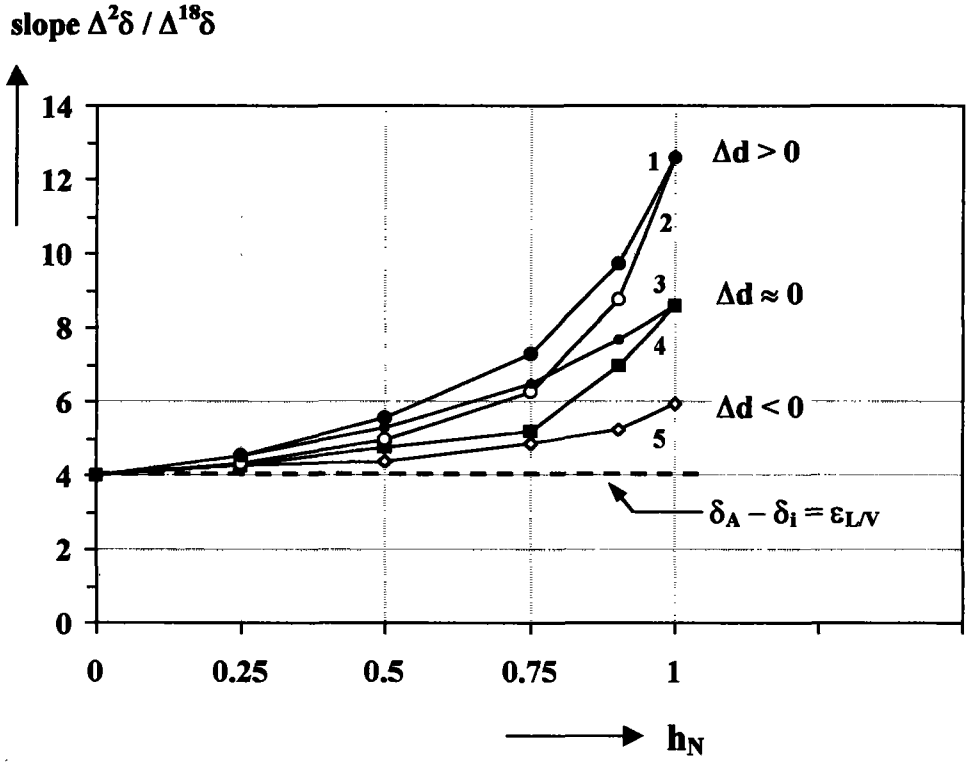

Fig.3.5 Slopes of the evaporation lines for an open water body as a function of the ambient humidity, for a number of assumptions concerning the ambient moisture. Calculations are based on an initial isotopic composition of the water body of $^{18}\delta_o = -5‰$ and $^{2}\delta_o = -30‰$; the d-excess = 10‰ and the temperature 20°C. The dashed line represents the condition of isotopic equilibrium between water and the ambient vapour, which at this temperature gives a difference of $\Delta d = -0.8‰$ between the δ values of the water and vapour (see Table 3.1). Line 1: moisture is derived from the evaporate with $\Delta\delta = +18‰$; line 2: data for a mixture of ambient and evaporated moisture with $\Delta\delta = +10‰$; line 3: $\delta_A = \delta_0$ and $\Delta\delta = 0‰$; line 4: $\delta_A = \delta_0 + \varepsilon_{V/L}$ and $\Delta\delta = -2.8‰$; line 5: the case where the air moisture is in equilibrium with ocean water at 20°C and $\Delta d = -10.8‰$.

3.2.2 THE CASE OF INCOMPLETE MIXING OF THE LIQUID RESERVOIR

The formulations given above can be applied to a well-mixed (homogeneous) water body, where at all times $\delta_{L,surface} = \delta_{L,bulk}$. This is not necessarily true for either an open-water body

under no-wind conditions, or for waters evaporating from within a porous medium, e.g. soil. Incomplete mixing then results in the surface water being enriched in the heavy isotopic species relative to the bulk of the liquid, and the establishment of a concentration gradient in the liquid boundary layer which opposes the fractionation in the air above.

In the Craig-Gordon model this needs to be taken into account by introducing an additional resistance ρ_L. Its maximum magnitude was found to be $\rho_L/\rho = 0.2$ (Siegenthaler, 1975).

On the assumption of a constant depth surface boundary layer, the flux through this layer is formulated as:

$$E_i = ER_L - \frac{R_S - R_L}{\rho_L}$$

Substituting this into Eq.3.3 (noting that R_L has to be substituted by R_S, the isotopic composition of the surface layer of the water):

$$E_i = \left[\alpha_{V/L} R_L (1 + E\rho_L) - h_N R_A\right] / (\rho_{Ai} + \alpha_{V/L}\rho_L)$$

so that

$$\frac{d \ln R_L}{d \ln N} = \frac{h_N (R_L - R_A)/R_L - \varepsilon_{V/L} - \varepsilon_{diff}}{(1 - h_N) - \varepsilon_{diff} + \alpha_{V/L} E\rho_L} \qquad \textbf{(3.11)}$$

compared to

$$\frac{d \ln R_L}{d \ln N} = \frac{h_N (R_L - R_A)/R_L - \varepsilon_{V/L} - \varepsilon_{diff}}{(1 - h_N) - \varepsilon_{diff}} \qquad \textbf{(3.12)}$$

if there is no liquid resistance.

Obviously when $\rho_L \neq 0$ the isotopic change is slowed down.

3.3 CLOUDS AND PRECIPITATION

3.3.1 IN-CLOUD PROCESSES

The formation of precipitation comes about as a result of the lifting of an air mass (dynamically or orographically). Due to adiabatic expansion, the air mass then cools until the dew point is reached. Provided appropriate condensation nuclei are present, cloud droplets are formed. These are believed to be in local isotopic composition with the moisture in the warm part of the cloud due to a rapid exchange which takes place between the droplets and the air moisture. In the cold part of the cloud, however, an additional isotope fractionation occurs due to the diffusion of the isotopic vapour molecules to the solid ice particles (Jouzel and Merlivat, 1984). This may then be conserved in the frozen cloud elements which are not subject to the isotopic exchange. As droplets coalesce and start to fall to the ground against

the rising air, further isotopic exchange takes place, which amplifies the fractionation between the liquid and gas phase. A number of authors have thus modelled clouds as a multistage vertical distillation column (Kirschenbaum, 1951; Tzur, 1971). Ehhalt (1967) found the vertical in-cloud gradient of isotopic composition to be described rather well by an ideal Rayleigh law (Chapter 2). At high levels of the clouds the depletion in the heavy isotopes becomes extreme, and values of $^2\delta \sim -450‰$ were measured on the top of the troposphere (Ehhalt, 1974). Only snow or hail keep a record of the isotopic composition of upper air, and hail is being used as a probe of a cloud's internal structure (Facy et al., 1963; Bailey et al., 1969; Macklin et al., 1970; Jouzel et al., 1975). The measured stable isotope content in the different layers of the hailstone can then be matched to a vertical isotope profile as predicted by a Rayleigh law (Volume I and Sect.3.1.5.1).

As far as the isotopic composition of the air under the cloud itself is concerned, all these models lead to the conclusion that *rain is close to equilibrium with the moisture in surface air*. This was indeed confirmed, on land, by the simultaneous collection of surface air moisture and precipitation (Craig and Horibe, 1967; Jacob and Sonntag, 1991; Rozanski et al., 1982; Matsui et al., 1983).

3.3.2 INTERACTION BETWEEN RAIN DROPLETS AND AMBIENT MOISTURE

A closer look at precipitating weather systems shows that the simplified view expressed above needs some qualification. First, it is obvious, that the different sizes of raindrops will represent equilibration with lower or higher levels in the cloud. Moreover, during the fall of the raindrops to the ground beneath the cloud base (where the air is undersaturated) some evaporation occurs, resulting in enrichment in the heavy isotopes. The degree of enrichment is a function of the size of the drop and thus of the rainfall intensity. Another factor to consider is the downdraft of air from higher levels, besides the cloud or within it, which will impart a negative isotopic signal. An extreme case is presented by the huge tropical clouds associated with the Intertropical Convergence Zone (ITCZ) (Salati et al., 1979).

The exchange of water molecules between a liquid drop and the ambient water vapour results in the establishment of isotopic equilibrium in those cases where the air is saturated with respect to the liquid at the prevailing temperature. Evaporation or condensation of water occurs if the air is undersaturated- or oversaturated, respectively. with respect to the saturated vapour pressure, accompanied by isotope fractionation characteristic of these processes. Once equilibrium has been established, a dynamic exchange of water molecules continues, without leading to a visible change.

The kinetic of the exchange process involves a few steps: a very rapid process at the very surface of the liquid, and much slower processes of diffuse mixing into the air and bulk of the liquid, controlled by the convective currents and turbulence in both these media. The situation

of a falling drop through the air, accompanied by currents engendered by this, enhances the efficiency of both of the latter processes.

The overall kinetics of the exchange process, like all exchange processes, follows first-order kinetics and can thus be characterised by a half-life or a relaxation time, i.e. the time to achieve 1/e of the final equilibrium state. For the case of falling droplets the size of the drop is a determining parameter, as it affects both the speed of fall and the size of the water reservoir involved. For raindrops falling at terminal free-falling velocities (at 10°C) the data given in Table 3.2 can serve as guidelines (Bolin, 1958; Friedman et al. (1962).

When the ambient air is under-saturated, evaporation of the droplets occurs. As a result there is an isotope enrichment of the water in the liquid phase, usually along ($^{18}\delta$,$^{2}\delta$) evaporation lines with slopes smaller than 8, causing a shift in the d-excess value. Rain samples will then not necessarily represent the in-cloud composition. Bolin (1958) calculated that only the heaviest showers, in excess of 10mm/hour, represent the relatively unmodified composition of the precipitation at cloud base, when that is up to an elevation of about 1000m above ground.

Table 3.2 Relaxation time and distance for the exchange process between falling water droplets and the ambient air moisture.

Drop radius (cm)	Relaxation distance (m)	Relaxation time (sec)
0.01	5.1	7.1
0.05	370	92.5
0.10	1600	246

The exchange and evaporation of the falling droplets is probably an important factor in the fact that in more arid regions the best fit Local MWLines show a slope smaller than 8. This effect may also explain the observed correlation between drop size and the depletion of their ^{2}H content (Woodcock and Friedman, 1963), and is responsible, in part, for the amount effect as discussed in Sect.4.5.

3.3.3 EVOLUTION OF THE ISOTOPIC COMPOSITION DURING A SHOWER

The evolution of the isotopic composition during a shower takes on many forms, and is intimately coupled with the synoptic pattern. There are still insufficient data to fully characterise shorter term isotopic changes during a storm or in between individual precipitation events. Such variations span a wide range of δ values, at times up to about 10‰ in $^{18}\delta$. Early studies by Epstein (1956), Bleeker et al. (1966), and Matsuo and Friedman (1967) indicated differences between rain produced by warm front uplifting or cold fronts and associated thunder clouds. These studies also showed that the early part of most rain showers is more enriched in the heavy isotopes, due to partial evaporation during the fall of rain

droplets through the air column. Later studies (Leguy et al., 1983; Rindsberger and Magaritz, 1983; Gedzelman et al., 1989; Rindsberger et al., 1990; Pionke and Dewalle, 1992; McDonnel et al., 1990) make it appear that these variations reflect mainly the source of moisture and its rainout history, and only to a smaller extent the local rain intensity. However, a notable exception to this rule is given by very strong tropical rains, associated with the ITCZ and its towering clouds, mentioned above, when precipitation with extremely depleted isotopic values is found at the peak of the downpour (Matsui et al., 1983). Some typical isotope patterns during a shower are shown in Fig.4.6.

3.4 SEAWATER AND THE MARINE ATMOSPHERE

As expected, surface waters of the world's oceans are slightly enriched in the heavy isotopes in those areas where E/P>1, whereas in estuaries and in polar regions the δ values become slightly negative. The highest degrees of enrichments are obtained in evaporative basins such as the Red Sea and the Mediterranean, where values go up to $^{18}\delta$ = +2‰ (Craig, 1966; Pierre et al., 1986).

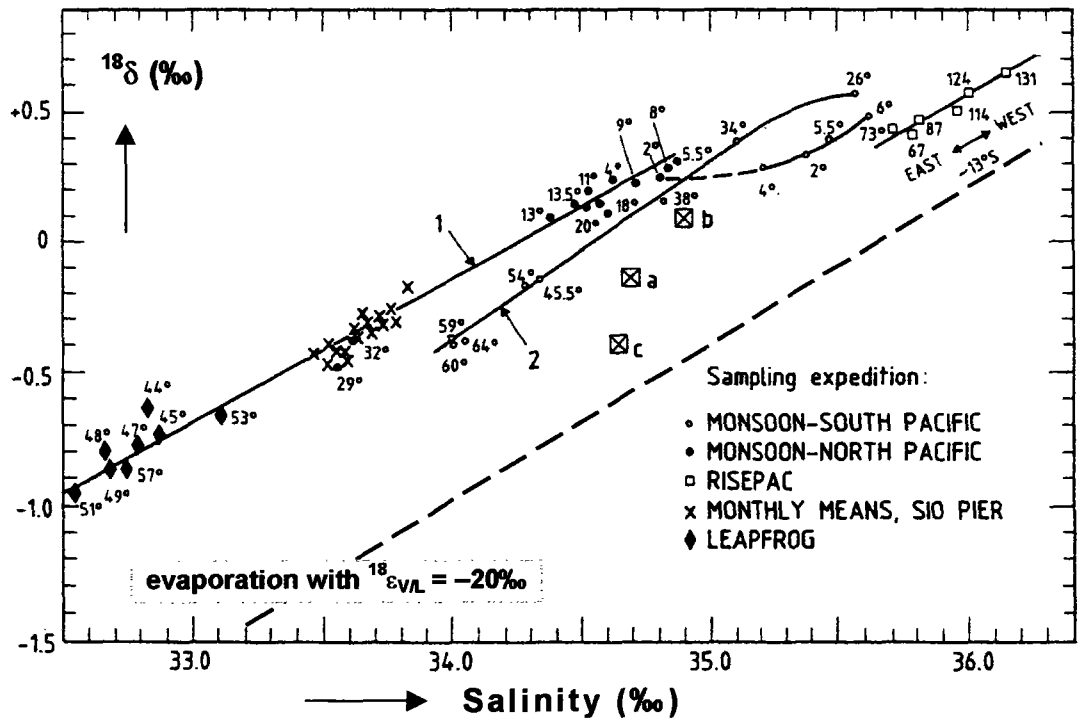

Fig.3.6 The isotopic composition of oceanic surface waters as a function of salinity; the degree of latitude is shown for some stations (from Craig and Gordon, 1965). If the seawater were evaporating with an ^{18}O fractionation of -20‰, the relation between $^{18}\delta$ and salinity would show the slope as indicated by the solid line.

The $^{18}\delta$ and $^{2}\delta$ values are usually well correlated with one another as well as with the salinity. $\Delta^{2}\delta/\Delta^{18}\delta$ is found to be 7.5, 6.5 and 6.0 for the North Pacific and North Atlantic (Craig and Gordon, 1965; Ferronski and Brezhgunov, 1989) and the Red Sea (Craig, 1966), respectively.

The Mediterranean Sea is an exception, portraying a relatively wide range of $^{18}\delta$ values with no commensurate increase in $^{2}\delta$ (= 8 ± 1‰) (Gat et al. 1996). The changes in the stable isotopic composition of the surface waters result from the interplay of the air-sea interaction process which determines the value of δ_E on the one hand and the δ value of the precipitation (and runoff) on the other. The latter more or less balances the evaporation flux.

The correlation with salinity is shown in Fig.3.6. The figure also contains a line indicating the slope of $^{18}\delta$ versus S in case the seawater is evaporating with an oxygen isotope fractionation of $^{18}\varepsilon = -20‰$.

There are very few direct measurements of the isotopic composition of the moisture in the marine atmosphere. Craig and Gordon (1965) report two profiles collected at mast height above the surface on a south-to-north track in the northern Pacific (Expedition Monsoon) and an east-to-west transect along latitude 20°N (Expedition Zephyrus) in the Atlantic. In both cases the $^{18}\delta$ value of the collected vapour was between -10.5‰ to -14‰, which is depleted by 3 to 4‰ relative to the value expected for equilibrium with the surface waters.

The fact that the marine vapour is neither constituted simply of the evaporation flux from the ocean, nor in local equilibrium with the surface ocean water was explained on the global scale as shown in Fig.3.7.

Because of the scarcity of vapour data one generally attempts to infer the isotopic composition of the atmospheric moisture based on the precipitation data, on the assumption of isotopic equilibrium between them. Unlike the case in a mid-continental location where the fact of such an equilibrium is fairly well established (Craig and Horibe, 1967; Jacob and Sonntag, 1991; Rozansky et al., 1982), one cannot rely on this as strictly over the oceans which are a source of vapour, so that a gradient upwards from the sea-surface is to be expected. A systematic difference in the isotopic composition of vapour collected at deck (20.35 m) and mast (27.9 m) height was reported for the 1995 cruise in the Mediterranean Sea by the RV METEOR.

3.5 THE CONTINENTAL ATMOSPHERE

3.5.1 THE RAYLEIGH REGIME

The further removed from the water source, the more depleted in the heavy isotopes are the meteoric waters. As described in Sect.3.2, the so-called *altitude*, *latitude* and *distance-from-coast* effects have been identified (Dansgaard, 1964). All of these effects are basically related

to the wringing out of moisture by cooling of the air masses and indeed the correlation with temperature appears as the overriding factor.

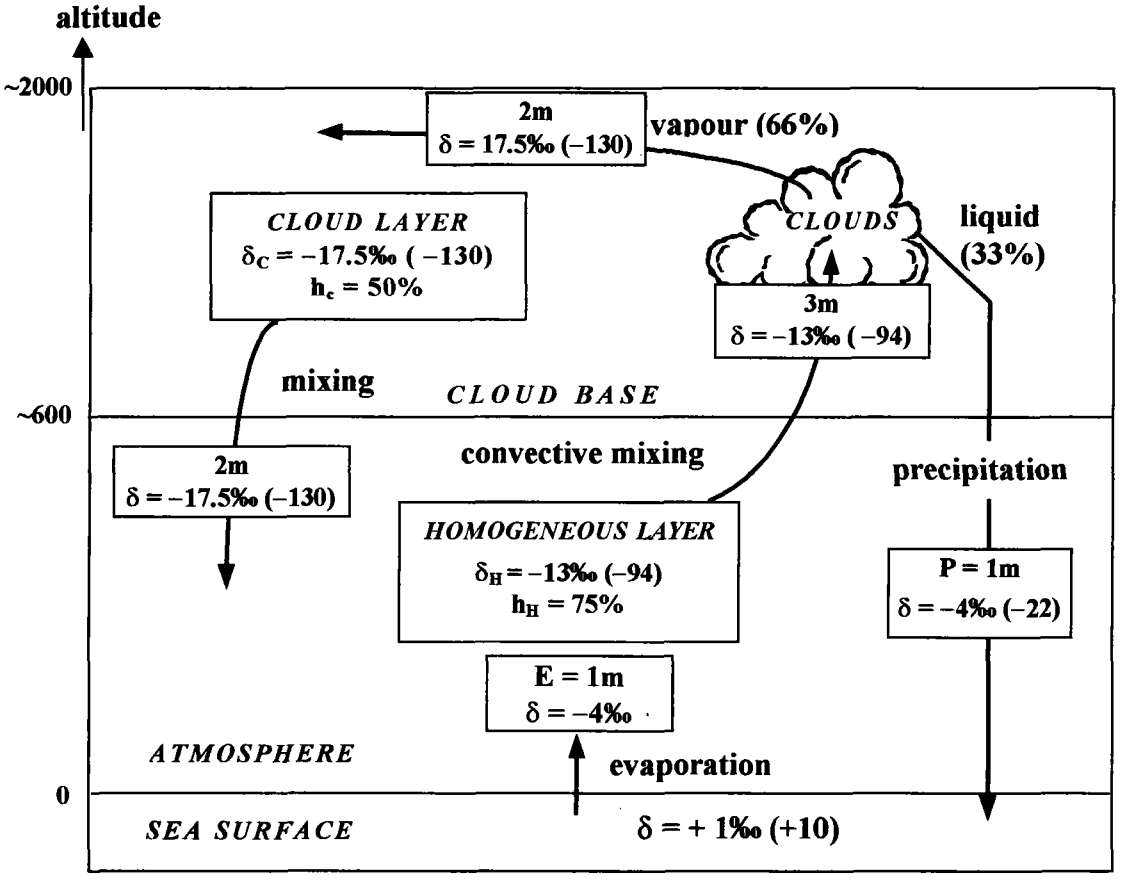

Fig.3.7 The marine-atmosphere isotope model of Craig and Gordon (1965) for the marine atmosphere. The δ values refer to $^{18}\delta$; $^{2}\delta$ is shown in parenthesis. The water transport fluxes are given in amounts of liquid water equivalents units of meter/year.

The conventional scenario envisages that, as the air mass cools, precipitation is formed in isotopic equilibrium with the vapour, At thermodynamic equilibrium between vapour and water the latter has a higher ^{18}O and ^{2}H content. Thus, the remaining vapour is continuously and thus progressively depleted in the heavy isotope. Fig. 3.8 presents the simple box model for this process. N_V is the number of water molecules, which closely equals that of the abundant, isotopically lighter molecules; R_V is the ratio of the isotopic molecules for either $^{2}H/^{1}H$ or $^{18}O/^{16}O$.

When dN_V molecules are removed with an accompanying fractionation factor $\alpha_{L/V}$ ($=1/\alpha_{V/L}$), the rare isotopic mass balance for the transported vapour is now written as:

$$R_V N_V = (R_V - dR_V)(N_V - dN_V) + (\alpha_{L/V}/R_V)dN_V \qquad \textbf{(3.13)}$$

resulting in:

$$dR_V/R_V = (\alpha_{L/V} - 1)(dN_V/N_V)$$

and, if we assume that the number of isotopically light molecules, N_V, equals the total amount of molecules, the solution for this equation is:

$$R_V / R_{V0} = (N_V / N_{V0})^{\alpha_{L/V}-1} \qquad \textbf{(3.14)}$$

where the subscript "$_0$" refers to the initial conditions, i.e. the source region of the water vapour.

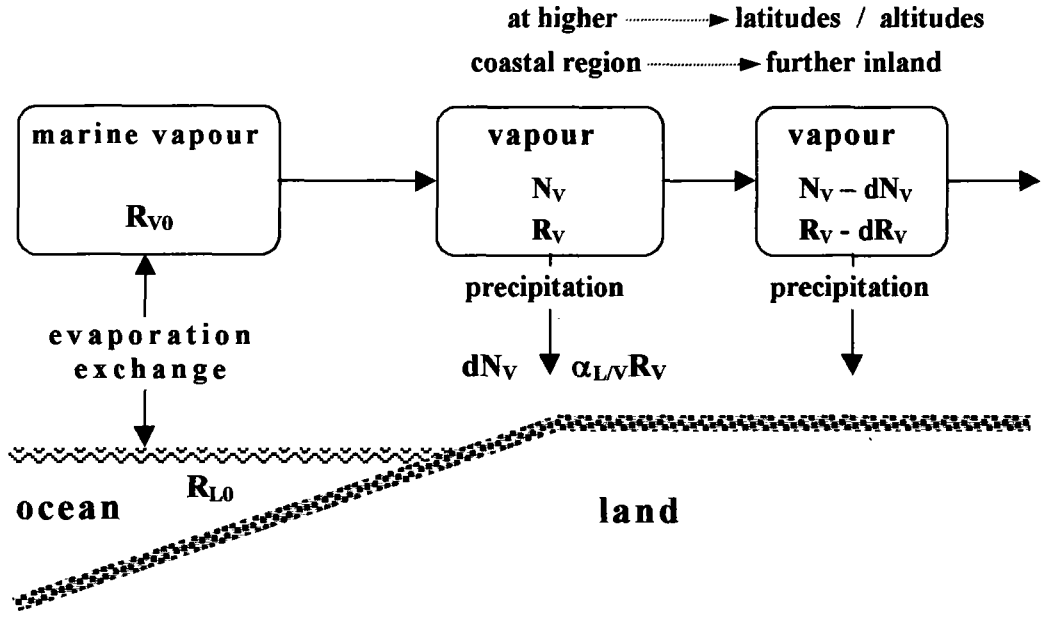

Fig.3.8 Schematic representation of a simplified (non-recycling) Rayleigh model applied to evaporation from the ocean and global precipitation. Water vapour originating from oceanic regions with strong evaporation moves to higher latitudes and altitudes with lower temperatures. The vapour gradually condenses to precipitation and loses $H_2{}^{18}O$ more rapidly than $H_2{}^{16}O$, because of isotope fractionation, causing the remaining vapour and also the "later" precipitation to become more and more depleted in both ^{18}O and ^{2}H.

For isobaric cooling the relative change in the amount of vapour is taken equal to the relative change in the saturated vapour pressure p_V:

$$dN_V/N_V = dp_V/p_V$$

Further, the relation between vapour pressure and temperature for an isobaric condensation process is presented by the law of Clausius Clapeyron:

$$p_V = C \exp(-D/T) \qquad \textbf{(3.15)}$$

where L = molar heat of evaporation = 44.4×10^3J/mole

G = gas constant = 8.3J/Kmole
D = L/G = 5349K
T = absolute temperature = t(°C) + 273.15K
C = constant for water (value here irrelevant)

From this we have:

$$dN_V/N_V = (D/T^2)dT$$

or:

$$N_V/N_{V0} = p_V/p_{V0} = \exp D(1/T_0 - 1/T)$$

so that

$$R_V/R_{V0} = \exp\{-D(1/T - 1/T_0)(\alpha_{L/V} - 1)\} \qquad \textbf{(3.16)}$$

where T refers to the temperature of the sampling station, T_0 to the source region of the water vapour.

For the temperature dependence of the fractionation between water vapour and liquid we choose the exponential equation (cf. Volume I, Sect.4.4):

$$\alpha_{L/V} = A \exp(B/T) = 0.9845 \exp(7.430/T) \qquad \textbf{(3.17)}$$

(exponential adjustment made from data by Majoube, 1971).

The use of this temperature relation is a refinement of the calculation by Dansgaard (1964), who used an average $^{18}\alpha$ value over the temperature range between source region and precipitation areas.

The isotopic ratio of the precipitation condensing from atmospheric water vapour is: $R_L = \alpha_{L/V}R_V$ where $\alpha_{L/V}$ is determined by the condensation temperature or rather the temperature at the cloud base. Combining Eqs.3.16, 3.17 and the value for $R_{V0} = R_{VSMOW}(1 + {}^{18}\delta_{V0})$ with ${}^{18}\delta_{V0} = -12‰$ (Sect.3.5) and considering that $R_{L0} = R_{VSMOW}$ leads to:

$$\delta_{\text{prec. at temp t}} = \delta_L = \alpha_{L/V}\,\frac{R_V}{R_{V0}}\,\frac{R_{V0}}{R_{L0}} - 1 \qquad \textbf{(3.18)}$$

This equation permits us to calculate curves of $^{18}\delta$ values versus temperature (Fig.3.8), which is to be compared with the observed variations in average annual $^{18}\delta$ values with latitude (Sect.4.1). Of course the model is too simple, as it is assumed that all vapour originates from regions around the thermal equator and all ocean evaporation at higher latitudes is neglected.

Using the above equations the temperature dependence of the latitude effect ranges from +0.8‰/°C at 0°C to +0.5‰/°C at 20°C (Fig.3.8).

The applicability of the Rayleigh relationship is based on the fact of the isotopic exchange between the falling droplets and the ascending air in the cloud, resulting in precipitation

which essentially "forgets" the isotopic label of very depleted isotopic values imprinted by the in-cloud processes, establishes isotopic equilibrium with the ambient air (Friedman et al., 1962). Indeed to a good approximation, the depletion in isotopic composition in precipitation correlates well with the near-ground temperature, as shown by Dansgaard (1964) and Yurtsever (1975), or more precisely with the temperature at the cloud base (Rindsberger and Magaritz, 1983). The result is to be compared with the observed values as presented in Sect.4.2.

This simple scenario which generally fits the data rather well, is modified under exceptional circumstances, namely:

1) in the case where snow or hail reaches the ground; the isotopic exchange between the air moisture and the precipitation element then does not occur, with the result that the precipitation is more depleted than in the equilibrium situation. Often, in addition, the solid precipitation shows higher d-values due to non-equilibrium condensation during the growth of ice particles (Jouzel and Merlivat, 1984);

2) in the case of precipitation from strongly convective systems (thunder clouds, cold fronts and tropical clouds associated with the ITCZ) which are characterised by strong local downdrafts. As a result the raindrops do not interact with an averaged sample of the ambient air but only with a portion of the in-cloud air.

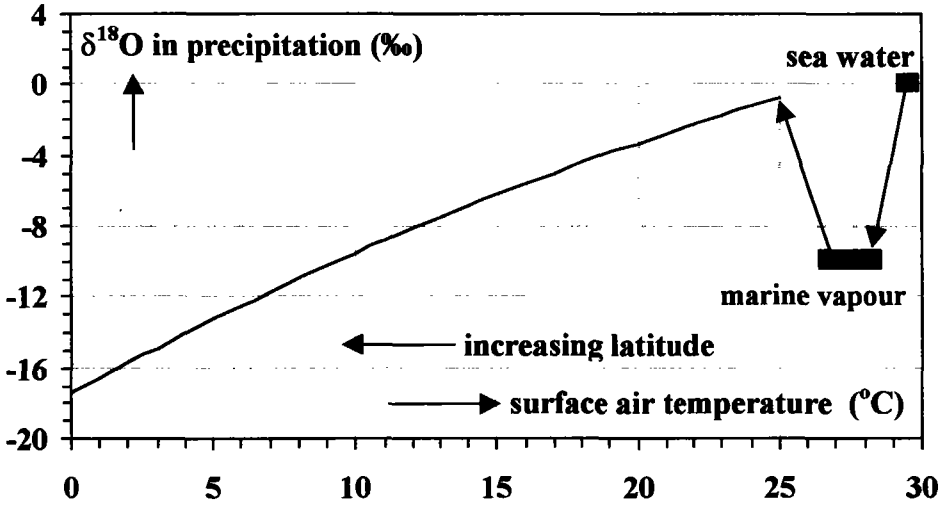

Fig.3.9 Result of calculating the temperature dependence of the latitude effect according to the simplified model of Fig.3.8 and Eq.3.18 ($^{18}R_{V0}/^{18}R_{L0}$ is taken 0.99, i.e. $^{18}\delta$ of the original marine vapour −10‰, and the evaporation temperature 25°C). The right-hand side of the drawing refers to the formation of water vapour from seawater and the subsequent condensation to form precipitation.

In these two cases the isotopic value in the precipitation is more depleted than the true equilibrium precipitation. These situations are then less effective in isotopic fractionation during rainout than the Rayleigh process proper, moderating the extent of isotopic depletion as a function of the rainout.

The meteoric water lines discussed so far, which in essence are Rayleigh lines, obviously describe a spatially distributed data set, describing the evolution of a particular precipitating air mass. They may also apply to different air masses with similar initial properties (water content, temperature and δ_{V0}), formed under comparable circumstances.

3.5.2 EVAPORATION AND TRANSPIRATION; RECYCLING OF MOISTURE OVERLAND

As rain falls on the ground it is partitioned into stagnant water pools and fluxes of surface runoff and of infiltration into the soil. As shown in Fig.3.10, part of the meteoric water is re-introduced into the atmosphere by virtue of direct evaporation or transpiration by the intermediary of the plant cover. Indeed some degree of evaporation already occurs as raindrops fall to the ground beneath the cloud base.

The largest share of the evapo-transpiration flux is carried by the transpiration of the plant cover, with evaporation from water intercepted on the canopy also accounting for an important share, up to 35% in the tropical rain forest (Molion, 1987). The total amount of re-evaporated water from the plants, from the soil and from open waters accounts in most cases for close to 50% of the incoming precipitation and approaches 100% in the arid zone. On a globally averaged basis the incoming moisture is recycled 1.5 times over the continents. Unlike the situation for transpired waters, evaporation from an open water body does not restore the ambient moisture's isotopic composition, since $\delta_E \neq \delta_P$. Moreover, it changes the d-excess of the atmospheric waters as explained below. However, complete drying-up of a surface water pool, as well as a terminal lake at hydrologic steady state, restores all of the incoming precipitation to the atmosphere so that the isotopic composition remains unchanged.

From the isotopic point of view, the transpiration flux is essentially non-fractionating (see Volume I, Sect.4.4.3), so that the addition of the transpired water restores the humidity lost by precipitation without a change in the isotopic composition. However, since the transpiration flux utilises the soil waters on a seasonally selective basis, and since usually there is a large seasonal cycle in the isotopic composition of precipitation, one finds a value different from the annual average, due to the selective utilisation of part of the rain (Sect.3.5.3).

The expression for the isotopic composition of the evaporate, given in Eq.3.5, depends among other factors on the composition of the water body which is evaporating. The value of δ_E in the δ^2 vs. $^{18}\delta$ graph is usually situated above the MWL, depending on how far the enrichment of the residual surface waters has progressed relative to the initial conditions.

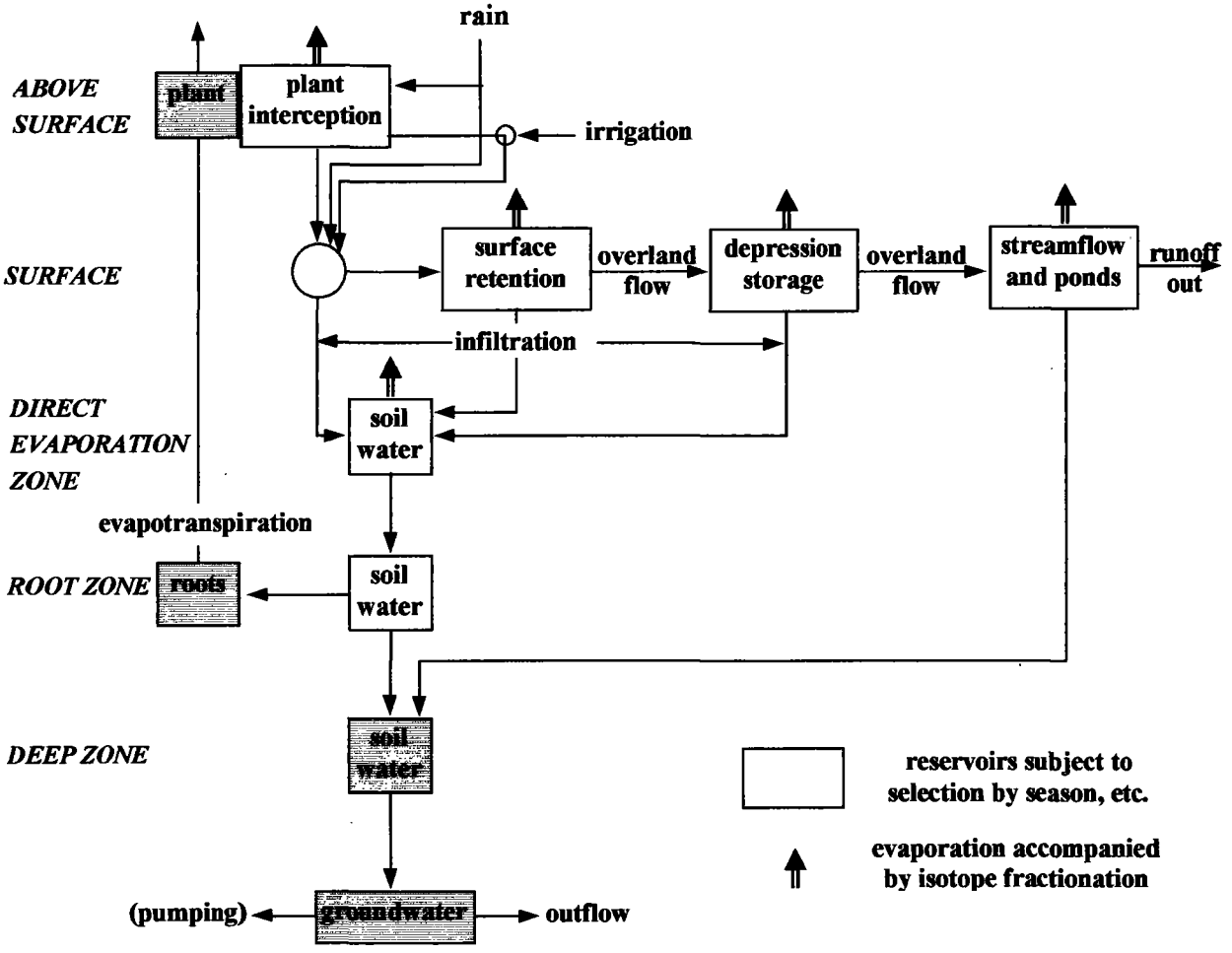

Fig.3.10 Scheme of the atmosphere/land surface interface, based on Gat and Tzur (1976). The backflux of water into the atmosphere by evapo-transpiration consists of 3 variants: 1. evaporation from open-water bodies with isotope fractionation; 2. transpiration from plants without isotope fractionation; 3. periodic evapo-transpiration from reservoirs where selection by season or based on rain amounts takes place (see also Sect.3.1.5).

As shown in Fig.3.3, when the isotopic composition of the residual waters is further and further removed from that of the initial (precipitation) value, then it is to be noted that the isotopic composition of the return flux to the atmosphere (δ_E) approaches that of the inflow (δ_{in}) and under terminal-lake conditions, when $\delta_E = \delta_{in}$, material balance considerations dictate that $\delta_E = \delta_{in}$. Thus, paradoxically, at the time that the effect on the isotopic composition of the lake water is maximal, the effect of the evaporation flux on the isotopic composition of the air moisture vanishes.

Writing Eq.3.6 for both the oxygen and hydrogen isotopes and remembering that

$$d = {}^{2}\delta - 8.{}^{18}\delta$$

we obtain an expression for d_E, the *d-excess value for the evaporation flux*, as follows:

$$d_E = \{d_w - h_N d_A - ({}^2\varepsilon_{L/V} - 8\,{}^{18}\varepsilon_{L/V}) - ({}^2\varepsilon_{diff} - 8\,{}^{18}\varepsilon_{diff})\}/(1-h_N) = \quad (3.19)$$

$$= \frac{d_w - h_N d_A - ({}^2\varepsilon_{L/V} - 8\,{}^{18}\varepsilon_{L/V})}{1-h_N} - n\Theta({}^2\Delta_m - 8\,{}^{18}\Delta_m)$$

where d_E, d_w and d_A are the d-excess values of the evaporation flux, the surface water and the atmospheric humidity, respectively.

The term $({}^2\varepsilon_{L/V} - 8\,{}^{18}\varepsilon_{L/V})$ is close to zero in all cases; $n({}^2\Delta_m - 8\,{}^{18}\Delta_m) = -100.3‰$ when $n = ½$, as applies to an open water body. Thus:

$$d_E - d_A \approx \frac{(d_w - d_A)}{(1-h_N)} + 0.1 \times \Theta \quad (3.20)$$

The value of $(d_E - d_A)$ does not depend on the discrete δ_A values. This is a very fortunate feature, since the value of d_A is never in doubt by more than a few ‰, even in the case where the values of δ_A may be uncertain due to the variable rainout history of the air masses (Gat, 1980) or due to the possibility of admixture of transpired water from the vegetation-covered continental areas (White and Gedzelman, 1984).

Eq.3.20 provides a scaling factor against which one can compare the measured change of d resulting from the admixture of the evaporate.

Due to the above-mentioned processes, one typically finds an increase of d in an air mass along a continental passage, as observed, for example, in the Amazon basin (Gat and Matsui, 1991).

The recycling of water over the continents, just described, affect the total atmospheric water cycle. Fig.3.11 is an attempt to show how the basic Craig-Gordon model is modified by the terrestrial part of the water cycle (Gat, 1996).

3.5.3 SELECTION VERSUS FRACTIONATION

The isotopic composition of precipitation is the primary signal whereby the derived meteoric waters, be these surface, soil or groundwater, can be related to the precipitation input, geographically or temporally. Further, their subsequent change by evaporation, mixing or interaction with the lithosphere can then be utilised to trace or quantify these processes.

Only in exceptional cases is the transfer from one compartment or phase to another indiscriminate, so that the original isotopic composition is fully preserved. One such case is the direct rainout on a mixed surface water, another obviously the total transfer of water from one system to another as occurs when a pool of water dries up completely.

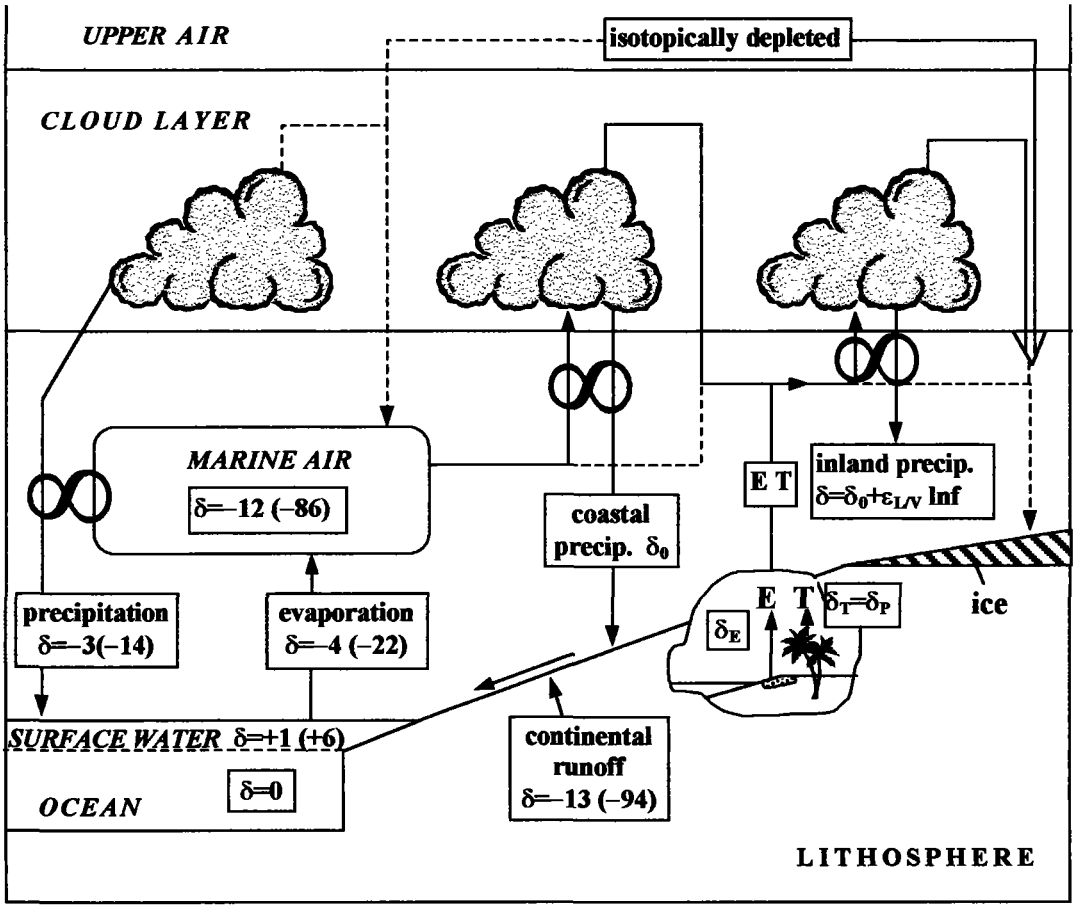

Fig.3.11 Adaptation of the Craig and Gordon model (Fig.3.7) to include the terrestrial part of the hydrological cycle. The double loop signifies that isotopic equilibrium is assumed between the precipitation and the ambient atmospheric moisture (Gat, 1996).

A difference in isotopic composition of the primary water pool to that transferred into another phase occurs, for example, by partial evaporation from an open-water body as discussed above or by uptake of water by plants from the soil during different parts of the year. These two examples differ, however, in that in the case of evaporation the different isotopic species of water, namely $^{1}H_2{}^{16}O$, $^{2}H^{1}H^{16}O$ and $^{1}H_2{}^{18}O$, partake at different rates in the evaporation, in which case a consistent isotope enrichment or depletion will occur. We have defined such a process as one with *isotope fractionation*. In the second case the momentary water transition is not fractionating with respect to the different isotopic species. However, the uptake can be unequal during different times of the year, e.g. favouring the growing season. Since the soil water pool is usually not a well mixed reservoir, and furthermore, since the isotopic composition of the precipitation varies seasonally, one will find a shift in isotopic composition in the remaining soilwater and its subsequent recharge to groundwater, based on a *selection* between rain events rather than on isotope fractionation directly. One more example out of many others is the favouring of intense rainfalls in the generation of surface

runoff, resulting in a selection based on the influence of the *amount effect* on the isotopic composition of the rain.

3.6 THE $^{17}O - ^{18}O$ RELATION

The two rare, heavy isotopes, of oxygen, ^{17}O and ^{18}O, occur with natural abundances of 0.037% and 0.204%, respectively (Table 2.1).

As must be clear from its omission in the preceding text, ^{17}O is hardly used, since nearly all ^{17}O and ^{18}O fractionation factors, and thus abundance variations have a fixed relation, independent of the (natural) processes and conditions that give rise to the fractionation:

$$\left(\frac{^{18}R_s}{^{18}R_r}\right) = \left(\frac{^{17}R_s}{^{17}R_r}\right)^{\theta} \qquad \textbf{(3.21)}$$

In this expression, the R's stand for the isotope ratio $^{17}O/^{16}O$ or $^{18}O/^{16}O$, depending on the superscript, and the subscripts "s" and "r" stand for "sample" and "reference", respectively.

This expression is commonly referred to as *mass dependent fractionation*.

Theoretically, the exponent θ is expected to be somewhat smaller than 2, but for the sake of simplicity, $\theta = 2$ is commonly assumed (Volume I, Sect.3.7) (Craig, 1957, Mook and Grootes, 1973, Allison et al., 1995)

The only field in which always ^{17}O was studied in relation to ^{18}O is cosmochemistry, the research of extraterrestrial material such as meteorites (Clayton, 1993). In the early 1980's, however, attention was drawn to observations of non-mass-dependent oxygen isotope fractionation in stratospheric ozone (Mauersberger, 1981), and later also in other stratospheric molecules such as CO_2 (Thiemens et al., 1991). A fractionation behaviour was observed that either obeyed Eq.3.21, but with θ very different from 2, or did not obey Eq.3.21 at all (Krankowsky and Mauersberger, 1996).

These quite unexpected ^{17}O-^{18}O anomalies in the earth's atmosphere brought new attention to the relation Eq.3.21. Actually, until recently, this relation never had been checked properly for meteoric waters, mainly due to practical facts: in the common analytical technique, that of Isotope Ratio Mass Spectrometry (IRMS) applied to CO_2 gas, the ^{17}O ($^{12}C^{17}O^{16}O$) signal is obscured by the much more abundant ^{13}C one ($^{13}C^{16}O_2$), both having mass 45.

Recently, however, two studies appeared, in which the ^{17}O-^{18}O relation of terrestrial material has been carefully analysed. The first (Meijer and Li, 1998) was based on the electrolysis of water and subsequent IRMS analysis of the oxygen gas thus formed. The authors studied a wide variety of natural waters (meteoric, ocean and lake water, and even fruit juice), and found a ($^{17}\delta$,$^{18}\delta$) relationship perfectly following Eq.3.21 with an exponent $\theta = 1.8936 \pm 0.00538$. Typical individual standard deviations of this study were 0.07 ‰ for $^{17}\delta$, and 0.10 ‰ for $^{18}\delta$ (note that the definitions of $^{18}\delta$ and $^{17}\delta$ are similar).

Miller et al. (1999) studied the ($^{17}\delta$,$^{18}\delta$) relationship of a large suite of rock and mineral samples, using the fluorination technique. They also found a relationship according to Eq.3.21, with $\theta = 1.9069 \pm 0.0009$. The individual standard deviations in this study were 0.04‰, and 0.08‰ for $^{17}\delta$, and $^{18}\delta$, respectively.

Although research in this field has not yet fully matured, and the two values for θ reported seem significantly different, it is safe to say at this point that, at least for isotope hydrological applications, $^{17}O/^{16}O$ does not carry additional information.

Studying the global carbon cycle, however, a new application of ^{17}O has been demonstrated by Luz et al. (1999) and Luz and Barkan (2000). The stratospheric processes, leading to ^{17}O-^{18}O anomalies in ozone and other oxygen-containing species, also influence the ^{17}O-^{18}O relation in molecular oxygen (Thiemens et al., 1995). Using IRMS for whole-air samples, this small effect can still be observed in sea-level oxygen. The stratospheric ^{17}O-^{18}O anomaly, however, is washed out by plant activity: photosynthesis (CO_2 consumption) as well as respiration and combustion (CO_2 production) show a ^{17}O-^{18}O relation fully complient with Eq.3.21. From the competition between these effects, and thanks to the high precision of the measurements, independent numbers can be deduced for marine and terrestrial biological activity (see further the related subjects in Sect.6.7 on O_2/N_2 measurements and the Dole effect).

4 OBSERVED ISOTOPE EFFECTS IN PRECIPITATION

In this chapter data are reported on the isotopic composition of precipitation. In principle variations in $^{18}\delta$ and $^{2}\delta$ are coupled, one way or the other: under conditions of isotopic (and thus also physical) equilibrium according to the meteoric water line with slope 8 (the GMWL), if the conditions are non-equilibrium by a more complicated kinetic process. For less detailed hydrological surveys it is generally assumed that $^{18}\delta$ and $^{2}\delta$ values are coupled as if in equilibrium. In the next sections we are therefore also reporting data from literature that are concerned with only $^{18}\delta$ or $^{2}\delta$.

However, it should be emphasised that measuring the oxygen as well as hydrogen isotopes often presents additional information; the combination of $^{18}\delta$ and $^{2}\delta$ is to be preferred.

4.1 THE LATITUDE / ANNUAL TEMPERATURE EFFECT

To explain in brief and numerically the stable isotopic composition of precipitation on a global scale, we have applied the Rayleigh model in Chapter 3, including two processes:

1) the formation of atmospheric vapour by evaporation in regions with the highest surface ocean temperatures
2) the progressive condensation of the vapour during transport to higher latitudes with lower temperatures.

The first step has been discussed in Sect.3.2. Atmospheric $^{18}\delta$ values were reported in Sect.3.4 The progressive rainout process based on the Rayleigh fractionation/condensation model, as shown in Fig.3.8 and discussed in Sect.3.5.1 results in a relation between the observed annually averaged $^{18}\delta$ and $^{2}\delta$ values of the precipitation and the mean surface temperatures in reasonable agreement with the observed values from the world-wide GNIP data network (Fig.4.1). The latitude effect is about

$$\Delta^{18}\delta \approx -0.6‰/\text{degree of latitude} \qquad (4.1)$$

for coastal and continental stations in Europe and the USA, and up to −2‰/degree of latitude in the colder Antarctic continent.

The observed relation between monthly temperature and isotopic composition shows much scatter and is not linear, except in the far north. The correlation improves by taking the

amount-weighted means. Based on north Atlantic and European stations from the GNIP network (Sect.3.1), Yurtsever (1975) reported the relation (t is the surface temperature in °C):

$$^{18}\delta = (0.521 \pm 0.014)t - (14.96 \pm 0.21)\,‰ \qquad (4.2)$$

This compares reasonably well with the relation originally reported by Dansgaard (1964) for the north Atlantic stations:

$$^{18}\delta = 0.695t - 13.6\,‰.$$

The simple model calculation for both $^{2}\delta$ and $^{18}\delta$ leads to the equation for the MWL as discussed earlier and is also reasonably consistent with Fig.4.1. The relation is further improved if the ground temperature is replaced by the cloud-base temperature (Rindsberger and Magaritz, 1983). It should be emphasised again that a global precipitation model can only give reliable results, if seawater evaporation is included over the entire range of seawater temperatures instead of being limited to the "thermal equator".

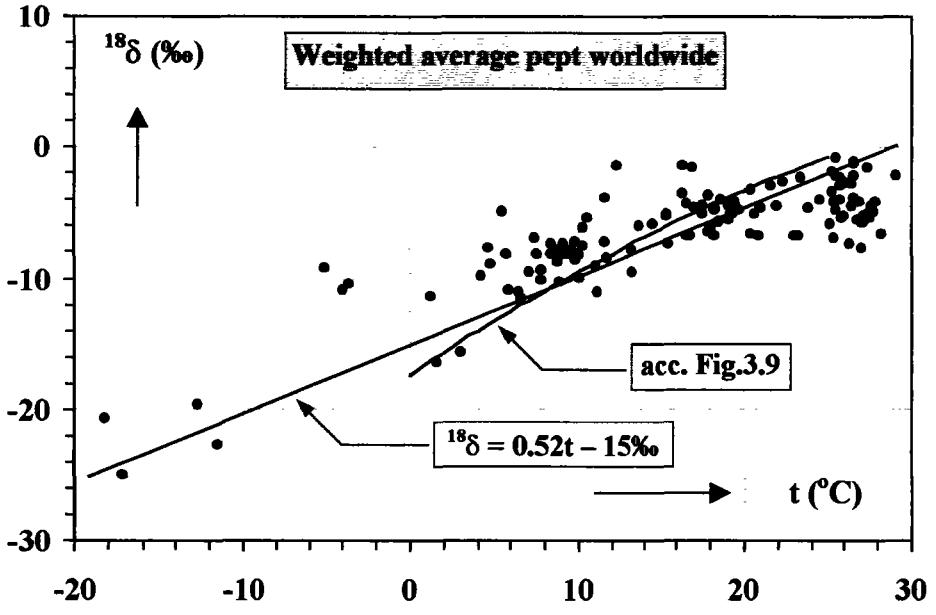

Fig.4.1 The *latitude or annual-temperature effect* on $^{18}\delta$ of precipitation (pcpt): weighted $^{18}\delta$ of total precipitation over periods of at least one decade from marine/coastal, continental and (Ant)arctic stations are shown as a function of the mean measured surface air temperature (data from the GNIP network). The (t,$^{18}\delta$) relation as reported by Yurtsever (1975) (Eq.4.2) and that according to Fig.3.9 are given for reference.

On the average global scale the ($^{18}\delta$, $^{2}\delta$) relation turns out to be satisfactorily described by the *Global Meteoric Water Line (GMWL)*, as is mentioned in Sect.3.1 (Fig.4.2). Regionally and

for certain periods (such as seasons) *Local Meteoric Water Lines* (LMWL) may be found, depending on the conditions for forming the local water source of each region (see next Section).

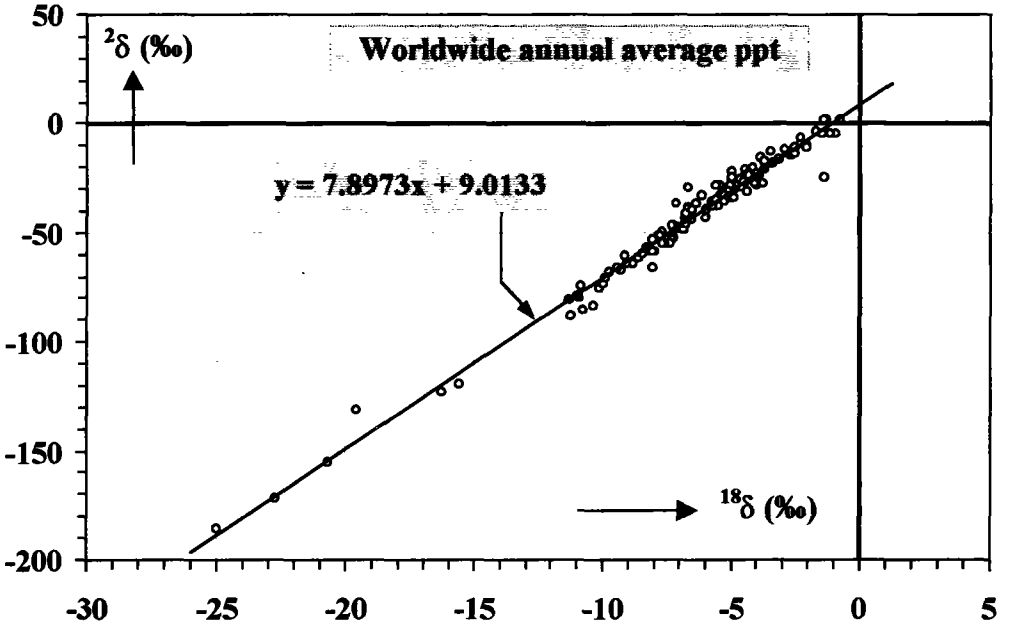

Fig.4.2 Relation between weighted average $^{18}\delta$ and $^{2}\delta$ values of total precipitation over periods of at least one decade from the same stations of the GNIP network as represented in Fig.4.1. The data confirm the general validity of the Global Meteoric Water Line (GMWL) reasonably well.

4.2 SEASONAL EFFECT

A seasonal temperature pattern is clearly followed by all but some marine stations (Fig.4.3). The dependence of the isotope variations on the local temperature (or the closely related parameter of the precipitable water content (Sonntag et al., 1983)) appears as the overriding parameter (Yurtsever, 1975; Fricke and O'Neil, 1999). Generally the temperature dependence of both δ values is smaller than shown by the latitude effect, varying from about 0.5‰/°C for some higher-latitude stations to ultimately 0‰/°C for tropical ocean islands (Fig.4.3 and 4.4).

From the simple model presented in the preceding section follows that the seasonal variations of $^{2}\delta$ and $^{18}\delta$ values of precipitation are bound to be smaller than the variations of yearly averages with latitude. The essence is in the $(1/T - 1/T_0)$ factor in Eq.3.16. During winter, the condensation temperature T_L is lower than during summer. However, the same is true for T_0,

the prevailing average temperatures in the region of evaporation. This partly masks the local temperature effect.

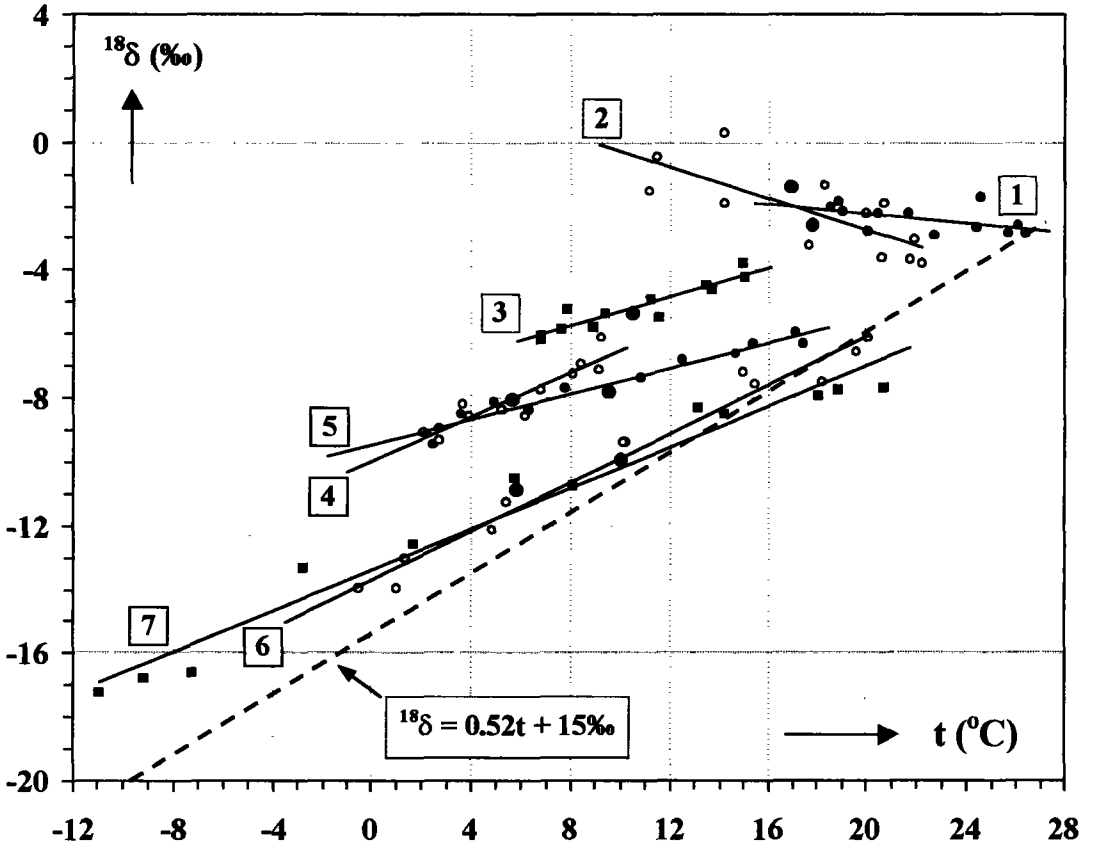

Fig.4.3 Comparison of the latitudinal and the seasonal temperature effect of ^{18}O in precipitation. In both cases the data show the averages over a large number of years. The dashed line refers to the latitudinal effect given by Eq.4.2, heavy dots represent the long-term annual averages., smaller dots the monthly averages. Numbers indicate the following stations:

1 Midway, Pacific Ocean 2 Pretoria, South Africa 3 Valentia, Ireland
4 Stanley, Falkland Isl. 5 Groningen, The Netherlands 6 Vienna, Austria
7 Ottawa, Canada

The opposite seasonal effect for Pretoria may be correlated with high precipitation intensity with often low $^{18}\delta$ values during summer (cf. Sect.4.5).

For instance, during winter in the northern hemisphere the highest temperatures are found south of the equator. Water vapour from this region is not easily transported to the northern hemisphere, however, so the effective evaporation region for the northern hemisphere has a lower T_0 value than during summer.

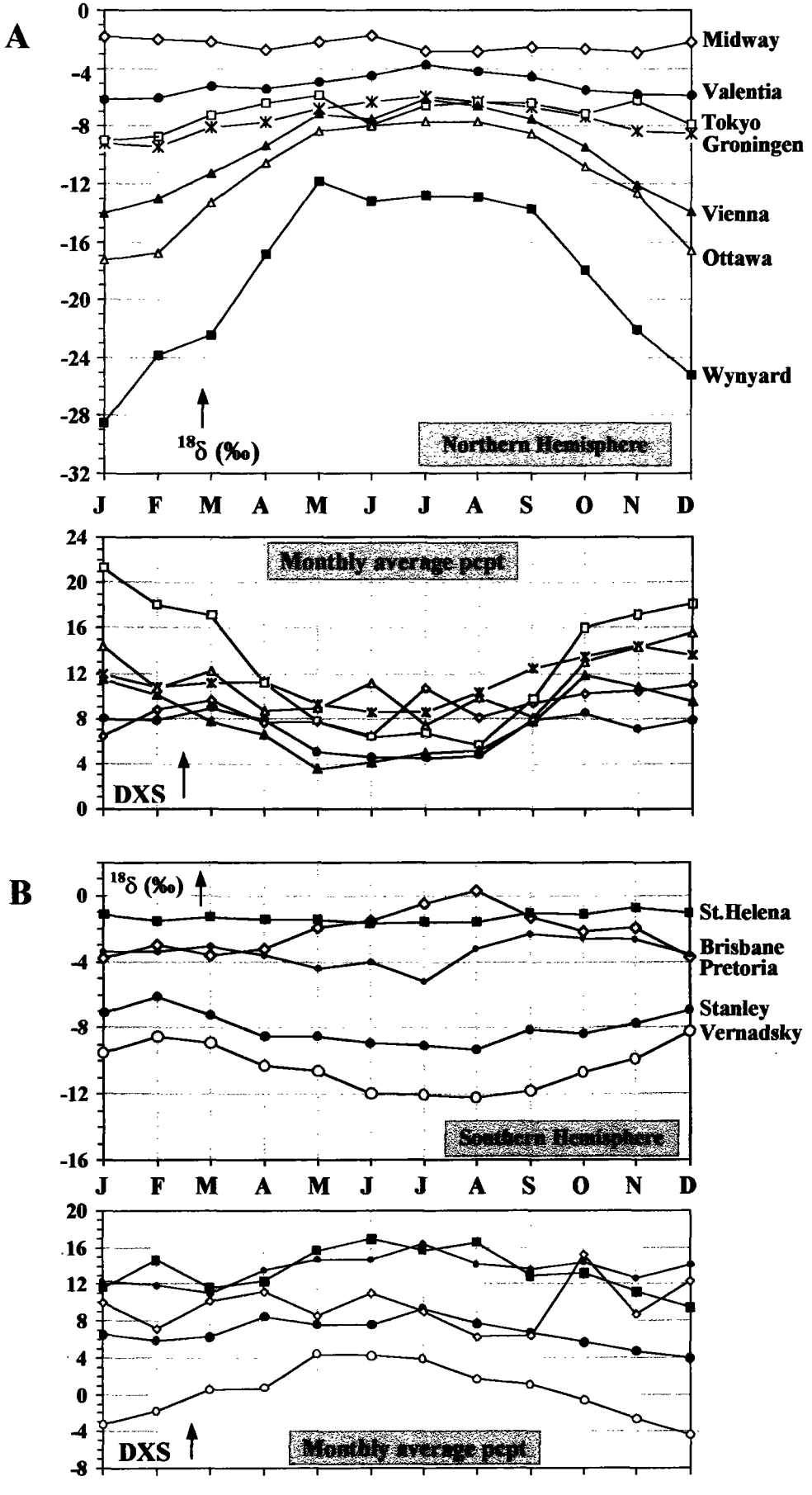
A
0
-4
-8
-12
-16
-20
-24
-28
-32
Midway
Valentia
Tokyo
Groningen
Vienna
Ottawa
Wynyard
$^{18}\delta$ (‰)
Northern Hemisphere
J F M A M J J A S O N D
24
20
16
12
8
4
0
Monthly average pcpt
DXS
B
$^{18}\delta$ (‰)
0
-4
-8
-12
-16
St.Helena
Brisbane
Pretoria
Stanley
Vernadsky
Southern Hemisphere
J F M A M J J A S O N D
20
16
12
8
4
0
-4
-8
DXS
Monthly average pcpt

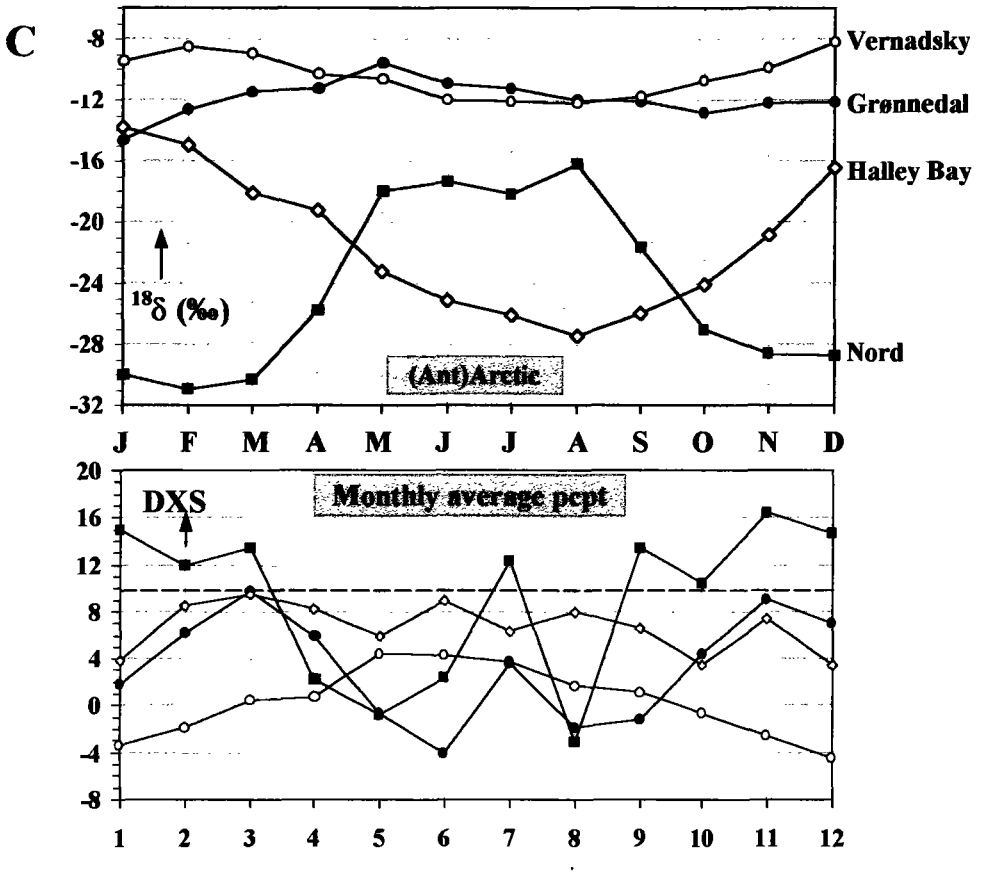

Fig.4.4 Seasonal variations in $^{18}\delta$ shown by weighted averages of monthly precipitation samples (pcpt) collected in some typical continental and island or coastal stations from **A)** the northern hemisphere, **B)** the southern hemisphere and **C)** some Arctic and Antarctic stations (data from the GNIP network, generally dating from the early 1960ies through 1997). The lower figures indicate the deuterium excess (DXS) values for the same stations (indicated by the same type of data points).

Stations situated in a mid-continental setting typically portray a seasonal change in the isotopic composition of the precipitation. These variations are correlated with the temperature, in most cases. At tropical islands, on the other hand, where the vapour source region essentially coincides with the region of precipitation ($T=T_0$) the temperature dependence almost disappears, as is shown in Fig.4.3 and 4.4.

If the weighted averages of monthly precipitation over a large number of years is considered, the ($^{18}\delta$,$^{2}\delta$) relation is very close to that of the Global Meteoric Water Line (Fig.4.5). However, looking in detail deviations exist.

The most pronounced factors which determine the offset of monthly data at any station from a classical meteoric water relationship are:

1) different source characteristics of the moisture, either due to the seasonal change of the meteorological conditions over the ocean, or different location of the source regions. This basically fixes a series of parallel meteoric water lines, for each of the seasons.

2) evaporative enrichment in the falling droplets beneath the cloud base, effective during warm and dry months when rain amounts are small. This partially evaporated rain is characterised by relatively higher $^{18}\delta$ values and small to negative d-excess values.

3) high values of the d-excess parameter (Fig.4.4) associated with snow or hail (Jouzel and Merlivat, 1984). These events are also associated with very depleted isotopic values.

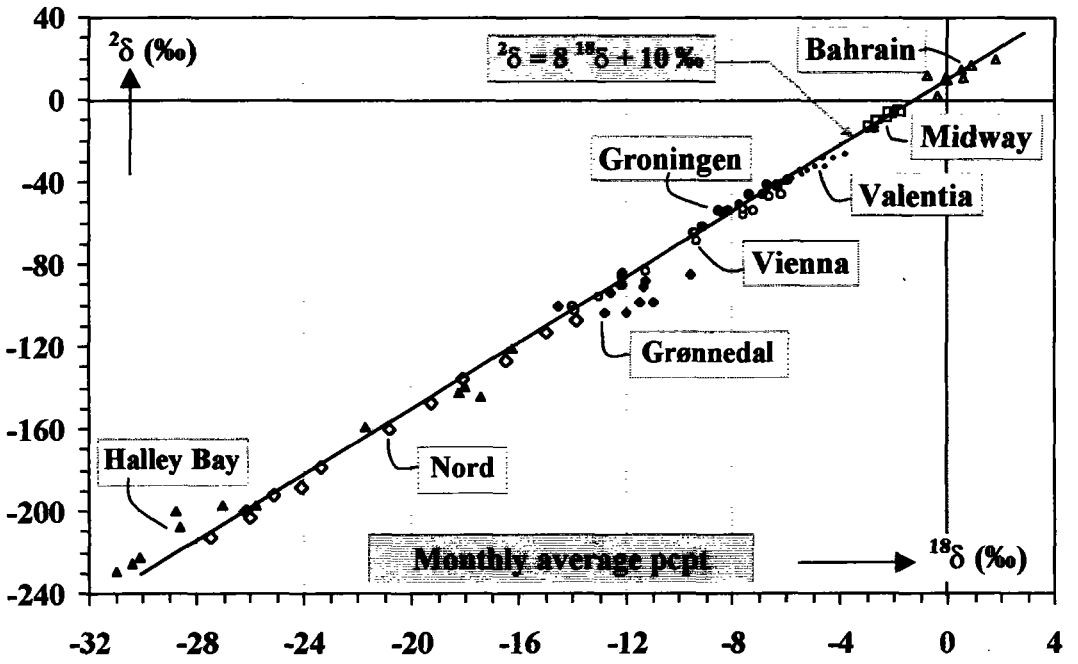

Fig.4.5 Seasonal influence on the ($^{18}\delta$,$^2\delta$) relation for average monthly precipitation at a number of stations, arctic, tropical, coastal and continental (data from the same series as in Fig.4.4).

The changes in $^{18}\delta$ are correlated with those of $^2\delta$. However, a local best fit for the ($^{18}\delta$,$^2\delta$) line is in most cases not a meteoric water line in the sense described before, namely one produced by varying degrees of rainout from an air mass of prescribed isotopic character. By and large, most of these effects combine to produce a low-slope ($^{18}\delta$,$^2\delta$) line (i.e. with a slope less than 8) which is not only indicative of the genetic and synoptic history of the rain events,

but also reflects the local conditions at the time precipitation occurs. Notably when the slope $\Delta^2\delta/\Delta^{18}\delta$ differs from the value of 8, then a simple linear fit is often not a satisfactory description of the relationships, because a variety of processes is at play, each process with its own set of rules concerning the isotope fractionation involved.

4.3 OCEANIC AND CONTINENTAL PRECIPITATION

Precipitation over the ocean, collected at island stations or weatherships, has the characteristics of *a first condensate* of the vapour. The range of most $^{18}\delta$ values is relatively small, between –0‰ to –5‰ with but little seasonal change in many cases (see Sect.4.2), and a lack of a clear correlation with temperature (Dansgaard, 1964; Rozanski et al., 1993). The same is true for the $^{2}\delta$ values. There is a relatively large variability in the value of the Deuterium-Excess especially notable close to the major source regions of the atmospheric moisture. This is obtained by imagining MWL's (having slope 8!) drawn through the data in Fig.4.4).

For comparison, Fig.4.4 also contains ($^{18}\delta$,$^{2}\delta$) data from inland or continental stations. In the case of oceanic precipitation, the scatter in d-excess predominates, whereas the isotopic data are fairly well aligned along meteoric water lines further removed from the coast, so that, even though the range of $^{18}\delta$ is much larger than in the marine domain, the values of $\sigma(d)$ are actually reduced. This characteristic can be quantified by the ratio of the spread in the d-excess, $\sigma(d)$, to the range of $^{18}\delta$ values, $\sigma(d) / <^{18}\delta>$. This ratio changes, for example over the European continent, from 2.0, 2.3, 1.8 and 2.8 at the coastal and island stations of Valentia (Ireland), Reykjavik, Faro (Portugal) and Weathership E in the northern Atlantic to values of 0.4, 0.35 and 0.7 at continental stations such as Berlin, Krakow and Vienna, respectively.

This observed pattern fits quite well a simplified scheme for the isotopes in the hydrologic cycle, wherein one views the d-excess value to be established at the site of the air-sea interaction. The offset from equilibrium conditions is then determined primarily by the humidity deficit above the sea surface, i.e. the value of $(1-h_N)$ (Merlivat and Jouzel, 1979). As will be discussed below, the d-excess value is basically conserved during the rainout over the continents.

Some apparently anomalous features of the marine data set (namely some relatively depleted isotopic values) can be explained, on the one hand, by the intense vertical mixing in the air column of tropical clouds in the presence of the ITCZ, as shown above. The amount effect, i.e. a correlation of the depletion of heavy isotopes with the amount of rain is explained on the other hand by the preferential isotopic exchange of the smaller droplets, which are predominant in light rains and drizzle, with the near-surface moisture. Heavier rains on the other hand maintain the depleted isotopic values from within the clouds.

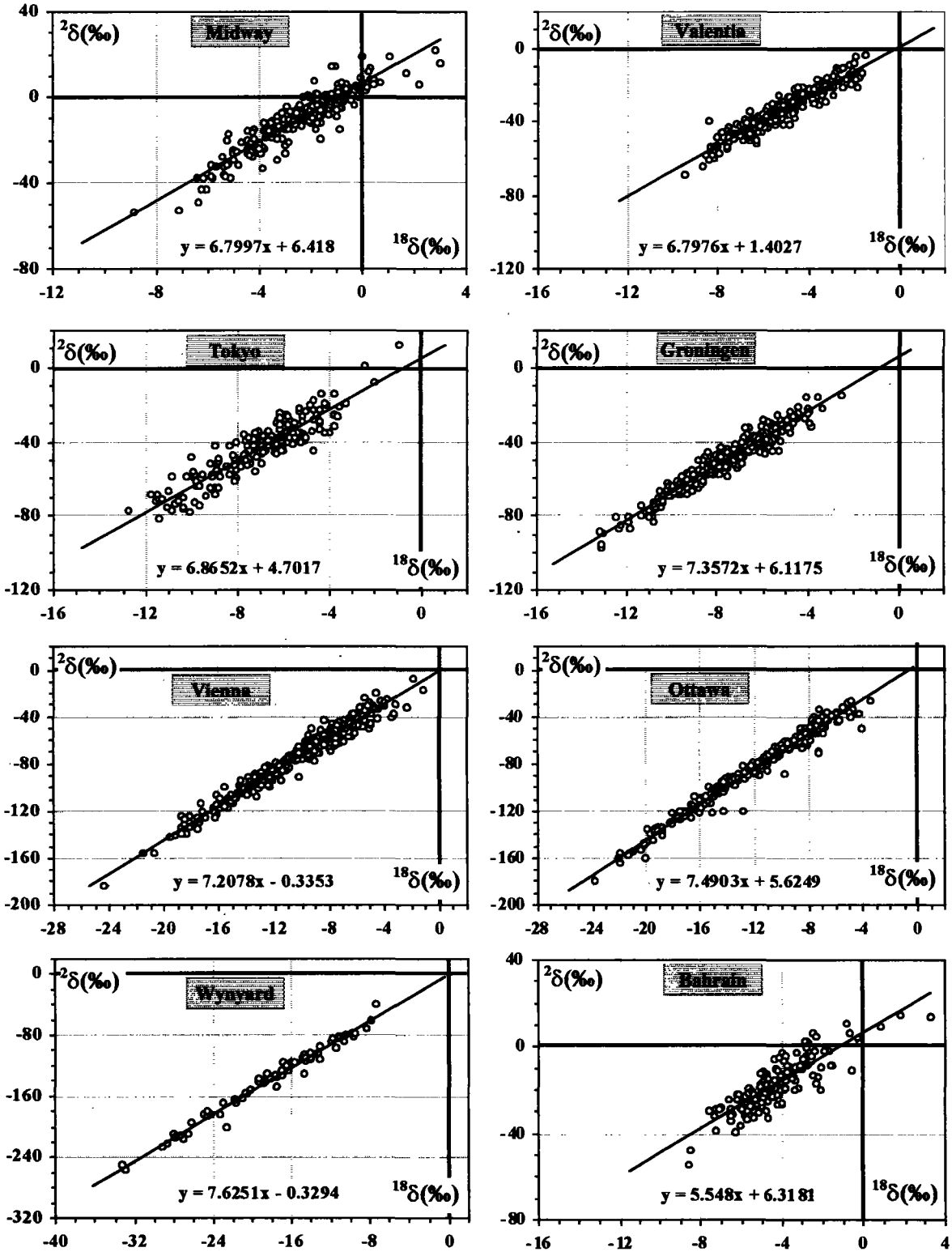
Midway
$^2\delta$(‰)
$^{18}\delta$(‰)
y = 6.7997x + 6.418
Valentia
y = 6.7976x + 1.4027
Tokyo
y = 6.8652x + 4.7017
Groningen
y = 7.3572x + 6.1175
Vienna
y = 7.2078x - 0.3353
Ottawa
y = 7.4903x + 5.6249
Wynyard
y = 7.6251x - 0.3294
Bahrain
y = 5.548x + 6.3181

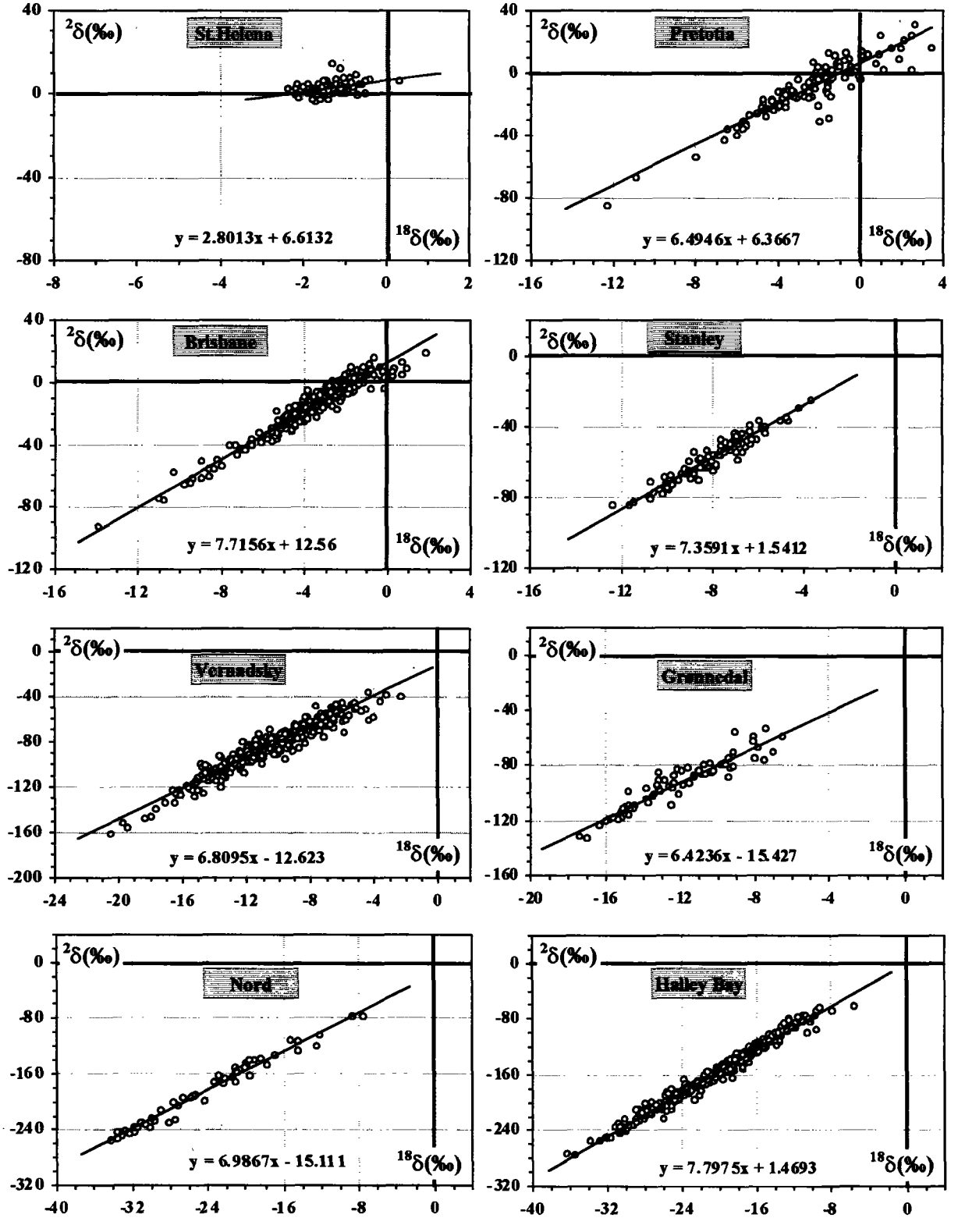

Fig.4.5 Regression lines for ($^2\delta$,$^{18}\delta$) relations of monthly precipitation samples from marine stations, continental tropic and (Ant)Arctic stations (data from GNIP); d-excess values to be estimated from lines with slope 8 through the data points, are highly variable, in agreement with Fig.4.4.

The *continental effect*, also referred to as the *distance-from-coast effect*, i.e. a progressive ^{18}O depletion in precipitation with increasing distance from the ocean, varies considerably from area to area and from season to season, even over a low-relief profile. It is also strongly correlated with the temperature gradient and depends both on the topography and the climate regime.

During the passage over Europe, from the Irish coast to the Ural mountains, an average depletion of 7‰ in $^{18}\delta$ is observed. However, the effect in summer is only about one fourth of the effect in winter. Eichler (1964) attributed this to the re-evaporation of summer rain.

An extreme case of the absence of an inland effect over thousands of kilometres, in spite of strong rainfalls en route, was reported over the Amazon (Salati et al., 1979). This is also attributed mainly to the return flux of the moisture by (non-fractionating) transpiration and thus invalidates the effect of the rainout. However, some of the return flux apparently occurs by evaporation from open waters. This process then results in some change in the isotopic composition, and in particular, an increase of the d-excess. Such an increase is indeed noted in the comparison of the precipitation from inland to coastal stations.

A similar effect of an increase of the d-excess will also result from the partial re-evaporation of rain droplets beneath the cloud base as these fall to the ground surface, as described by Dansgaard(1964) in the case of precipitation at Adis-Abeba in north-east Africa.

The continental effect in $^{2}\delta$ is nicely shown by the iso-$^{2}\delta$ contours reported by Taylor (1972) for the United States. However, from an evaluation of the IAEA data, it turns out that there are continental stations without a *continental effect* Many results for coastal stations appear to deviate from the lines in Fig.4.1, whereas several continental stations have precipitation in agreement with these (t,$^{18}\delta$) relations. The extent to which a continental effect occurs probably depends on the prevailing direction of the movement of air masses, rather than simply on distances from the ocean.

4.4 ALTITUDE EFFECT

As a rule the isotopic composition of precipitation changes with the altitude of the terrain and becomes more and more depleted in ^{18}O and ^{2}H at higher elevations. This has enabled one of the most useful applications in isotope hydrology, namely the identification of the elevation at which groundwater recharge takes place.

This *altitude effect* is temperature-related, because the condensation is caused by the temperature drop due to the increasing altitude. Due to the decreasing pressure with increasing altitude (-1.2%/100 m), a larger temperature decrease is required to reach the saturated water vapour pressure than for isobaric condensation. Therefore, dN_V/N_V per °C and thus $d\delta_L/dT$ is smaller than for the isobaric condensation process which produces the latitudinal effect. The molar amount of vapour is proportional to the barometric pressure, b. The relative decrease in vapour content is then given by:

$$dN_V/N_V = dp/p - db/b$$

Siegenthaler and Oeschger (1980) calculated this decrease to be -3.6%/100 m (directly caused by a temperature drop of -0.53°C/100 m and +1.2%/100 m, respectively. The value of $(dN_V/N_V)dT$ is then 2.4/0.53 = 4.5%/°C. From Eqs.3.16 and 3.17 we can then deduce the temperature effect:

$$\frac{d^{18}\delta}{dT} \quad +0.4‰/°C \approx -0.2‰/100m$$

and **(4.3)**

$$\frac{d^{2}\delta}{dT} \quad +3‰/°C \approx -1.5‰/100m$$

However, other factors need to be considered that change the isotopic composition, besides the basic Rayleigh effect. One is the evaporative enrichment of ^{18}O and ^{2}H in raindrops during their fall beneath the cloud base, which is larger at low altitudes where the cloud base is typically high above ground level. This so-called pseudo-altitude effect (Moser and Stichler, 1974) is observed in inter-mountain valleys and on the lee side of a mountain range. This evaporative enrichment, unlike the primary Rayleigh rainout effect, also results in a decrease of the d-excess and thus marks these situations clearly. This effect is illustrated for the case of a traverse across the Judean mountain range and in the distribution of the d-excess parameter throughout the area, closely following the topography (Gat and Dansgaard, 1972).

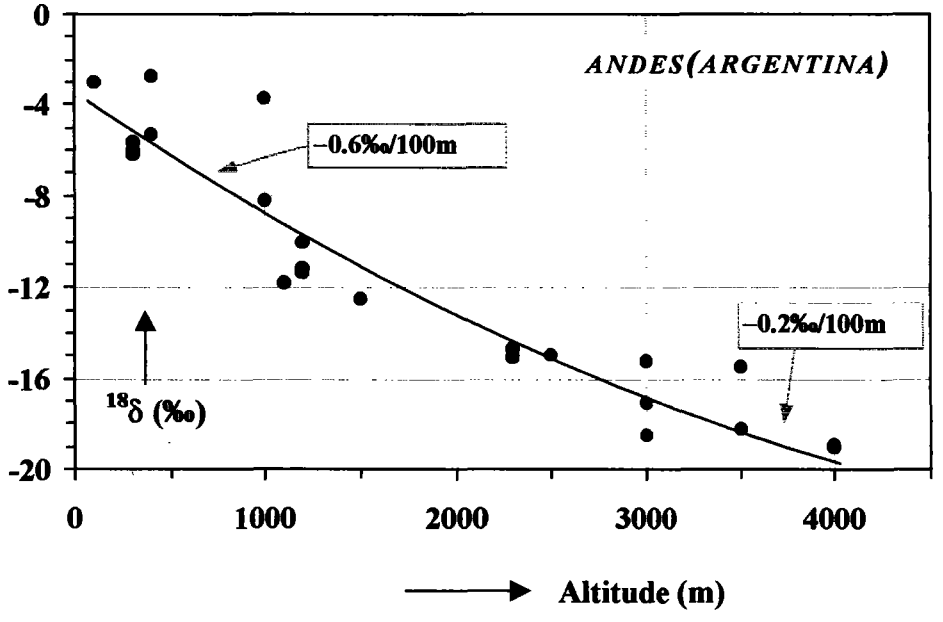

Fig.4.7 Example of the altitude effect on precipitation for the eastern slopes of the Andes mountains, as deduced from samples of undeep groundwater/soilwater, collected from springs. The magnitude of the effect is increasing from –0.2 to –0.6‰/100m (Vogel et al., 1975).

The most elusive factor is where different air masses with different source characteristics affect the precipitation at the base and crest of a mountain. A prominent case is that of the western slopes of the Andes in South America: precipitation near the crest results predominantly from air from the Atlantic with a long continental trajectory, whereas air from the Pacific Ocean, with predominantly oceanic attributes, affects the precipitation in the lower elevations. Under such conditions one encounters apparently anomalously large altitude effects.

An opposite effect results when the long-term samples (e.g. monthly, seasonal or annual composites) represent different time series at the varying altitudes. As an example can be cited the case of a low-altitude and a high-altitude station in Cyprus (Gat et al., 1962). Frontal rains affect both stations and show a normal altitude effect. In the mountain, however, rain also occurs orographically at times that no rain falls in the plain, so that in the composite sample of the mountain station the frontal rains are diluted by precipitation representing a 'first condensate", with relatively enriched isotopic values.

The observed ^{18}O effect generally varies between –0.1‰ and –0.6‰/100 m of altitude often decreasing with increasing altitude (Vogel et al., 1975) (Fig.4.7). Values in this range have also been reported for mountain regions in Czechoslovakia (Dinçer et al., 1970), Nicaragua (Payne and Yurtsever, 1974), Greece (Stahl et al., 1974), Cameroon (Fontes and Olivry, 1977), Italy (Bortolami et al., 1978) and Switzerland (Siegenthaler and Oeschger, 1980).

Friedman et al. (1964) reported data on the altitudinal effect on $^{2}\delta$, showing roughly –4‰/100m for the coastal region of the western United States, whereas Moser et al. (1978) report a value of –2.5‰/100m, observed in S.W. Germany and values ranging from –1‰/100m to –4‰/100m for Chile (Moser et al., 1972).

In many cases the d-excess is found to increase with altitude, possibly for a variety of reasons. This issue has not been finally resolved.

4.5 AMOUNT EFFECT

Dansgaard (1964) observed a relation between the amount of precipitation and $^{18}\delta$. For example, the very strong tropical rainfalls at times of the passage of the Intertropical Convergence Zone (ITCZ), characterised by towering clouds and strong downdrafts, may be extremely depleted in $^{18}\delta$ and $^{2}\delta$, the former by as much as –15‰. Similar, though smaller effects are observed in thunderstorm-engendered precipitation. In north-western Europe during convective storms changes in $^{18}\delta$ have been found of –7‰ within 1 hours. Examples are shown in Fig.4.8. Probably, the dip in the $^{18}\delta$ curve for seasonal precipitation at Tokyo in June (Fig.4.4), quite consistent over several years, is due to the high rain intensity during this month. The same may be true for the opposite seasonal temperature effect over Pretoria (Figs.4.3).

In other (isolated) cases amount effects are not consistent and appear to depend critically on the meteorological conditions at the time of the precipitation. In the eastern Mediterranean some of the largest rainfall events result from air masses whose origin differs from that of the usual winter precipitation and which show rather enriched isotopic values, compared to the rest of the precipitation.

Among island stations, where temperature variations are small, a dependence of $^{18}\delta$ on rain intensity is observed to the extent of −1.5‰/100mm of monthly precipitation. It turns out that if this is taken into account, the temperature correlation is improved.

On the other hand, small amounts of rain are, as a rule, enriched in the heavy isotopes along typical evaporation lines, especially in the more arid regions. This effect obviously results from the evaporation of rain droplets on their fall to the ground. However, no further consistent amount effect is noted for rain intensities in excess of about 20mm/month.

The conclusion is that one should refrain from generalisations and explore the local amount effect individually in each case, by running a special sampling programme.

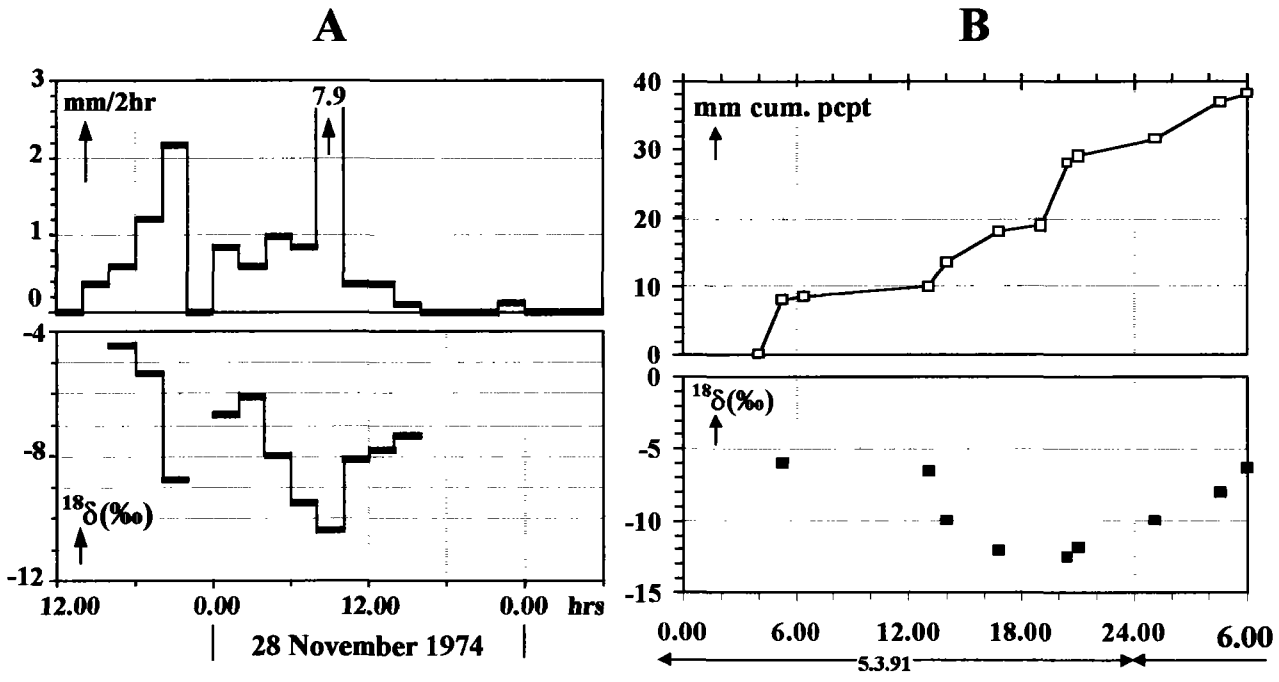

Fig.4.8 Time sequence of the isotopic composition of precipitation during showers; examples are shown for two cases of convective storms: **A)** rain intensity in mm/2 hours (Mook et al., 1974); **B)** cumulative rain over variable periods.

4.6 INTERANNUAL VARIATIONS

Yearly average $^{18}\delta$ values vary from year to year. In temperate climates the values generally do not vary by more than 1‰, and a large part of the spread is caused by variations in the average annual temperature. Figs.4.9 and 4.10 present annual variations for a number of stations,

showing a certain spread of the weighted annual precipitation $^{18}\delta$ as well as $^{2}\delta$. In semi-arid climates, with a less regular rain distribution in time, larger variations occur. In those cases only hydrological systems that pool precipitation inputs over many years can be related to the average rain input over many years.

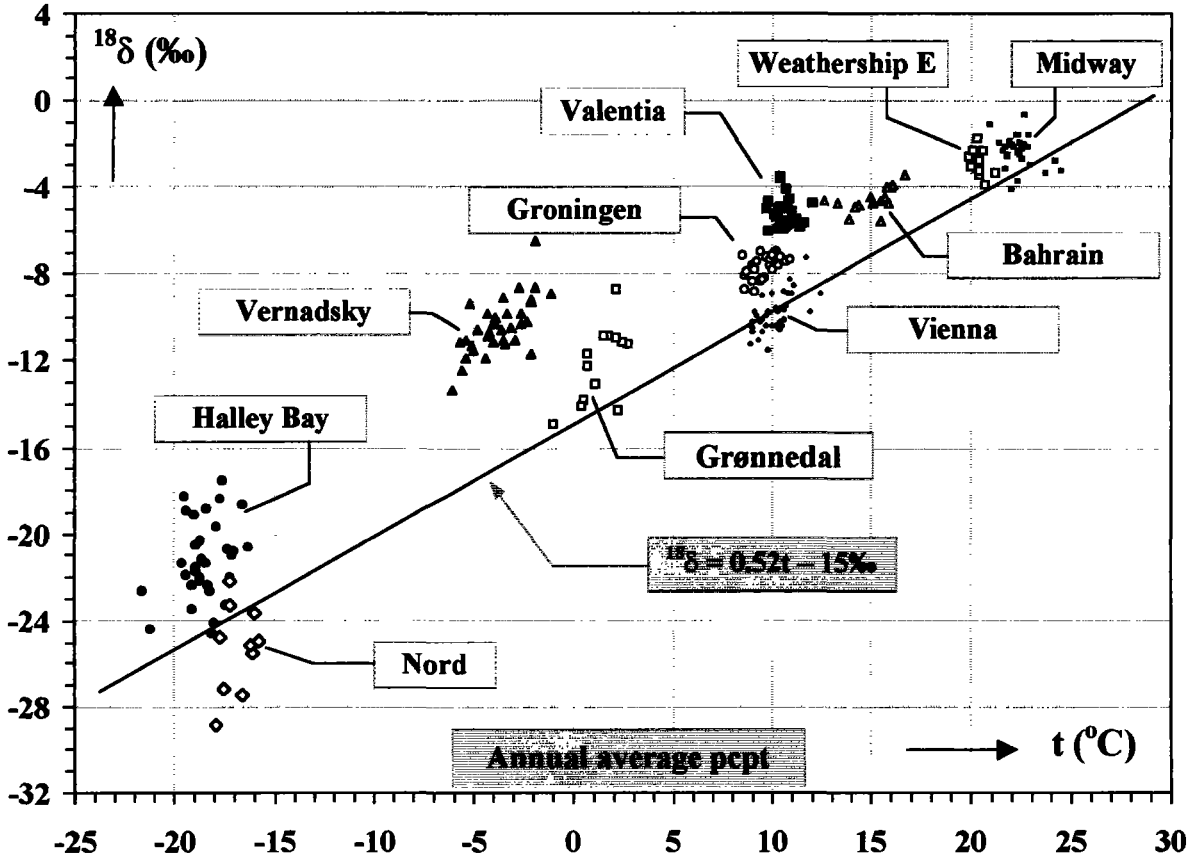

Fig.4.9 Weighted average annual values of $^{18}\delta$ in precipitation (pcpt) vs the mean surface air temperature, showing the variations from year to year (data from the GNIP network).

4.7 SMALL-SCALE VARIATIONS

4.7.1 SMALL-SCALE SPATIAL VARIATIONS

It is important to establish, for instance for $^{18}O/^{16}O$ tracer studies in which $^{18}\delta$ or $^{2}\delta$ variations in rain are related to those in run-off, that short- and long-term variations of $^{18}\delta$ of precipitation with distance have not occurred over the region of interest.

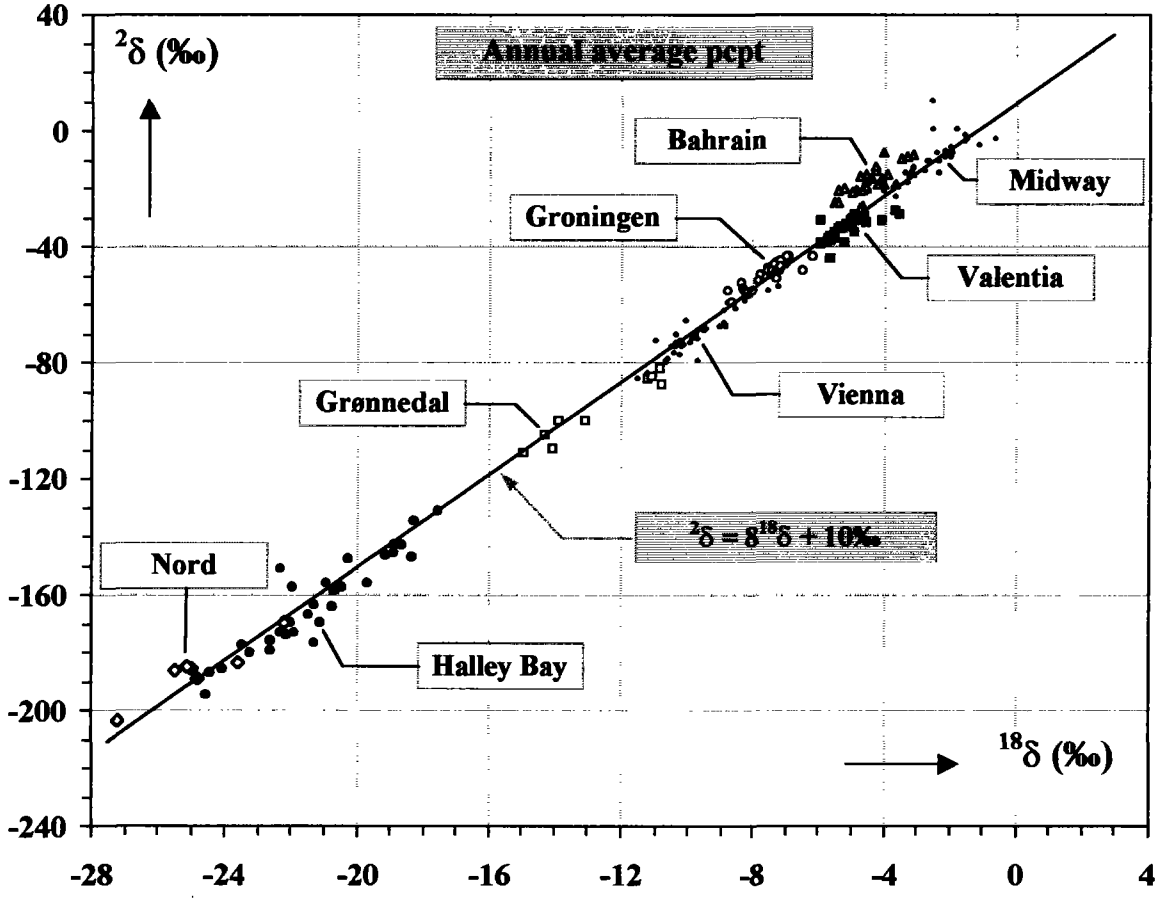

Fig.4.9 Spread of the weighted annual values of the ($^{18}\delta$,$^2\delta$) relation for precipitation (pcpt) (data from the GNIP network).

In the temperate climate of north-western Europe it has regularly been observed that the $^{18}\delta$ values of rain samples collected over periods of 8 and 24 hours from three locations within 6 km^2 at equal elevations agree within 0.3‰ (Mook et al., 1974). Similar results were obtained from the semi-arid climate of Israel (Rindsberger et al., 1990).

At larger distances, especially with single convective storms, larger differences are to be expected. Over a periods of a months $^{18}\delta$ in rain has a similar pattern, even over distances of a few hundred kilometres. Despite the similarities, single monthly samples might differ significantly, although the average values are only slightly ($\approx$ 1‰) different. The $^2\delta$ and $^{18}\delta$ values probably closely obey the MWL.

4.7.2 SMALL-SCALE TEMPORAL VARIATIONS

Rapid variations in $^{18}\delta$ of rain can occur. In Sect.3.1.7 we have mentioned such variations in samples collected during successive two-hour periods. The magnitude of this effect depends on

the character of the precipitation process such as convective storms or weather fronts. Fig.4.8 showed an example, in the framework of the amount effect.

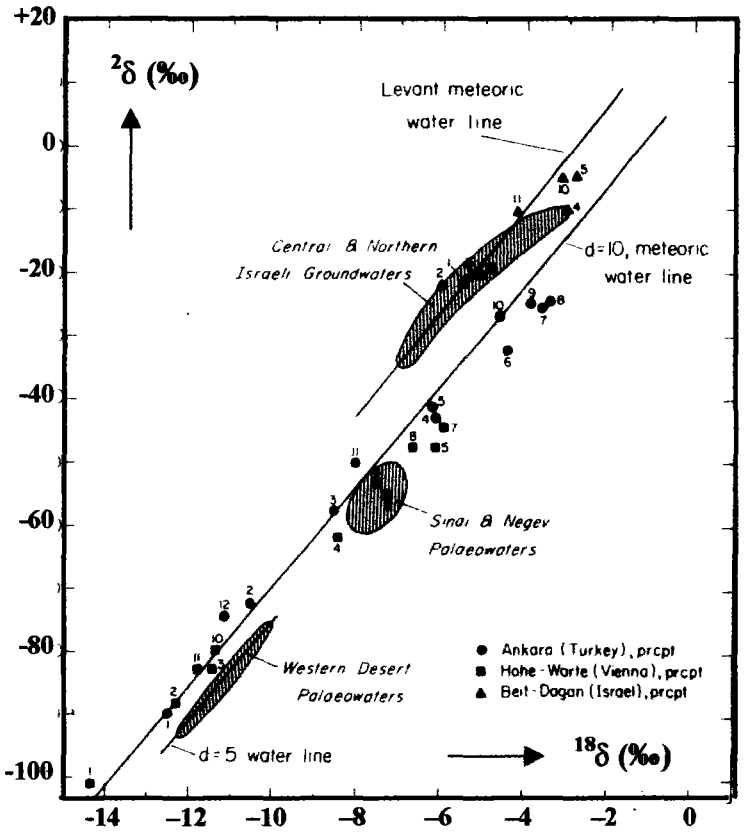

Fig.4.11 Isotopic composition of modern meteoric waters and of palaeowaters in the eastern Mediterranean Sea area. The average monthly precipitation are from Ankara, Vienna and Beit-Dagan; the numbers 1-12 refer to calendar months. Furthermore, the range is indicated of groundwater sources of the modern and palaeohydrologic cycle in the Levant; data from palaeowater of the western desert (Egypt) are shown for comparison (Gat, 1983).

4.8 PALAEOCLIMATE RECONSTRUCTION

The good correlation established between the isotopic composition of precipitation at many sites (especially in a continental setting) and climate variables, such as the ambient temperature and amount of precipitation (Yurtsever, 1975), suggested the use of the isotopic signal both as a monitor and record of climate changes, i.e. changes in the temperature and meteorological regimes.

The 30-year time series of the GNIP program has enabled one to identify a trend of increase in $^{18}\delta$ in parallel with a temperature increase in continental stations in Europe (Rozanski et al. 1992). Shorter term fluctuations in the isotopic composition of precipitation have been shown to coincide with changes in the synoptic pattern of the rain producing air masses, for instance for the Mediterranean, contemporaneous with a cold phase in northern Europe (Kukla and Kukla, 1974; Gat and Carmi, 1987).

Longer records of isotopes in meteoric waters are the ice accumulation on glaciers, where the record can be traced back for thousands of years (see Volume I: Sect.7.2.5).

Meteoric waters originating from precipitation in the distant past, named palaeo-waters (Fontes, 1981) are encountered as deep groundwater in those areas where the present-day replenishment of groundwaters is slow, predominantly in arid ones. In most cases their isotopic composition differs appreciably from that of the modern precipitation in the recharge zone. Fig.4.10 shows some examples.

The isotopic composition can also be preserved in materials related to the meteoric water cycle which are more ubiquitous than the water itself. Such materials, named *climate proxies* are:

- interstitial waters in lake sediments
- carbonates and silicates in lake sediments
- concretions in soils and stalactites
- cellulose in treerings and other plant material
- phosphates in biomass
- peat bogs.

In some of these proxies, e.g. cellulose and interstitial waters, both ^{18}O and ^{2}H variations can be measured. In other cases, only the oxygen isotopic composition is amenable to measurement.

Based on the changes in the isotopic composition of the proxies one seeks to infer the change in the meteoric waters, so as to relate these then to climate parameters such as temperature and humidity. In order to do so two palaeoclimate effects need to be considered. On the one hand, the changing isotope composition of the precipitation (the primary climate signal) and on the other hand, there is the effect of climate change on the relationship between the isotopic composition of precipitation and that of the proxy. The latter in itself is made up of two components, namely the relationship between the isotopic composition of the incident rain and the water body which imprints its isotopic signature on the proxy material (see for example the discussion of Gat and Lister, 1995 in the case of lake sediments) and further the transfer from the relevant water body (be it lakewater, soilwater or groundwater, etc.) to the proxy material.

As discussed in section 3.5.2., the transfer of precipitation into the terrestrial aquatic systems is neither complete nor indiscriminate. As rain falls on the land surface it is partitioned into fluxes of surface runoff, infiltration into the ground and a return flux to the atmosphere by means of evaporation and transpiration. The isotopic composition is modified as a result of these processes, both due to the isotope fractionation which accompanies evaporative processes near the surface and also due to the selective utilisation of rainfall with different isotope composition in these different pathways. Obviously this shift in the isotope composition which accompanies the recharge – runoff processes, which were named the Isotope Transfer Function (ITF) (Gat,1998) depend on and change with changes of the ambient conditions. These shifts are especially significant under two extreme environmental situations; namely on the one hand in lake and wetland country and, on the other hand , in an arid environment. The common denominator of these two regions is the prominent role of surface waters in their hydrological cycle.

The safest way to asses the changing isotope values in precipitation during past period appears to be through the medium of global circulation models; estimates of the possible changes in the ITF and the transfer into proxy material must depend on a in-depth understanding of the processes concerned,

Summarising, there are two palaeoclimate effects that need to be considered. On the one hand, there is the effect of the changing system on the relationship between the isotopic composition of precipitation and that of the proxy, on the other hand the changing isotopic composition of the precipitation (the primary climate signal).

As far as the latter is concerned, the most probable relation between $^{18}\delta$ (or $^{2}\delta$) of precipitation in the region and average temperature at the time of precipitation is similar to the present-day latitudinal temperature dependence at that specific temperature (Sect.4.1). For the ice cores in polar regions the effect of temperature may be larger than +0.5 to +0.7‰/°C as in non-arctic regions.

5 TRITIUM IN THE ATMOSPHERE

5.1 CHARACTERISTICS OF TRITIUM

The radioactive isotope of hydrogen of mass 3 (^{3}H, or *tritium*) has a half-life of about 12 years and thus a lifetime commensurate with many hydrological processes (more details are given in Volume I). By and large, ^{3}H is introduced into the hydrological cycle in the atmosphere, where it is produced naturally by the interaction of cosmic radiation with atmospheric components. The major reaction involved is that of thermal neutrons with nitrogen

$$^{14}N(n,^3H)^{12}C \qquad (5.1)$$

High-energy spallation reactions and direct accretion of ^{3}H from the solar wind are believed to be of less importance (Nir et al., 1966).

As from the early 1950s anthropogenic sources, especially from nuclear tests in the atmosphere, overshadowed the natural production for more than a decade, as will be discussed.

In groundwater-hydrology and oceanography ^{3}H concentrations are generally given as TU (Tritium Unit), equivalent to a concentration of 10^{-18}. Other disciplines may use the specific radioactivity in Bq (Bequerel) or mBq, related to TU by:

$$1\,TU \equiv 0.118\ Bq/L \text{ of water } (\equiv 3.19\ pCi/L)$$

or: $$1\ Bq/L \equiv 8.47\ TU$$

The most up-to-date value for the half-life is 12.32 year (Lucas and Unterweger, 2000).

Fig.5.1 shows the ^{3}H concentration in monthly precipitation at Vienna (data from the GNIP network). Data from the Ottawa station show that the ^{3}H increase started already during the 1950ies.

From known-age wine samples Begemann (1959) and, independently, Roether (1967) estimated that the natural ^{3}H content of rain before the nuclear test series in the 1950s began was about 5 TU in central Europe. The average natural production rate was estimated to be about 0.20 ^{3}H atoms/cm^{2}sec. The production of ^{3}H takes place preferentially in the upper troposphere and lower stratosphere. It is introduced into the hydrologic cycle following oxidation to tritiated waters (^{3}H^{1}HO), seasonally leaking down into the troposphere mainly through the tropopause discontinuity at mid-latitudes.

At the peak ^{3}H concentration during spring 1963 the ^{3}H content of precipitation at the northern hemisphere was about 5000 TU (Fig.5.1). Considering the rough estimate of the amount of water in the troposphere of about 2×10^{16} kg ($\approx$ 4 g/cm^2), the total ^{3}H inventory in the northern troposphere was then in the order of 10 kg or roughly 3 kmole. This is to be compared with an estimated amount of simultaneously present ^{14}C of about 50 kmole (Chapter 6). The cross section for the nuclear reaction, however, is more than a few hundred times smaller than that for ^{14}C production (Libby, 1965). The conclusion then must be that the bomb-derived ^{3}H largely originated from a direct release of ^{3}H from the bombs, rather than by the nuclear reaction by neutrons released during the explosions. Mason et al. (1982) established that the direct ^{3}H injection in the atmosphere by fusion bombs is about 1.5 kg per megaton of explosive force.

The pattern shown in Fig.5.1 is repeated at most northern hemisphere stations, albeit with slightly varying amplitudes and phase shifts. The notable feature of this curve is a yearly cycle of maximum concentrations in spring and summer and a winter minimum, with typical concentration ratios of 2.5 to 6 between maximum and minimum values. The annual cycle is superimposed upon the long-term changes which have ranged over three orders of magnitude since 1952.

There is a marked latitude dependence: concentrations are highest north of the 30th parallel, with values lower by a factor of 5 or so at low-latitude and tropical stations. In the southern hemisphere (represented by Pretoria) the yearly cycle is displaced with the season by half a year, and the mean ^{3}H levels in atmospheric waters are lower than at comparable north-latitude stations. This is a reflection of the predominant northern location of weapon testing sites and the slow inter-hemispheric transport of tracers. Consequently, in the southern hemisphere the increase has been a factor of 10 to 100 smaller (Fig.5.1), because of the equatorial barrier in the global air mass circulation and the fact that the annual ^{3}H injected during spring from the stratosphere into the troposphere is removed from the latter very efficiently within weeks.

5.2 GEOPHYSICAL ASPECTS

Tritium concentrations and inventories, like that of other atmospheric components of stratospheric origin, are dominated by the timing, location and intensity of exchange of tropospheric and stratospheric air masses, as well as, of course, the ^{3}H concentration in the stratosphere at the time that such an exchange takes place. Exchange occurs predominantly during late winter and in spring (the so-called spring leak of the tropopause) in the region of baroclinic zones and tropopause discontinuities of the mid-latitudes (Newell, 1963).

The changing ^{3}H inventory of the stratosphere of recent years reflects the massive injections by weapon tests in 1954, 1955, 1958 and again during 1961-1962, mostly in the northern hemisphere, reaching high altitudes in the stratosphere.

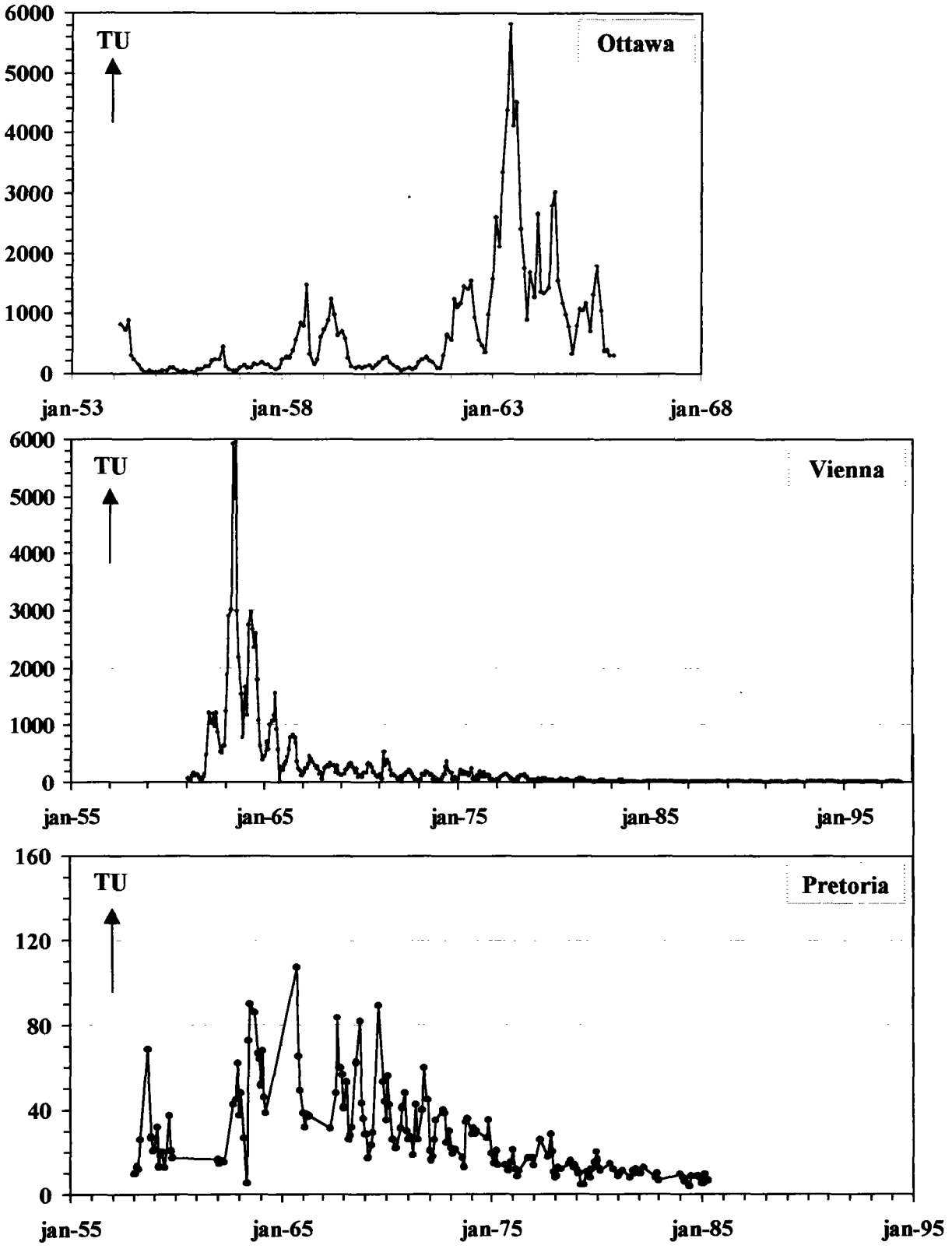

Fig.5.1 ^{3}H in monthly precipitation samples of stations representative for the northern (Ottawa, Vienna) and the southern hemisphere (Pretoria) (data from the GNIP network) (data valid for the year of sample collection).

At any time, the inventory decreases by 5.5% per year through radioactive decay and some of the ^3H leaks into the troposphere from where it is lost into the ocean or groundwater, both of which can be considered a sink for the stratospheric ^3H. Estimated residence times of tritiated water vapour in the lower stratosphere are of the order of a few years. Inter-hemispheric mixing in the stratosphere seems to occur on a similar time scale.

The residence time of water in the lower troposphere, on the other hand, is of the order of 5 to 20 days. This is a short period relative to large-scale north-to-south mixing in the troposphere, but within the time scale of horizontal atmospheric motions. As a result ^3H is deposited onto the surface of the earth within the latitude band of its penetration from the stratosphere or more precisely of its distribution on top of the so-called moist layer, which extends to 500mbar approximately (Eriksson, 1966).

From measurements on atmospheric vapour by Ehhalt (1971) it appears that above the 2-km level the ^3H content is uniform over both land and sea, along each latitude band. Over the continents during summer, there is an increase in ^3H amount in the lowest 2 km, apparently due to re-evaporation of part of the winter and spring precipitation. In contrast, ^3H levels are low over the sea throughout the year, as a result of the uptake of ^3H by molecular exchange into the oceans. Moisture evaporated from the ocean is consequently low in ^3H content due to the long residence time of water in the ocean. The delay in the appearance of the annual ^3H peak in precipitation relative to the time of its injection (June vs. the late winter months) is attributed by Ehhalt to this re-evaporation of moisture from the continents, which provides an additional source of ^3H to the atmosphere during summer.

^3H build-up over the continent comes about as a result of the cutting off of the supply of low activity oceanic vapour, while influx from aloft continues. The inland gradient could be expected to be highest during late winter, spring and summer when the downward flux is at its peak value. This effect is, however, somewhat balanced by the lower content of vapour in the winter atmosphere.

As stated, re-evaporation of moisture from the continent during summer acts to extend the spring maximum of ^3H concentrations into the summer, but does not affect the inland build-up of ^3H content (expressed in ^3H units) except when there is a hold-up (delay) of water, so that the re-evaporated moisture has a noticeably different ^3H age than the atmospheric moisture. Ages of a few years are quite typical for soil moisture or for waters in sizeable inland lakes. During periods of rising ^3H levels, such as the decade of 1952-1963, the continental water reservoirs were relatively low in ^3H content and their evaporation reduced the continental gradient. During years with declining atmospheric ^3H levels, the continental reservoirs may retain the memory of high ^3H levels of the past and reverse the normal ^3H flux, contributing ^3H to the atmosphere. In this case the inland ^3H gradient is increased.

Build-up of ^3H concentrations over continents is quite gradual. For example, TU levels double over Central Europe over a distance of 1000 km. The interaction over the ocean, on the other hand, becomes effective over very short distances, especially when the continental air is very

unsaturated relative to ocean surface waters. An extreme case is found in the Mediterranean Sea, where the intense sea-air interaction is mirrored in the extreme drop in ^3H activity, to 10% of the continental value. The inland gradient on the Eastern Mediterranean shore also is more abrupt than usual, the TU doubling length being about 100 km (Gat and Carmi, 1970) due to the limited extent and intra-continental position of the Mediterranean Sea.

Precipitation is the main mechanism for removing ^3H from the atmosphere over the continent. Moreover it is the vehicle for the downward transport of ^3H within the troposphere. As a result of the rapid exchange of isotopes between the rain droplets and ambient vapour, the falling rain drops contribute ^3H to the lower troposphere during the period where strong vertical ^3H gradients exist. Indeed, Ehhalt (1971) has noticed an additional source of ^3H in the lower atmosphere, at a height just below the freezing level. Only the frozen phases, i.e. hail and snow, are not subject to this exchange and can carry the high ^3H levels all the way to the ground.

On a global average, however, the molecular exchange of water between the air and the ocean needs to be added to loss of ^3H by precipitation. This exchange appears to increase the rate of ^3H loss by a factor of up to 1.9 (Lipps and Helmer, 1992).

The atmospheric moisture system has been treated as a box model by Bolin (1958) and Eriksson (1967). In these models ^3H is added from aloft (F_T); loss occurs through rainout and exchange with the ^3H deficient surface waters over the ocean while over land the loss is to the groundwater systems or through runoff. The soil, which returns most of the precipitated ^3H through evapotranspiration acts as a buffer which maintains high continental ^3H levels.

Fig.5.2A shows the ^3H budget of the atmosphere in a box model representation. a, a' and b are the water content in continental and marine atmosphere and in the soil column, respectively. S_a, $S_{a'}$, S_b, S_0 = ^3H content of these reservoirs and of the oceanic surface layers, respectively (in TU); S_b*, the ^3H content of recharging waters, may differ from S_b because of hold-up of water in the soil column. F_T = ^3H influx from aloft (in moles/s). P_c, P_m, E, E_T, R_s, R_G and X = the precipitation amounts (continental and marine), evaporation and evapotranspiration fluxes, surface and groundwater runoff and the molecular exchange flux between ocean and atmosphere, respectively.

Fig.5.2B is a schematic picture of deposition of ^3H and concentration of ^3H in precipitation in a westerly zonal air current (Eriksson, 1967). The length of the arrows is proportional to the rate of vertical transports. The dashed line indicates the smoothing in the concentrations which will take place due to longitudinal eddy mixing.

During recent years, the atmospheric reservoir has been practically exhausted of the ^3H introduced by the nuclear tests so that the atmospheric ^3H levels have almost returned to the pre-1952 levels, except for some local anthropogenic releases of ^3H from the nuclear industry and other uses of tritiated materials.

In the next sections we will discuss some points of special hydrological interest in the ^3H curves.

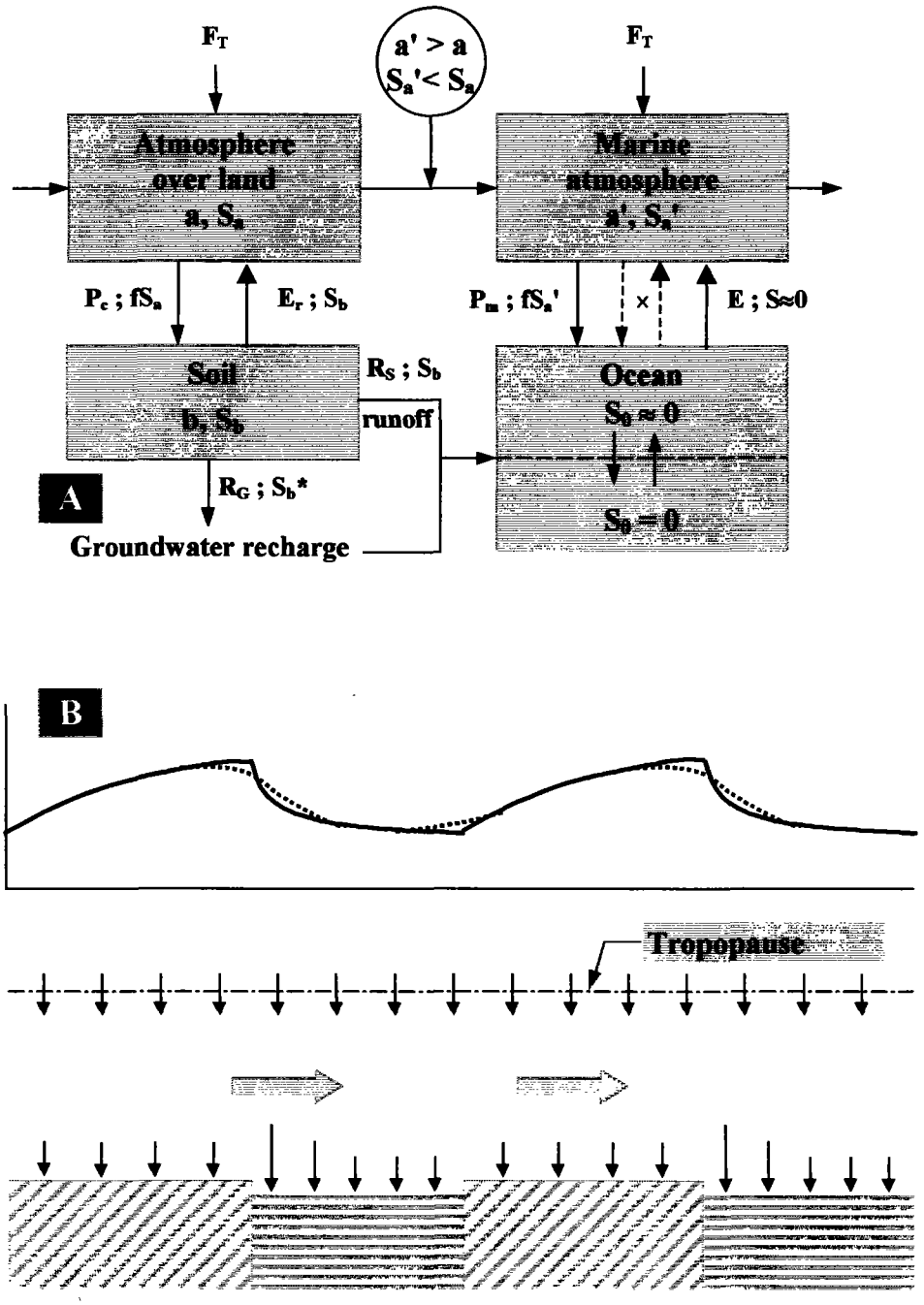

Fig.5.2 **A.** ^3H budget in the atmosphere in box model representation (after Bolin, 1958 and Begeman, 1960); a, a' and b are the water content in continental, marine and soil layer; s values refer to the respective ^3H contents; F_T is the ^3H influx from aloft.

B. schematic presentation of the concentration of ^3H and its deposition on land or sea in a westerly air current (Eriksson, 1967).

5.3 HYDROLOGICAL ASPECTS

For the hydrologist it is of interest to be able to judge ^3H concentrations in the underground, in order to have an first impression of the hydrological situation, and of the necessity and specific conditions of sample collection. Since the ^3H content of precipitation has decreased almost to their natural level, part of the applications exploited during the 1960ies and 1970ies are no longer possible. Nevertheless, excess ^3H is still present in the ground and in surface waters. Therefore, knowledge of possible variations is still relevant.

In the next sections we will give a broad survey of ^3H variations in precipitation.

5.3.1 LONG-TERM RECOVERY OF NATURAL ^3H LEVELS

There are two reasons why ^3H in precipitation has returned quickly to its natural level, at least in comparison with ^{14}C in atmospheric CO_2:

1) ^3H has a relatively short half-life (12.32 years; Lucas and Unterweger, 2000). This means that by decay alone the peak concentration from 1963 would become reduced by a factor of $2^{10} \approx 1000$ in a period of about 120 years (= 10 half-lives) provided no further nuclear tests in the atmosphere are made. In the period of three half-lives since 1963 the peak concentration has been reduced by a factor of 8. Fig.5.3 shows the data for Vienna and Pretoria from Fig.5.1 when corrected for radioactive decay.

2) The atmospheric water circulation through ocean-air exchange is very vigorous. The water in the troposphere is replaced about every 10 days. Therefore, bomb ^3H is rapidly transported to the ocean, even though ^{14}C is not (Sect.6.4). On the other hand, most of the ^3H produced by fusion bombs entered the stratosphere, from which it has only gradually been leaking back to the troposphere, so that ^3H stayed in the atmosphere for a longer time.

Because of the short turn-over time of atmospheric water and not much ^3H is left in the stratosphere, the tropospheric ^3H concentration has decreased to the relatively stable original level. It is only since the seventies, following a long period of limited nuclear test activity, that the northern and southern hemisphere ^3H concentrations are becoming comparable.

5.3.2 SEASONAL VARIATIONS IN ^3H

The seasonality of the stratosphere-to-troposphere transport results in the marked seasonal cycle in the ^3H content of precipitation (Fig.5.1), opposite in phase between the northern and southern hemisphere.

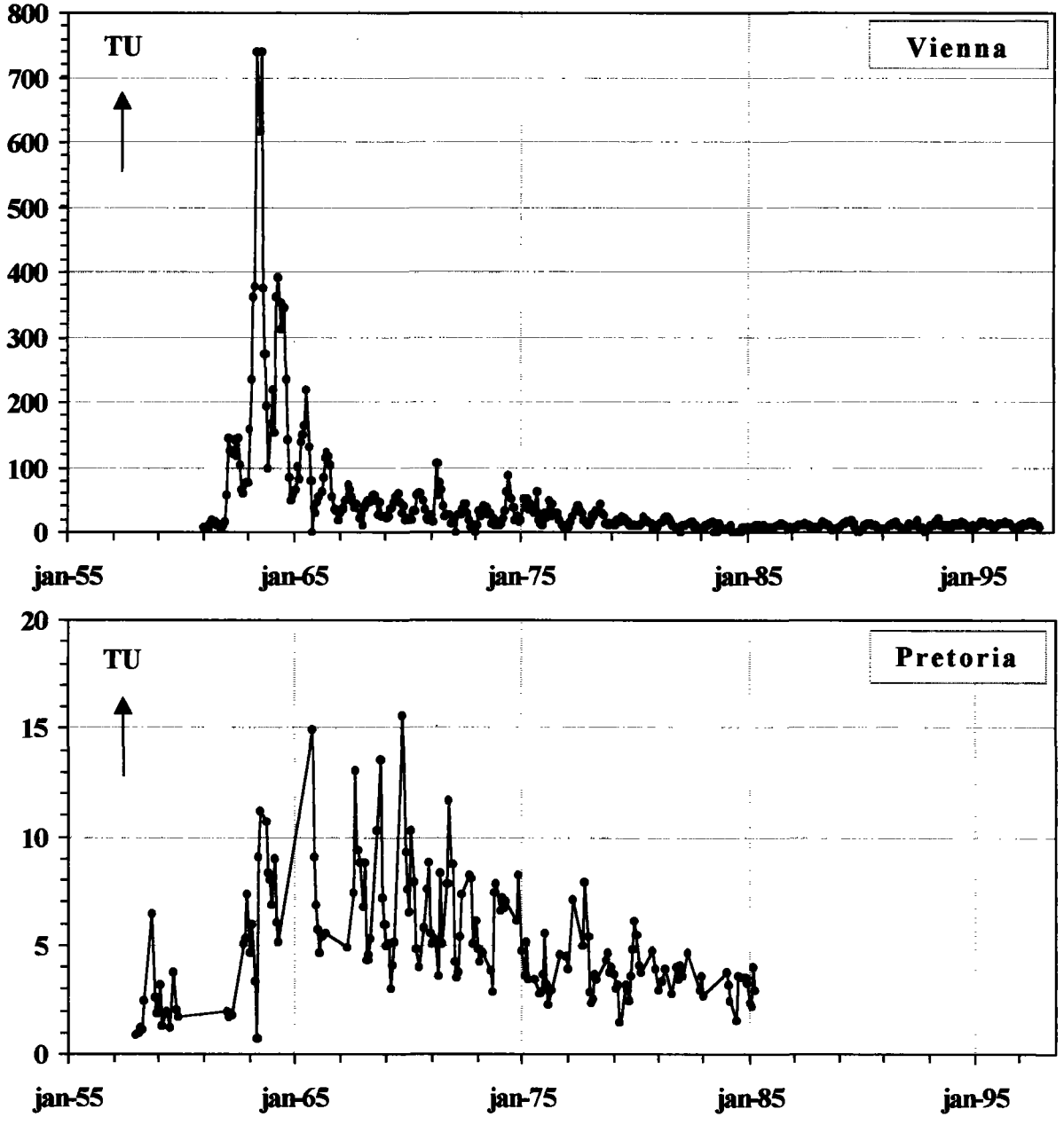

Fig.5.3 ^{3}H in precipitation at Vienna (representing the northern hemisphere) and Pretoria (representing the southern hemisphere), corrected for radioactive decay during the period between the moment of sampling and the year 2000 (original data from Fig.5.1).

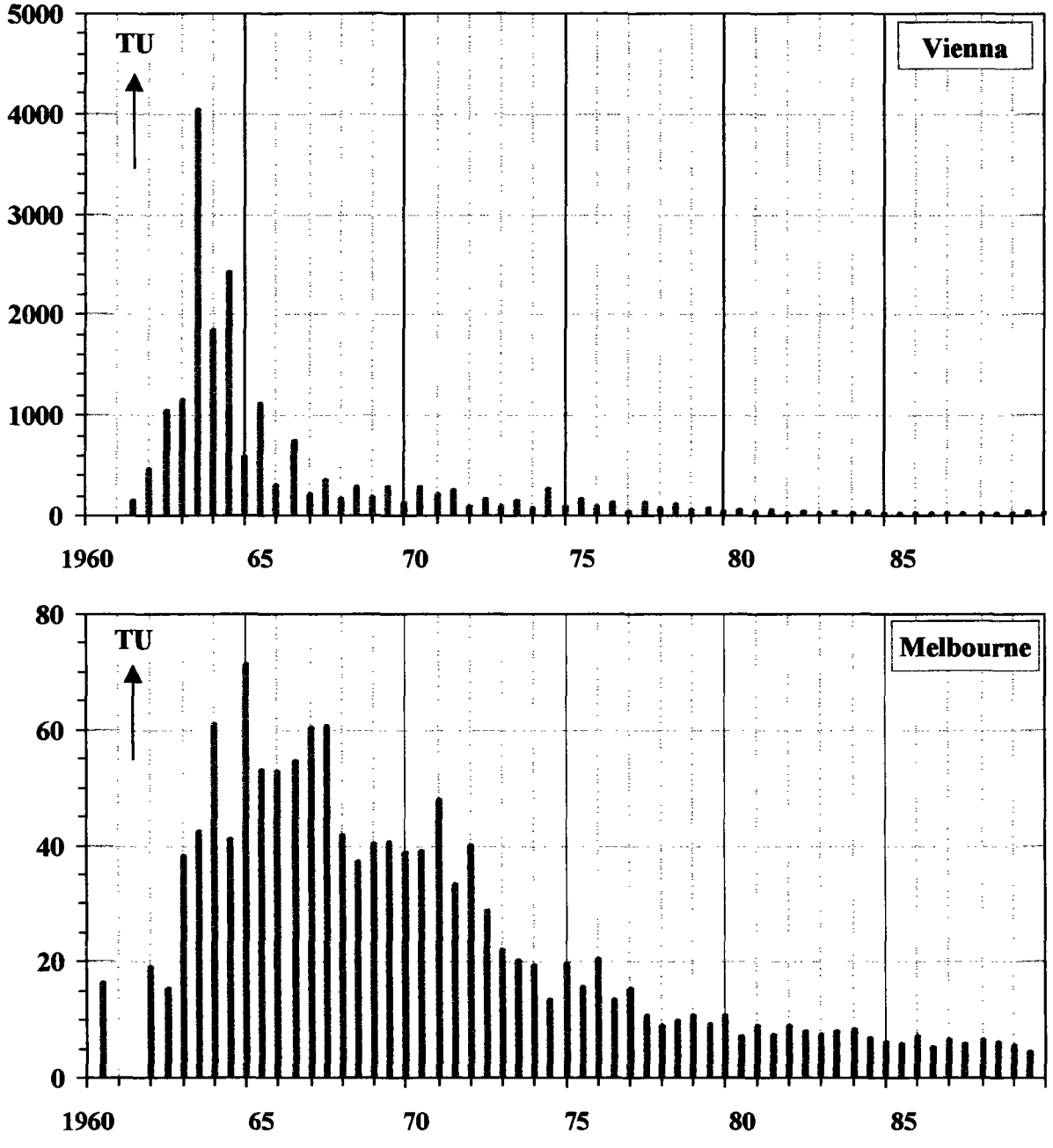

Fig.5.4 ^{3}H values for "winter" (October-March) and "summer" (April-September, between scale divisions) precipitation in Vienna, representing the northern hemisphere and similar values for Melbourne at the southern hemisphere. The seasonal cycle for the latter series is less pronounced (weighted averages from the GNIP network). In the southern hemisphere the ^{3}H (and ^{14}C) maxima have a phase shift of half a year, because the leak between stratosphere and troposphere occurs in early spring. Fig.5.5 shows an example of the absence of high "summer" values in the unsaturated zone in a dune area in NW Europe, meaning that here the "summer" rain did not reach the groundwater table (see also: Volume IV, Sect.5.1.4.2) (data valid for the year of sample collection).

Fig.5.4 contains two graphs of separate "winter" and "summer" ^3H patterns, one containing the weighted means for the months October-March, taken as representative for winter, April-September for the summer months at the northern hemisphere, whereas similar data of Melbourne represent the southern hemisphere. This phenomenon is caused by temporary mixing between the stratosphere and troposphere at high latitudes in early spring, so that ^3H, originally injected into the stratosphere by nuclear explosions, can return to the troposphere.

For hydrologists this is a very important aspect of the temporary elevated ^3H levels about 30 years ago. The reason is that the infiltration of precipitation is not a phenomenon distributed evenly over the year. Generally groundwater recharge occurs after heavy rainfall and without significant (evapo)transpiration of the vegetation. In moderate climates infiltration is therefore limited to the "winter-period" with relatively low ^3H values (see later Fig.5.5). This point is illustrated in Fig.5.5 where a ^3H profile in a sandy dune area with presumably vertical infiltration is compared with ^3H in winter precipitation (October-March). Because for this region no ^3H data are known for the early 1960ies, we have used for comparison the data from Vienna and Ottawa which are comparable for the later overlapping period. A degree of dispersion has been allowed for equivalent to a running average of the ^3H data of 5 consecutive years. Obviously the summer precipitation does not significantly infiltrate.

5.3.3 GEOGRAPHICAL VARIATIONS IN ^3H

In Figs.5.1 and 5.4 we have compared the ^3H content of precipitation at different stations. As we have seen, the most striking point is that the very high ^3H levels are confined to the northern hemisphere: in the southern hemisphere, the ^3H content increased by a factor of hardly more than 10 above the pre-bomb levels. The variations at stations in the N. hemisphere show generally the same pattern. However, the ^3H concentrations themselves may be quite different from one station to another.

By an effect similar to the continental effect and the (small) seasonal effect for ^{18}O and ^2H, low ^3H values are found near the ocean. A large fraction of the local water vapour, and thus of the precipitation, consists of oceanic vapour which is low in ^3H. The highest values apply to samples from the North Atlantic Ocean (Östlund and Fine, 1979; Weiss et al., 1979).

5.3.4 SMALL-SCALE ^3H VARIATIONS

Local variations are likely to be small, because the ^3H content in rain is not influenced by temperature variations (as are ^{18}O and ^2H). Although also ^3H is fractionated during evaporation and condensation processes -at twice the extent as ^2H (Bolin, 1958)-, the variations involved are in the order of 16% (twice 80‰), equivalent to just one year of radioactive decay. Therefore, they can not be clearly distinguished in hydrological realities and are thus neglected.

Under normal conditions we would not expect significant variations in the ^3H content of the vapour within one air mass.

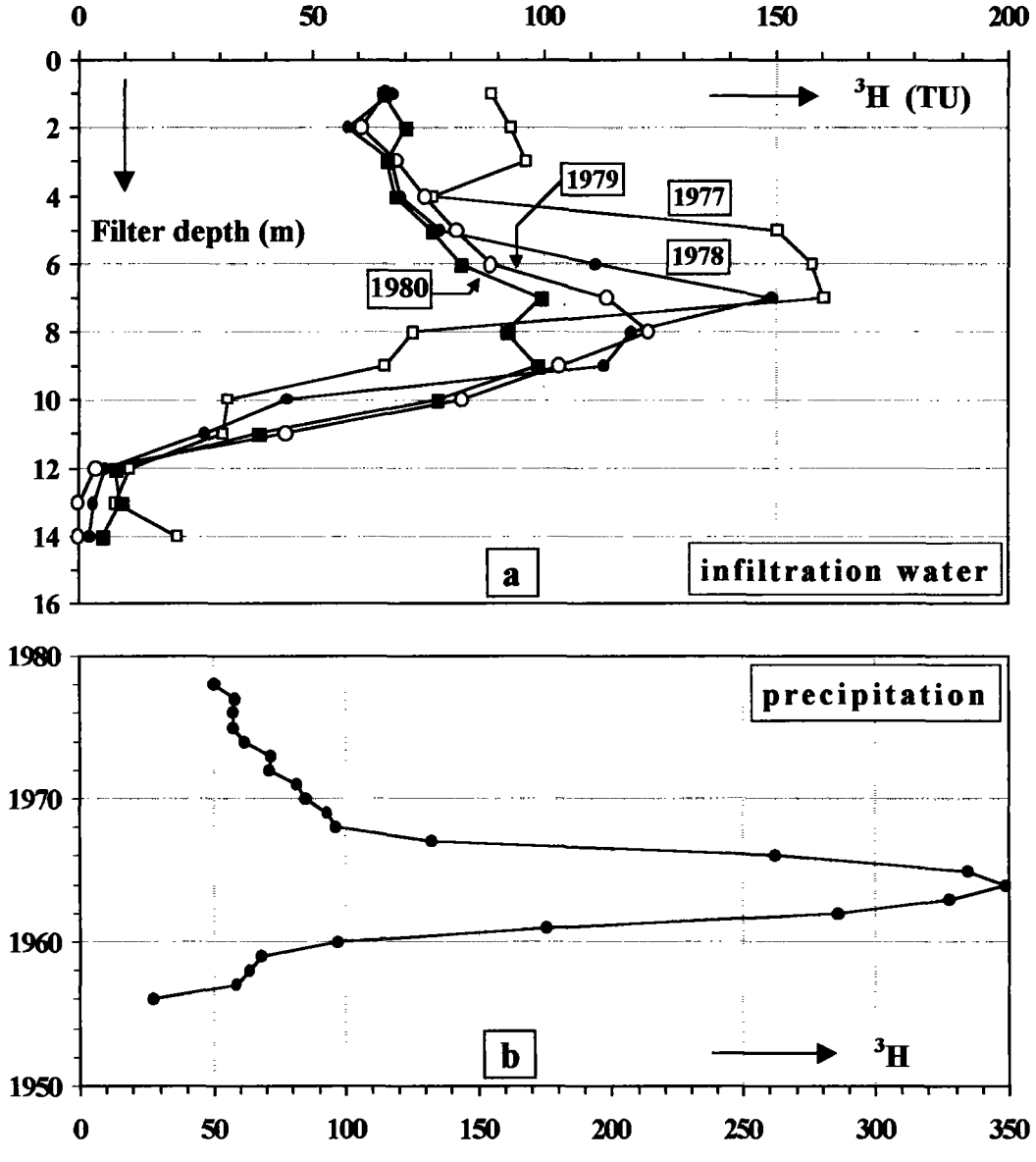

Fig.5.5 **a)** ^3H profile of infiltrated water in a dune area in NW Europe (Monster, the Netherlands). The high ^3H level of 1963 did not reach the groundwater (all data corrected for radioactive decay till 1980);

b) ^3H in precipitation at Vienna/Ottawa, reasonably representative for precipitation in the study area. The values refer to winter precipitation (October-March); a dispersion has been introduced equivalent to 5 years moving average (all data valid for 1980).

5.3.4.1 SMALL-SCALE SPATIAL ^{3}H VARIATIONS

From a series of ^{3}H data of monthly precipitation from 15 stations within the small country of the Netherlands (about 30 000 km^2) we concluded that between the stations there are no significant regular differences in seasonal effect. Existing differences over this region are irregular and small. Averaged over the year, however, a small continental effect is apparent.

Another example over a longer period is presented by four stations within 50 km around Vienna. The seasonal variations are parallel and the yearly averages are comparable. Discrepancies between the stations do not seem to be systematic.

5.3.4.2 SMALL-SCALE TEMPORAL ^{3}H VARIATIONS

Fast fluctuations in ^{3}H can be expected, if in a short period different air masses contribute to the precipitation at a site. Precipitation collected during a severe convective storm showed no significant differences within a period of 30 minutes (Groeneveld, 1977), although significant variations in ^{18}O and ^{2}H were noted. A fast change in ^{3}H might occur during the passage of another air mass, for instance correlated with a cold front. Large differences in ^{3}H content have been observed within a hurricane, resulting from complicated meteorological conditions (Östlund, 1967)

6 ISOTOPES IN ATMOSPHERIC CO_2 AND O_2

6.1 ATMOSPHERIC CO_2 CONCENTRATIONS

The concentration of CO_2 in the atmosphere is expressed as the CO_2 partial pressure P_{CO2} or as the CO_2 mixing ratio C_{CO2}, the ratio of the mole amount of CO_2 per m^3 to the mole amount of air per m^3. At present (AD 2000) the CO_2 concentration is about 370 μmole/mole (in short: ppm) (CDIAC). This level is considerably elevated compared to natural conditions, due to the massive anthropogenic CO_2 production caused by fossil fuel combustion. CO_2 mixing ratio measurements in air bubbles trapped in ice caps have shown that the pre-industrial CO_2 mixing ratio was about 275 ppm, with a natural variability of about ± 5 ppm (Etheridge et al., 1996).

The carbon contained in the atmospheric CO_2 is closely connected to the other global carbon reservoirs: the carbon dissolved in the oceans, the carbon contained in the terrestrial plants, in the soils, and finally inside the earth's crust, the so-called lithosphere. The latter reservoir is very large, but it interacts very slowly with the other compartments, and therefore, for a time scale of hundreds of years, it can be safely neglected. The coupling between the other compartments is very fast and intensive: in the course of a single year, about 25% of the atmospheric carbon get exchanged with one of the other containers. This total system of interacting carbon reservoirs is called the global carbon cycle.

The atmospheric CO_2 concentration is generally given as the *CO_2 mixing ratio*, the concentration ratio of CO_2 and air (~78% N_2 + 21% O_2 + ~1% Ar). Fig.6.1 shows the results of measurements of the atmospheric CO_2 concentration over an extended period of time, on three locations: Point Barrow (Alaska, 71°N) in the north polar region, Mauna Loa (Hawaii, 20°N) in the Central Pacific Ocean and on the South Pole. Both differences and similarities can be observed. The clearest phenomenon, observable in all three observations, is the steady increase. This is caused by the emission of CO_2 from fossil fuel combustion, and to a lesser extent from changes in land use (mainly deforestation). On a closer comparison, one can observe a weak north-south gradient in the CO_2 mixing ratio. This gradient is the result of the fact that the vast majority of the fossil fuel emission takes place in the northern hemisphere, and even though the mixing ratio of the atmosphere is very high (typically north-south mixing time is 1.5 years) this effect is not completely washed out.

The second phenomenon observed, which differs greatly between the three shown measurement series, is the seasonal cycle. In the high northern latitudes, there are massive landmasses, and plant activity is highly seasonal. In the tropical regions much less seasonality

is observed, in accordance with the lack of strong seasonal variations in plant activity. In fact, most of the still observed seasonal signal at Mauna Loa is due to atmospheric transport of the higher northern seasonal signals.

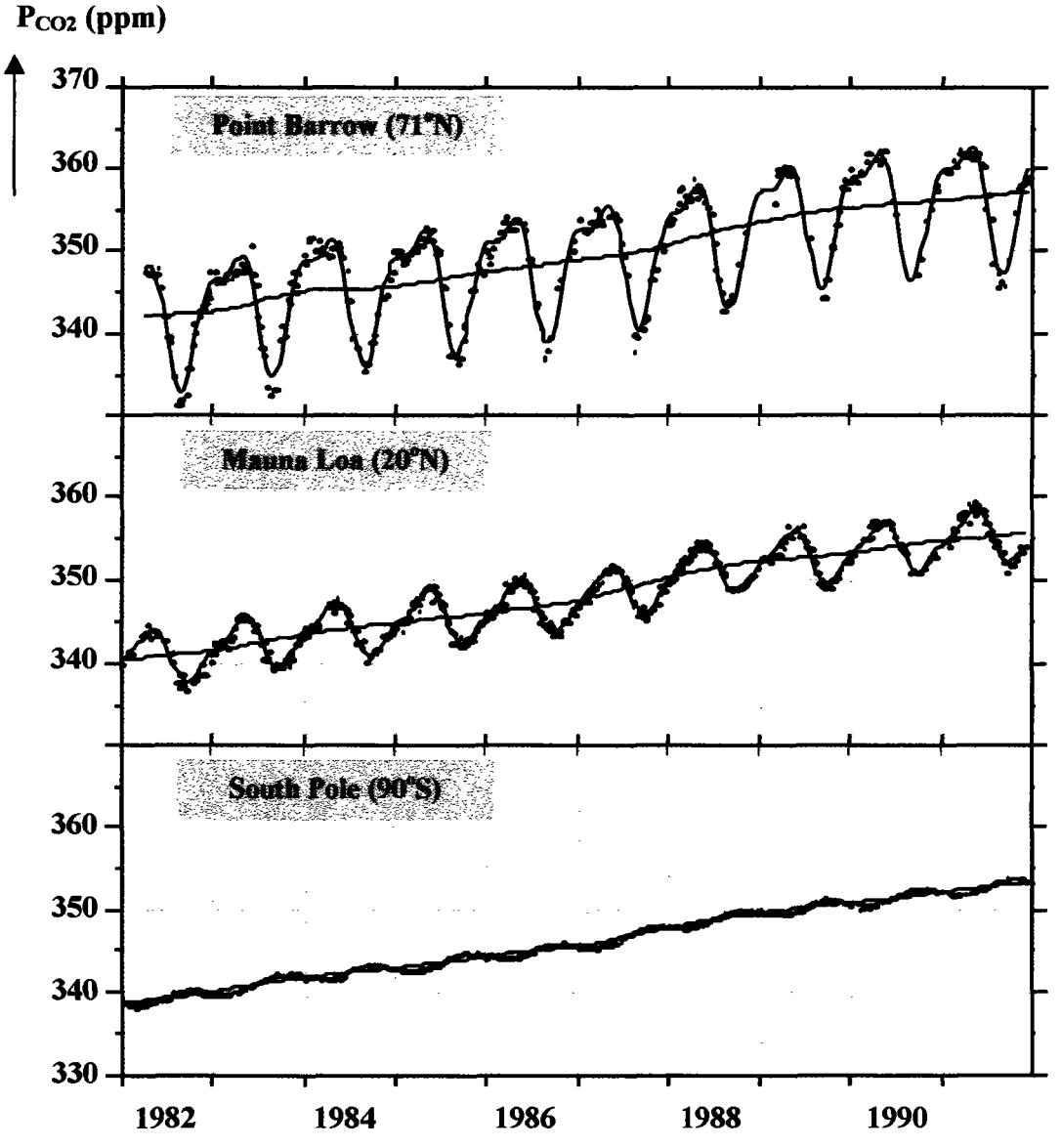

Fig.6.1 Atmospheric CO_2 concentrations (as mixing ratios) for three monitoring stations (data from Keeling et al. 1989; 1995).

In the far south, a very weak seasonal signal is observed, which is in anti-phase with the other two. This is the southern hemisphere seasonal signal, which is much weaker, since most of the higher southern hemisphere is either ocean, or without vegetation.

The global carbon cycle is enjoying still increasing attention. The human-caused increase of atmospheric CO_2 is likely to cause substantial climatic change, and this fact has become known to the general public and to policy-makers.

Scientific effort has therefore also seen a considerable growth. At present, many CO_2 monitoring stations exist world-wide (WMO), the most prominent programs among them being those of Scripps Institute of Oceanography, USA (Keeling et al., 1995, also the earliest by far (Keeling, 1958)), NOAA, USA (Conway et al., 1994), and CSIRO Australia (Francey et al., 1995). The so-called Intergovernmental Panel on Climate Change (IPCC), a group of specialised scientists, collects scientific knowledge, and periodically produces reports (for an updated list see the IPCC web site). According to the latest IPCC report (1995), the best representation of the global carbon cycle is shown in Fig.6.2. The specific anthropogenically caused fluxes are listed in Table 6.1.

Table 6.1 Annual average anthropogenic carbon budget. CO_2 sources, sinks and storage in the atmosphere are expressed in GtC (= Pg or 10^{15}g carbon) per year (values according to IPCC Report 2001).

CO_2 sources	**GtC**
(1) Emissions from fossil fuel combustion	5.4 ± 0.3
(2) Net emissions from changes in land-use	1.7 ± 0.9
Total anthropogenic emissions	**7.1 ± 1.0**
CO_2 sinks	**GtC**
(1) Remains in the atmosphere	3.3 ± 0.1
(2) Ocean uptake	1.9 ± 0.6
(3) Uptake by (North.Hemisph.) forest regrowth + Inferred sink (uptake by terrestrial biosphere)	1.9 ± 1.5
Total sink	**7.1**

The carbon content of all reservoirs and fluxes is expressed in GtC (gigatons = billion tons of carbon) or in Pg (10^{15}g) carbon. Fig.6.2 shows the "best values" for the fluxes, Table 6.1 shows the uncertainties as well. As one can see, there are still large uncertainties in the annual fluxes. The most certain aspects are the yearly emission of fossil fuel CO_2 (based on trade statistics) and the yearly increase of atmospheric CO_2 (direct measurements by the atmospheric CO_2 monitoring networks).

The most remarkable feature, as far as the anthropogenic influences are concerned, is the fact that almost half the amount of carbon introduced into the atmosphere by fossil fuel combustion is taken up by the oceans and the land plants. The exact breakdown between these two sinks, as well as the regional distribution of the sinks, is still accompanied with large uncertainties. For the study of ocean-atmosphere and terrestrial plants – atmosphere the

isotopes of CO_2 can be put to use. More recently, ultra-sensitive monitoring of the atmospheric O_2 mixing ratio can also assist in discrimination of land vs. ocean effects.

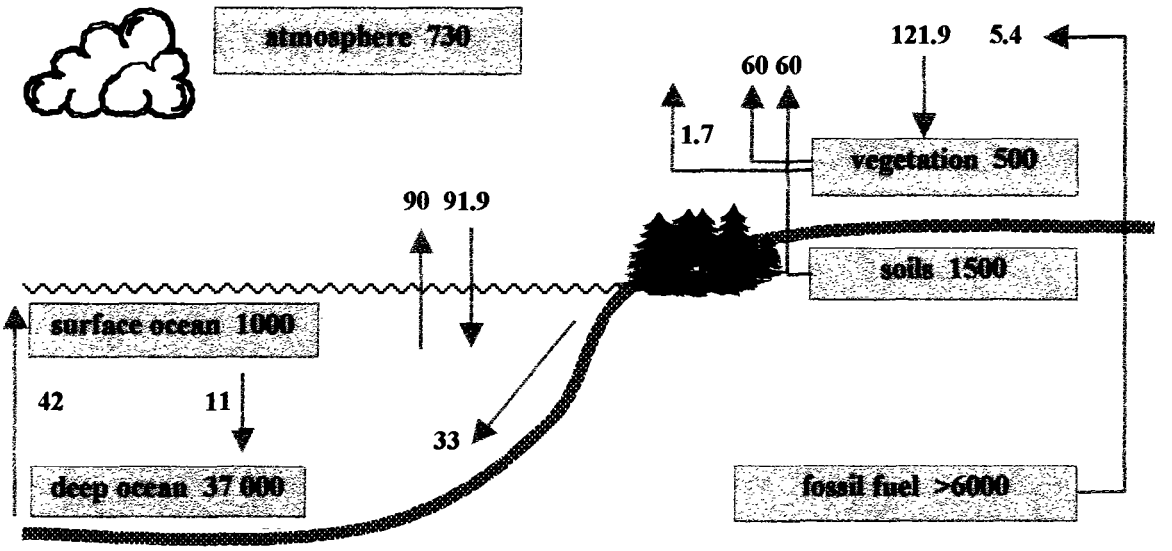

Fig.6.2 Schematic drawing of the global carbon cycle. The numbers represent reservoirs sizes and the fluxes of carbon in GtC or Pg (values according to IPCC report 2001). The CO_2 input and output data as given in this scheme result in annual increase of the atmospheric CO_2 content of 3.3 GtC.

6.2 STABLE CARBON ISOTOPES IN ATMOSPHERIC CO_2

The different $^{13}\delta$ signature of the various compounds of the global carbon cycle (see Volume 1, Sect.7.1.4) can be put to use to measure the size of the (annual) fluxes, and to discriminate between the various processes. Especially the ocean-atmosphere exchange of CO_2 can be discriminated from the terrestrial exchange, as well as from fossil fuel input. The effective fractionation for ocean uptake of CO_2 from the atmosphere is only about –2‰, whereas terrestrial photosynthesis yields a fractionation of –17‰ (for C3 plants). Table 6.2 shows average $^{13}\delta$ values for the various components of the global carbon cycle, as well as fractionations for a flux out of each component into the other ones (where appropriate) (see Volume I for more details). The potential for discrimination using $^{13}\delta$ is clear. However, due to the large size of the atmospheric carbon reservoir, even the large fluxes in Fig.6.2 will only appear in $^{13}\delta$ of atmospheric CO_2 in a very dilute way. This puts high demands on the accuracy of $^{13}\delta$ measurements of atmospheric CO_2.

Nevertheless, there is an ever-increasing number of atmospheric stations, where the CO_2 mixing ratio measurements have been supplemented by $^{13}\delta$ analyses. Fig.6.3 shows the $^{13}\delta$ measurements over the years for the same stations as in Fig.6.1.

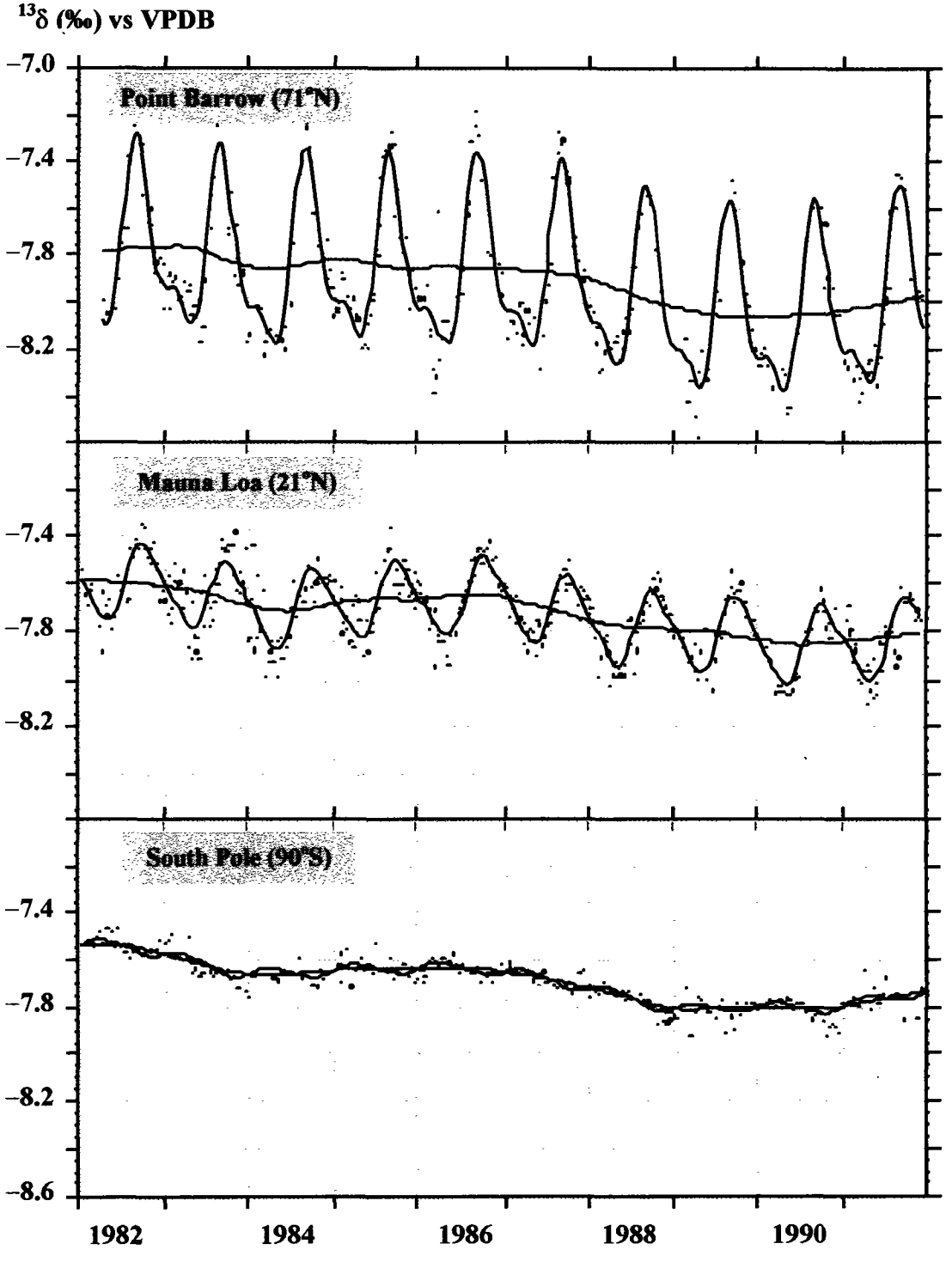

Fig.6.3 The $^{13}\delta$ results for the same CO_2 samples as reported in Fig.6.1.

Table 6.2 An overview of the main global carbon cycle components from a $^{13}\delta$ perspective. The grey boxes contain the average $^{13}\delta$ values (in ‰) for the various components, the off-diagonal elements give values for the ^{13}C fractionation (‰) for a flux from the component in the left column into the other ones (where appropriate). The values are indicative (cf. Volume I).

	(1)	(2)	(3)	(4)	(5)	(6)
(1) Atmosphere	**–8**	–2	-	–17	-	-
(2) Surface Ocean (DIC)	–10	**+1.5**	0	-	-	-
(3) Deep Ocean	-	0	**+1**	-	-	-
(4) Land plants (C3)	0	-	-	**–25**	< 0	-
(5) Soils	–2 ± 2	-	-	-	**–25**	-
(6) Fossil Fuel	0	-	-	-	-	**–28**

As a first example we shall take a closer look at the $P_{CO2} - {}^{13}\delta$ relation in the seasonal cycles. To this end we shall, for the moment, "force" steady state conditions over the years by separating the (average) seasonal cycle and the increasing trend from the CO_2 and $^{13}\delta$ records. We can now describe the relation between the observed P_{CO2} and $^{13}\delta$ by two compound mixing (see Volume I, Sect. 4.3 and 7.1):

$$C_T\delta_T = C_{Bk}\delta_{Bk} + C_{add}\delta_{add} \qquad (6.1)$$

in which C_T, C_{Bk} and C_{add} are the amount of CO_2 (usually expressed as mixing ratios) in total, the background air, and the added, respectively, and the δ's their respective $^{13}\delta$ values. Since of course:

$$C_T = C_{Bk} + C_{add} \qquad (6.2)$$

we can easily deduce:

$$\delta_T = \delta_{add} + \frac{1}{C_T}\left[C_{Bk}(\delta_{Bk} - \delta_{Add})\right] \qquad (6.3)$$

This way of presenting two-component mixing is called a "Keeling plot" (after C.D. Keeling, 1958). It is widely used in atmospheric research: the quality of the linear fit shows whether the two-component approximation is valid, and if so, the intercept of the fit directly yields the $^{13}\delta$ value of the "added" compound.

Fig.6.4 shows such a Keeling plot, for three different years, for the Point Barrow $^{13}\delta$ record. To this end, the record shown in Fig.6.3 has been carefully detrended first. The results for

δ_{add}, shown in the figure, confirm that the seasonal cycle at Point Barrow is caused by plant activity.

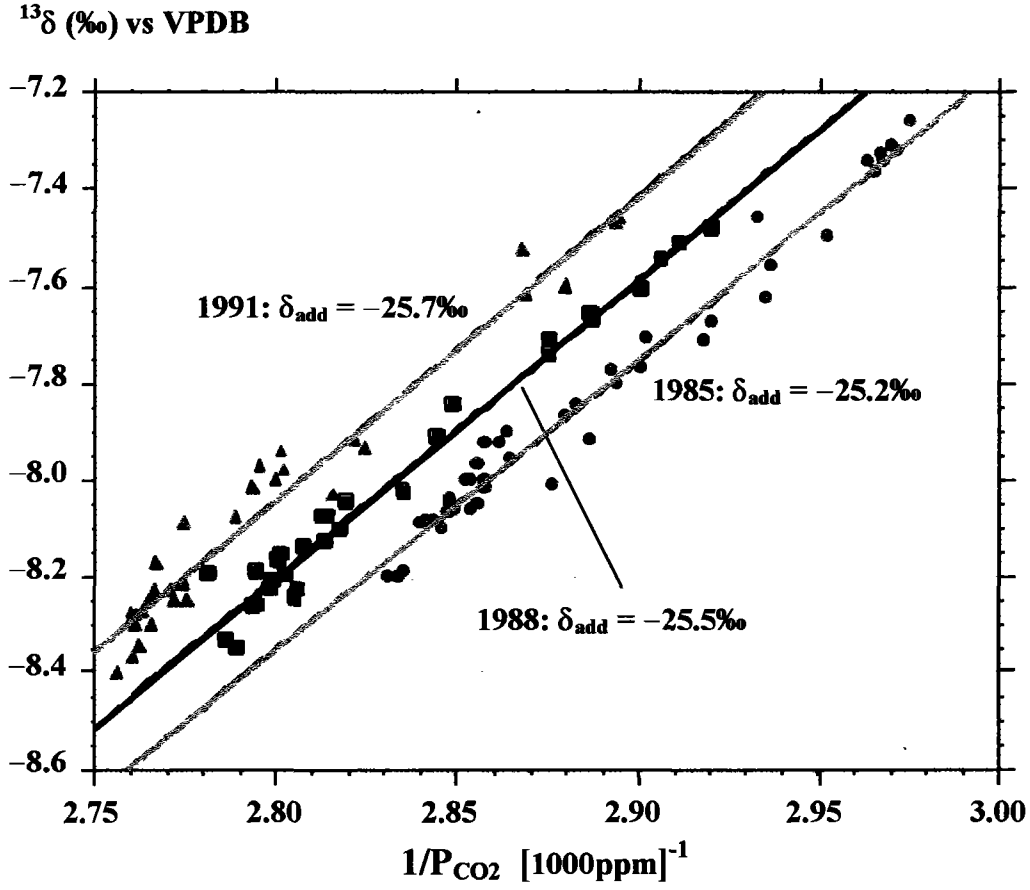

Fig.6.4 The Keeling plot for three years from the Point Barrow records (Figs.6.1 and 6.3). The results for δ_{add}, shown confirm that the seasonal cycle at Point Barrow is caused by plant activity. The differences between the years are not significant.

The relation between the trends in the P_{CO2} and $^{13}\delta$ as observed is not straightforward. The increasing trend in P_{CO2} and the decreasing trend in $^{13}\delta$ are qualitatively consistent with the continuous addition of fossil fuel-derived CO_2 with their lower $^{13}\delta$ values (Table 6.2). However, an attempt to describe their relation as two-compound mixing would produce an unrealistic source $^{13}\delta$ of about −14‰ (as well as a bad fit quality). The reason that this number is so far off the real $^{13}\delta$ values for fossil fuels is that isotopic exchange between the atmospheric CO_2 and that of the ocean tends to wash out the original signature of the fossil fuel CO_2 to a large extent. The terrestrial biosphere does not show this behaviour, because the carbon reservoir is not mixed as in the ocean: most of the CO_2 taken up in the growing season returns into the atmosphere later in the year, with identical $^{13}\delta$.

Evidently this effect of smeared-out signature does not make the atmospheric CO_2 measurements useless; on the contrary, since the $^{13}\delta$ signature of the input fossil fuel CO_2 is relatively well-known, the relation between the long-year trend in $^{13}\delta$ and P_{CO2} is a valuable measure for both the partition of uptake over the oceans and the terrestrial biosphere, as well as for the CO_2 fluxes going in and out of the ocean annually (Keeling et al., 1989; Tans et al., 1990; Ciais et al., 1995).

A summary of the concentration and $^{13}\delta$ data, together with the current annual changes –both valid for 01/01/1990 is given in Table 6.3. The P_{CO2} and $^{13}\delta$ trends are described by:

$$P_{CO2} = C + (\text{year} - 1990)\Delta C$$

$$^{13}\delta = D + (\text{year} - 1990)\Delta D$$

or

$$^{13}\delta = D + (\text{year} - 1990)\Delta D/\Delta C$$

Table 6.3 only shows the trend data; the actual P_{CO2} and $^{13}\delta$ values during a year of course have to include the seasonal variation as well (cf. Roeloffzen et al., 1991).

Table 6.3 Concentrations and carbon isotopic compositions of atmospheric CO_2 and annual changes therein for three stations, more or less representing the high and medium latitudes of the northern hemisphere and the southern hemisphere (P_{CO2} data from C.D.Keeling, Scripps Inst. of Oceanography, La Jolla, Cal.; isotopic data from the Centre for Isotope Research of Groningen Univ., the Netherlands).

Valid for 01/01/1990	C (ppm)	ΔC (ppm/year)	D (‰)	ΔD (‰/year)	ΔD/ΔC (‰/ppm)
Point Barrow	350	1.75	–7.9	–0.035	–0.012
Mauna Loa	348	1.59	–7.7	–0.021	–0.013
South Pole	346	1.49	–7.7	–0.024	–0.016

6.3 STABLE OXYGEN ISOTOPES IN ATMOSPHERIC CO_2

The situation for the $^{18}\delta$ signature of atmospheric CO_2 is remarkably different from $^{13}\delta$. This difference is caused by the oxygen isotopic exchange that can occur between CO_2 and (liquid) water through the carbonic acid formation (see Volume I, Sect. 7.2.2 and 10.2.1). This effect causes $^{18}\delta$ of atmospheric CO_2 to be dominated by the $^{18}\delta$ signature of both ocean water and precipitation.

An increasing number of networks of atmospheric stations also analyses $^{18}\delta$ of atmospheric CO_2 routinely. In fact, a mass spectrometric $^{13}\delta$ analysis of CO_2 yields a $^{18}\delta$ result as well.

Still, $^{18}\delta$ causes additional experimental problems (in precision of measurement and calibration), due to the risk of CO_2–H_2O isotopic exchange that may occur anywhere in the sample treatment from the moment of sampling until the input of the sample in the mass spectrometer.

Fig.6.5 shows, for the same three stations as before, the $^{18}\delta$ signals. The most striking feature is the huge north-south gradient (cf. Fig.6.3). If one considers the intense mixing of the atmosphere, one has to conclude that there must be huge sources/sinks for the oxygen isotopes, or rather that the CO_2-H_2O isotopic exchange capacity must be very large to be able to counteract the atmospheric mixture to such extent.

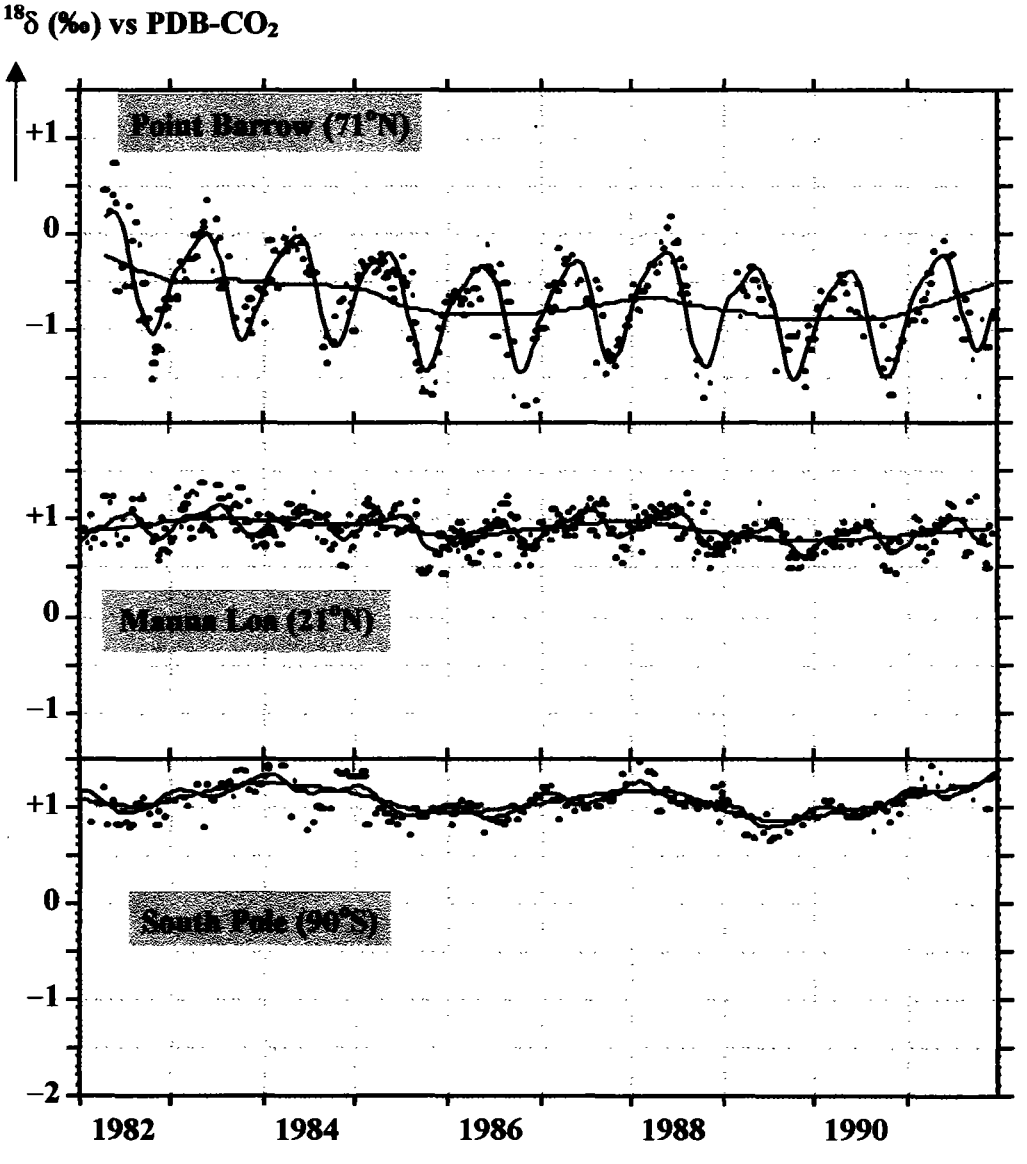

Fig.6.5 The $^{18}\delta$ results for the same set of CO_2 samples as in Figs.6.1 and 6.3.

This huge exchange capacity puzzled researchers for years, since the CO_2–H_2O isotopic exchange is a slow process (see Volume I, Sect.10.2.1). The solution to this problem is the enzyme carbonic anhydrase that is present in plants, and to a certain amount also in soils. From every 3 CO_2 molecules that enter a plant leaf through the stomata only one is taken up by photosynthesis. The two others become equilibrated with the leaf water almost instantly due to the acceleration of the equilibrium process by the carbonic anhydrase, but then return to the atmosphere without actually been taken up by the plant. This huge flux therefore only influences the $^{18}\delta$ signature of the atmospheric CO_2, and has no influence on either the CO_2 concentration or its $^{13}\delta$ value. Francey and Tans (1987) were the first to describe the influence of this effect on the atmospheric $^{18}\delta$ signal, followed some years later by Farquhar et al. (1993) with a quantitatively more correct model.

Generally, this enzyme-enhanced isotopic exchange, together with the seasonal isotopic signature of precipitation and leaf water, explain both the huge global gradient, and the strong seasonal cycle in the Northern Hemisphere (for a more thorough discussion, see: Ciais and Meijer, 1998).

The $^{18}\delta$ signal carries information about land biospheric activity in a way not present in the P_{CO2} or the $^{13}\delta$, but much other information (fractionation effects, the $^{18}\delta$ distribution of ground water, precipitation and water vapour over the world) is needed in order to extract this information. Thanks to the existing network of GNIP (Global Network of Isotopes in Precipitation, see Chapter 3, this Volume) much of this information is available. The many fractionation effects involved -especially diffusion through the soil- are more problematic. Still, recent detailed modelling work (Ciais et al, 1997a, 1997b) shows promising results.

6.4 RADIOCARBON IN ATMOSPHERIC CO_2

As explained in Volume I (Sect.8.1) the radioactive isotope of carbon, ^{14}C (also called radiocarbon) occurs naturally. In the natural situation the ^{14}C concentrations of the various carbon containing reservoirs on earth are in steady-state. Of course, depending on their interaction with the atmospheric CO_2 , these steady state values vary between being equal to the atmospheric ^{14}C concentration (leafs, young plant material) to virtually zero (ocean sediments, fossil fuel).

In the twentieth century, two anthropogenic effects caused a situation of pronounced disequilibrium:

1) The combustion of fossil fuels produces CO_2 which is ^{14}C-free, due to the high age of this material. This ^{14}C free, or "dead" CO_2 dilutes the ^{14}C in the atmosphere. This effect is called the *Suess effect* (Suess, 1955). Direct observations of this Suess effect are not possible, because the ^{14}C bomb peak, described above, completely obscures this effect at present. However, treerings from the period before AD 1950 have archived the atmospheric ^{14}C concentration at that time, and the Suess effect can be clearly seen.

2) Above-ground nuclear bomb tests gave rise to a considerable additional production of ^{14}C in the troposphere and stratosphere, which caused a fast and strong increase of ^{14}C in atmospheric CO_2 (up to a factor of 2 in the Northern Hemisphere in the early 1960's). After the end of the above-ground nuclear test explosions in 1963 the atmospheric ^{14}C concentration started to decrease again, due to exchanges with various components: the Northern-Southern hemisphere atmospheric mixing, mixing with the terrestrial biosphere, and –primarily- mixing with the oceans. Final re-establishment of equilibrium is very slow, due to the slow mixing between the ocean surface and the deep ocean waters.

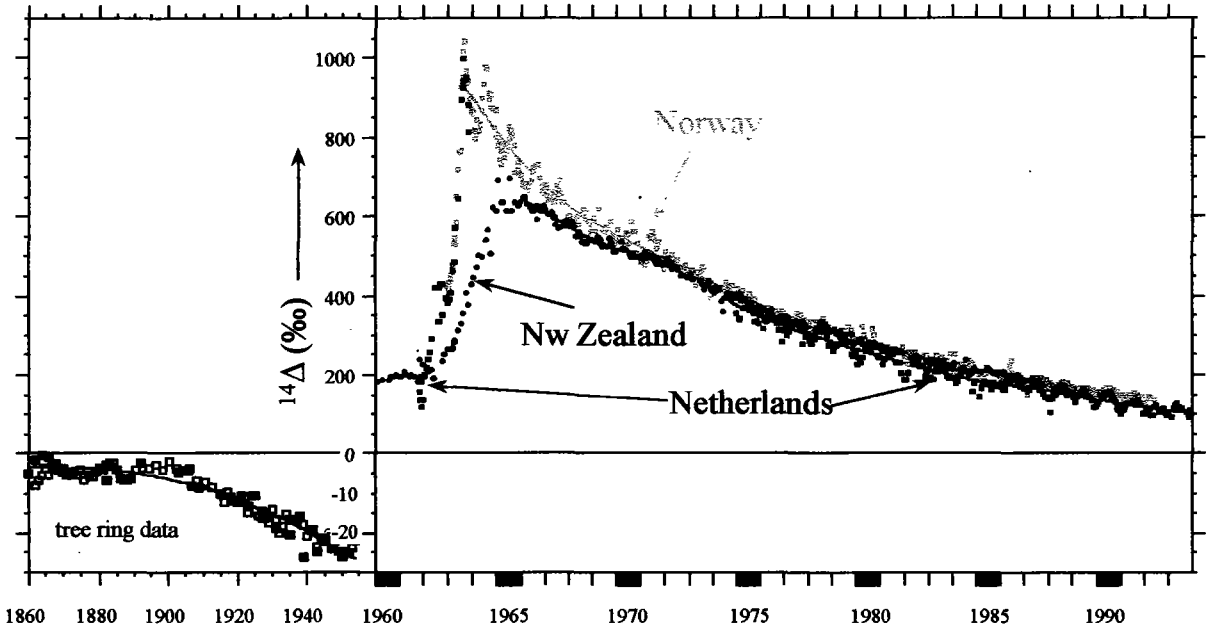

Fig.6.6 Combination of the pre-1950 Suess effect and the post-1960 bomb peak (mind the different scales) (^{14}C data on Suess effect from Tans et al. (1979), De Jong, 1981 and Stuiver and Quay (1981); nuclear bomb data according to Meijer et al. (1995) and Manning et al. (1990).

Fig.6.6 combines the pre-1950 Suess effect and the post-1960 bomb peak (mind the different scales). At present, the amount of CO_2 produced from fossil fuel combustion is about four times as high as in the 1950's. Extrapolating the Suess effect measurements from Fig.6.6 one can estimate that the total Suess effect presently must be typically -100‰ in total since pre-industrial times, and growing at a pace of about -1.5‰ per year.

Several networks monitor the ^{14}C content of atmospheric CO_2 for various stations (Nydal and Lövseth, 1983; Manning et al., 1990; Meijer et al., 1995; Levin et al., 1995). The different features of the signal (the pulse-like rise in the early 1960's, the long decay signal due to several mixing processes, the increasing Suess effect, which is "hidden" behind the bomb peak decline, the seasonal variations) make it a valuable additional piece of information for global carbon cycle research. In particular, the decline of ^{14}C builds a strong test case for all carbon cycle models.

6.5 ATMOSPHERIC OXYGEN

6.5.1 ATMOSPHERIC OXYGEN CONCENTRATION

In recent geological time, the atmospheric oxygen concentration has been remarkably constant. On a short time scale, in which large scale weathering processes etc. can safely be neglected, the O_2 concentration is coupled with the amounts of reduced and oxidised carbon that are present in the global carbon cycle (see 6.1). However, the amount of O_2 present in the atmosphere ($\sim 3\times10^{19}$mol) is large compared to the amount of oxidised ($\sim 3\times10^{18}$mol) and especially reduced ($\sim 10^{18}$mol) carbon. Therefore, even the combustion of all reduced carbon (i.e. the complete biosphere and the fossil fuels) would only reduce the atmospheric O_2 concentration by 2-3%, as pointed out by Broecker (1970).

Yet small variations in the atmospheric oxygen concentration can be expected due to the seasonal variation in oxidation and reduction processes in the global carbon cycle (Fig.6.1), but they will be in the ppm range. Also, the gradual increase of atmospheric CO_2 due to fossil fuel combustion must have its equivalent decrease in the atmospheric oxygen concentration.

Keeling (1988) was the first to develop an analysis method sensitive enough to measure these very small effects on the atmospheric O_2 concentration in a reliable and reproducible way. His method was based on the measurement of the refractive index of the air. A few years later Bender et al. (1994) made the measurements more practical by applying Isotope Ratio Mass Spectrometry (IRMS). In this technique, the ratio of atmospheric O_2 and N_2 is measured for a sample and a reference gas, as if these molecules were each other's isotopes.

The value of these measurements, additional to the analyses of CO_2 concentration and isotopic composition, is that the O_2 measurements discriminate very clearly between land and ocean processes. For land processes, the changes in O_2 concentration are inversely proportional to those in the CO_2 concentration (with the stoichiometry of the specific combustion or photosynthesis process as the coefficient). Oceanic processes, on the other hand, deliver their O_2 and CO_2 signals distinctly different to the atmosphere for three reasons:

1) O_2 is simply dissolved in water to a certain extent, directly proportional to the atmospheric partial O_2 pressure (solubility of O_2 = 31.6mL/L of water at 25°C and 1atm of pressure). Therefore, any process in the water producing or consuming O_2, will immediately lead to

delivery to or from the atmospheric O_2 concentration above the water; for CO_2 this is not the case because of the carbonic acid equilibrium

2) the solution of gases is temperature-dependent: the lower the temperature, the more gas dissolves; for CO_2, the seasonal temperature cycle is in counter-phase with the oceanic CO_2 production, again having a damping effect on the way CO_2 is delivered to or taken from the atmosphere; for O_2, temperature and production are in phase, thereby enhancing the atmospheric signal

3) because of fossil fuel combustion, the atmospheric CO_2 concentration is in disequilibrium with the ocean, causing the ocean to be a net sink of CO_2 (Table 6.1); of course, this process has no counterpart in O_2.

Fig.6.7 shows a sketch of CO_2 and oxygen measurements from a Northern and a Southern hemisphere station (based on the data by Keeling and Shertz, 1992). It is clear that in the Northern hemisphere, where land processes dominate, the O_2 and CO_2 measurements are to a large extent each others inverse (compare the situation for Point Barrow, for which station it was shown by $^{13}\delta$ (Fig.6.4) that its seasonal cycle is caused by plant activity). In the Southern hemisphere, where oceanic processes dominate, there is hardly any CO_2 seasonal cycle visible, but there is a profound O_2 seasonality. The difference between the two is caused by the points mentioned above.

The O_2/N_2 measurements are already in full use for the evaluation of the global carbon cycle, also in the latest IPCC report (IPCC 2001; Prentice et al., 2001). For further details we refer to (R.F.Keeling et al., 1998; Stephens et al., 1998).

6.5.2 ISOTOPES IN ATMOSPHERIC OXYGEN

The $^{18}\delta$ value of atmospheric oxygen is profoundly different from that of ocean water. Kroopnick and Craig (1972) determined $^{18}\delta$ of atmospheric O_2 to be +23.5‰ relative to VSMOW(water), the latter actually resembling the isotopic composition of "mean" ocean water. This difference is called the Dole effect (after its discoverer Malcolm Dole (Dole, 1935; Dole et al.,1954)). It is caused by the balance of isotope fractionation effects for photosynthesis and respiration. According to Bender et al. (1994), the O_2 produced during photosynthesis in the ocean is isotopically essentially the same as the water, so O_2 with $^{18}\delta$ (relative to VSMOW(water)) $\approx$ 0‰ is delivered to the atmosphere. The oxygen consumption processes, however, are characterised by an average fractionation of about -18.9‰ of the air O_2. If the $^{18}\delta$ value of air-O_2 is denoted by $^{18}\delta_{air\text{-}O2}$ the δ value of the O_2 consumed is then $(^{18}\delta_{air\text{-}O2} - 18.9)$ ‰.

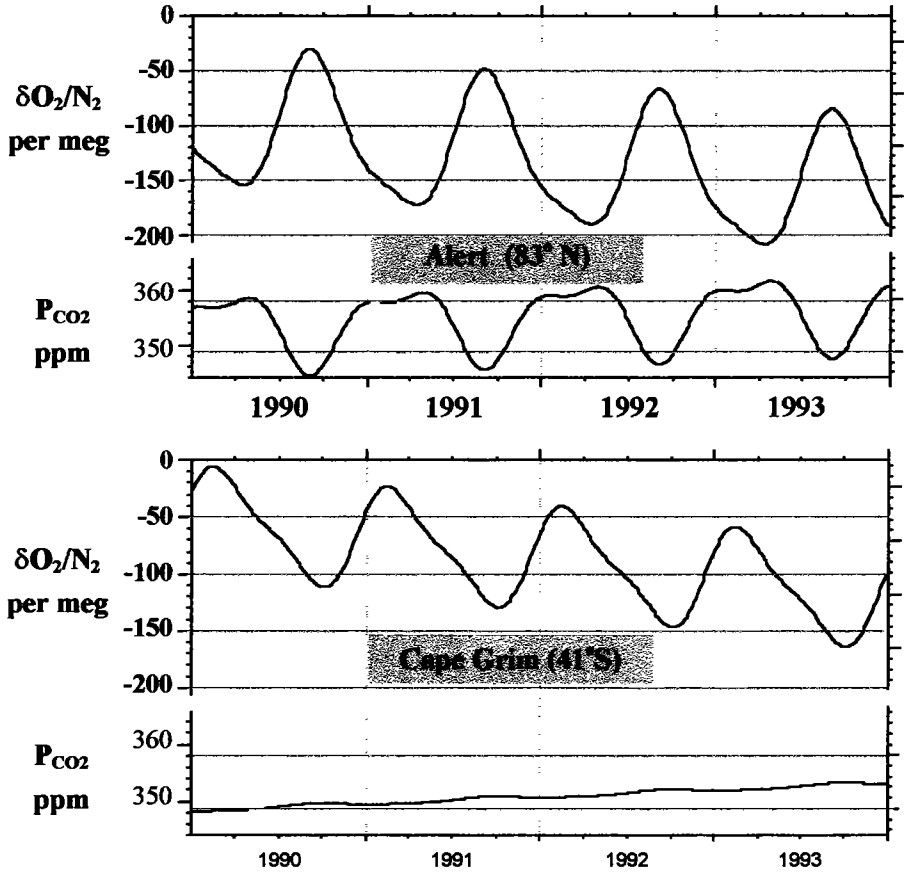

Fig. 6.7 Sketch of atmospheric oxygen and CO_2 measurements from a Northern (Alert, north-east Canada) and a Southern (Cape Grim, Tasmania) hemisphere station. The curves are based on the data by Keeling and Shertz (1992). Scaling is such that the O_2 and CO_2 curves correspond with each other on a mole to mole basis. For both stations, the steady decrease of Oxygen is visible, corresponding to the steady increase of CO_2. (cf. Fig.6.1) For both stations, O_2 shows a clear seasonal cycle. For Alert, the CO_2 pattern is to a considerable content inversely proportional to the O_2 curve, demonstrating the relative importance of the terrestrial signal at that latitude. At Cape Grim, CO_2 hardly shows any seasonality at all (cf. South Pole, fig 6.1), indicating that the O_2 cycles are caused by oceanic processes exclusively.

In land plants the $^{18}\delta$ of O_2 from photosynthesis is also essentially equal to that of the plant water. This $^{18}\delta$ is governed by the global hydrological cycle, and is additionally increased by a several ‰ enrichment compared to the local groundwater, due to evaporation. Relying on Farquhar et al. (1993), Bender et al. (1994), take as the "photosynthesis-weighted, global average $^{18}\delta$" a number of +4.4‰. For respiration (O_2 consumption), a similar fractionation applies as for the marine case (18.0‰). Fig.6.8 illustrates the main processes.

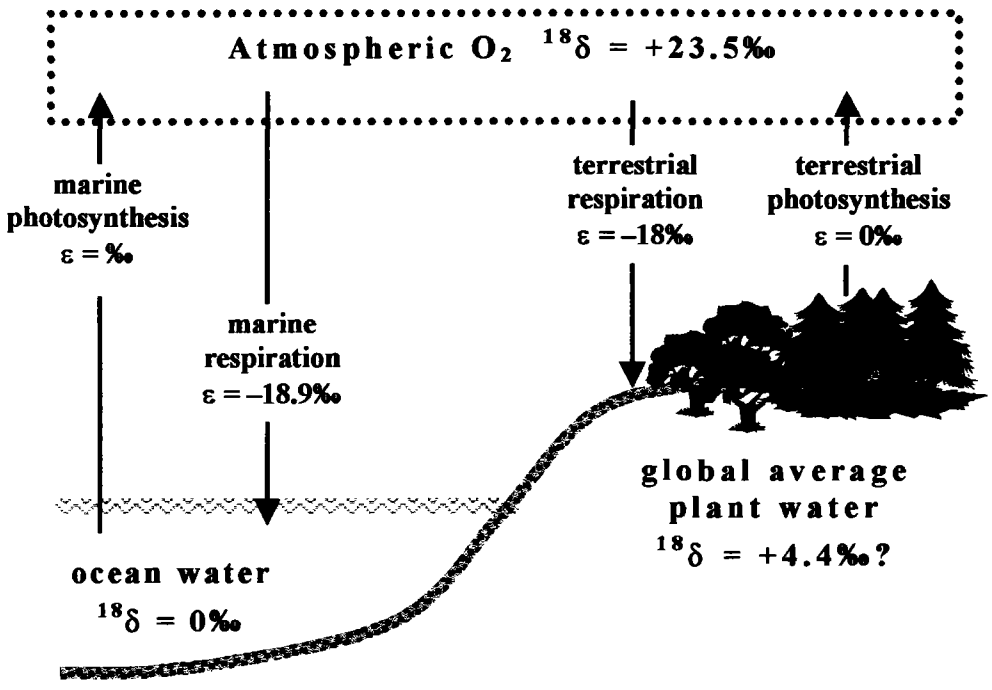

Fig.6.8 Illustration of a simple model to explain and quantify the Dole effect (after Bender et al., 1994). For oxygen, both the marine and the terrestrial photosynthesis processes do not fractionate, and thus pass the $^{18}\delta$ value of their respective surrounding water, i.e. ocean water for the marine environment ($^{18}\delta$ = 0 ‰), and plant water for the terrestrial situation, enriched by evaporation. Both respiration processes do fractionate with almost equal amounts. If one knows the relative terrestrial:marine productivity, one can calculate the value of $^{18}\delta_{air\text{-}O2}$ from this diagram. Bender et al. (1994), using a ratio 54:46, find $^{18}\delta_{air\text{-}O2}$ = +20.8‰, significantly lower than the actual value for $^{18}\delta_{air\text{-}O2}$ = 23.5‰. One reason may be that the $\delta^{18}O$ value for the plant water, being most unreliable number in their model is taken too small.

For studying the global carbon cycle and its reservoirs, it is interesting to compute $^{18}\delta_{air\text{-}O2}$ from this model. For this the relative flows of oxygen of marine and terrestrial origin are needed. Using a ratio of 54:46 for terrestrial and marine activity, respectively (based on global carbon cycle models), Bender et al. (1994) find $^{18}\delta_{air\text{-}O2}$ to be +20.8‰, in fact almost 3‰ too light. They consider a too low value for the terrestrial plant water as a likely explanation (adjusting this value from 4.4 to 8.5‰ would bring their simple Dole effect model in accordance with reality. However, they also discuss other, smaller effects (such as stratospheric O_2 isotopic enrichment) as a possible cause for the discrepancy.

In summary, it is clear that the isotopic composition of atmospheric oxygen is dependent on several main climatological parameters, such as the hydrological cycle (determining the $\delta^{18}O$

of plant water) and the ratio between oceanic and terrestrial photosynthesis activity. Also, obviously, the $^{18}\delta$ of atmospheric oxygen will depend on the $^{18}\delta$ of ocean water.

Gas bubbles in deep ice cores preserve the composition of the earth's atmosphere, in principle, for the last several 100 000 years. Recently it has become possible to reconstruct the Dole effect (or rather the $^{18}\delta_{air\text{-}O2}$ value) through glacial times (Bender et al., 1994; Malaize et al., 1999). The Dole effect appears to have been surprisingly stable with variations over two glacial-interglacial era's within ± 0.5‰, and it appeared to be hard to distinguish between the main effects that can either increase or decrease the Dole effect. Nevertheless, data on the Dole effect put important constraints on palaeo-climate models, in particular considering the hydrological cycle (Jouzel et al., 1994), and terrestrial/marine photosynthesis.

REFERENCES

Allison, G.B., Gat, J.R. and Leaney, F.W., 1985. The relationship between deuterium and oxygen-18 values in leaf water. Isotope Geoscienc. 58: 145-156.

Allison, C.E., Francey, R.J., and Meijer, H.A.J., 1995. Recommendations for the reporting of stable isotope measurements of carbon and oxygen in CO_2 gas. In: Reference and intercomparison materials for stable isotopes of light elements, IAEA-TECDOC 825 155-162 IAEA, Vienna.

Andrews, J.E., Brimblecombe, P., Jickells, T.D. and Liss P.S., 1966. An Introduction to Environmental Chemistry. Blackwell Science Ltd.

Baertschi, P., 1976. Absolute ^{18}O content of Standard Mean Ocean Water. Earth Planetary Science Lett. 31: 341-344.

Baily, I.H., Hulston J.R., Macklin, W.C. and J.R. Stewart, 1969. On the isotopic composition of hailstones. J. Atmosph. Sc. 26: 689-694.

Barnes, C.J. and Allison, G.B., 1988. Tracing of water movement in the unsaturated zone using stable isotopes of hydrogen and oxygen. J. Hydrol. 100: 143-176.

Begemann, F., 1960. Natural tritium. In: Nuclear Geology, Varenna: 109-128.

Bender, M., Sowers, T., and Labeyrie, L., 1994. The Dole effect and its variations during the last 130 000 years as measured in the Vostok ice core. Global Biogeochemical Cycles 8: 363-376.

Bender, M.L., Tans, P.P., Ellis, J.T., Orchardo, J., Habfast, K., 1994. A high-precision isotope ratio mass spectrometry method for measuring the O_2/N_2 ratio of air. Geochim. Cosmochim. Acta 58: 4751-4758.

Benton, G.S. and Estoque, M.A., 1954. Water vapour transfer over the North-American continent. J. Meteorol. 11: 462-477.

Bleeker, W., Dansgaard, W. and Lablans, W.N., 1966. Some remarks on simultaneous measurements of particulate contaminants including radioactivity and isotopic composition of precipitation. Tellus 18: 773-785.

Bolin, B., 1958. On the use of tritium as a tracer for water in nature. In: Proc. 2nd UN Conference on the Peaceful Uses of Atomic Energy, Geneva, 18: 336-344.

Bortolami, G.C., Ricci, B., Susella, G.F. and Zuppi, G.M., 1979. Isotope Hydrology of the Val Corsaglia, Maritime Alps, Piedmont, Italy. Proc. Conf. Isotope Hydrology Vol. I, IAEA, Vienna: 327-350.

Broecker, W.S., 1970. Man's oxygen reserves. Science 168: 1537-1538.

Brutsaert, W., 1965. A model for evaporation as a molecular diffusion process into a turbulent atmosphere. J. Geophys. Res. 70: 5017-5024.

Budyko, M.I., 1962. Teplovoi Balans Zemli. Trans. Vses. Nauchu. Meteorolog Sov. 1: 113-124.

CDIAC, Carbon Dioxide Information Centre, Oak Ridge, Tenessee, U.S.A. Web page http://cdiac.esd.ornl.gov/pns/current_ghg.html.

Chapman, S. and Cowling, T.G., 1951. Mathematical theory of non-uniform gases (2nd edn). Cambridge University Press, Chapter 10: 14.

Chow, V.T., 1964. Handbook of Applied Hydrology. McGraw Hill, New York.

Ciais, P., Tans, P.P., White, J.W.C., Trolier, M., Francey, R.J., Berry, J.A., Randall, D.R., Sellers, P.J., Collatz, J.G. and Schimel, D.S., 1995. Partitioning of ocean and land uptake of CO_2 as inferred by $\delta^{13}C$ measurements from the NOAA climate monitoring and diagnostics laboratory global air sampling network. J.Geophys. Res. 100(D3): 5051-5070.

Ciais, P., Denning, A.S., Tans, P.P., Berry, J.A., Randall, D.A., Collatz, G.J., Sellers, P.J., White, J.W.C., Trolier, M., Meijer, H.A.J., Francey, R.J., Monfray, P. and Heimann, M., 1997a. A three-dimensional synthesis study of $\delta^{18}O$ in atmospheric CO_2, I Surface fluxes. J. Geoph. Res. D 102 (1997): 5857-5872.

Ciais, P., Tans, P.P., Denning, A.S., Francey, R.J., Trolier, M., Meijer, H.A.J., White, J.W.C., Berry, J.A., Randall, D.A., Collatz, G.J., Sellers, P.J., Monfray, P. and Heimann, M., 1997b. A three-dimension synthesis study of $\delta^{18}O$ in atmospheric CO_2. II Simulations with the TM2 transport model. J. Geoph. Res. D 102: 5873- 5883.

Ciais, P. and Meijer, H.A.J., 1998. The $^{18}O/^{16}O$ isotope ratio of atmospheric CO_2 and its role in global carbon cycle research. In: H. Griffiths (Editor), Stable Isotopes, Intergration of Biological, Ecological and Geochemical Processes, BIOS Scientific Publishers, Oxford, ISBN 1 85996 135 5.

Clayton, R.N., 1993. Oxygen isotopes in meteorites. Ann. Rev. Earth Planet. Sci. 21: 115-149.

Conway, T.J., Tans, P.P., Waterman, L.W., Thoning, K.W., Kitzis, D.R., Masaric K.A. and Zhang, N., 1994. Evidence for interannual variability of the carbon cycle from the National Oceanic and Atmospheric Administration/Climate Monitoring and Diagnostics Laboratory Global Air Sampling Network. J.Geophys. Res. 99 D11: 22831-22855.

Craig, H., 1957. Isotopic standards for carbon and oxygen and correction factors for mass spectrometric analysis of carbon dioxide. Geochim. Cosmochim. Acta 12 133-149.

Craig, H., 1961a. Isotopic variations in meteoric waters. Science 133: 1702-1708.

Craig, H., 1961b. Standards for reporting concentrations of deuterium and oxygen-18 in natural waters. Science, 133: 1833-1834.

Craig, H. and Gordon, L.I., 1965. Deuterium and oxygen-18 variations in the ocean and marine atmosphere. In: E. Tongiorgi (Editor), Stable Isotopes in Oceanographic Studies and Paleo-Temperatures. Pisa, Lab. Geol. Nucl.: 9-130.

Craig, H., 1966. Isotopic composition and origin of the Red Sea and Salton Sea geothermal brines. Science 54: 1544-1547.

Craig, H. and Horibe, Y., 1967. Isotope characteristics of marine and continental water vapour. Trans. Am. Geophys. Union 48: 135-136.

Dansgaard, W., 1961. The isotope composition of natural waters. Medd. Grønland 165 (2): pp.120.

Dansgaard, W., 1964. Stable isotopes in precipitation. Tellus 16: 436-468.

De Jong, A.F.M., 1981. Natural ^{14}C variations. Thesis Groningen University: pp114.

De Wit, J.C., Van der Straaten, C.M. and Mook, W.G., 1980. Determination of the absolute D/H ratio of VSMOW and SLAP. Geostandards Newslett. 4: 33-36.

Dincer, T., Payne, B.R., Florkovski, T., Martinec, J. and Tongiorgi, E., 1970. Snowmelt runoff from measurements of tritium and Oxygen-18. Water Res. Res. 5: 110.

Dole, M., 1935. The relative weight of oxygen in water and in air. J. Am. Chem. Soc. 57: 2731.

Dole, M., Lane, G.A., Rudd, D.P., and Zaukelies, D.A., 1954. Isotopic composition of atmospheric oxygen and nitrogen. Geochim. Cosmochim. Acta 6: 65-78.

Doney, S.C., Glover, D.M. and Jenkins, W.J., 1992. A model function of the Global Bomb Tritium Distribution in precipitation 1960-1986. J. Geophys. Res. 97: 5481-5492.

Ehhalt, D., 1967, Deuterium and tritium content of hailstones: additional information on their growth. Trans. Amer. Geophy. Union.

Ehhalt, D.H., 1971. Vertical profiles and transport of HTO in the troposphere. J. Geophys. Res. 76: 7351-7367.

Ehhalt, D., 1974. Vertical profiles of HTO, HDO and H_2O in the troposphere. NCAR Techn. Note, NCAR-TN/STR-100: pp 131.

Eichler, R., 1964. Über den Isotopengehalt des Wasserstoffs in Niederschlag, Boden und Grundwasser. PhD Thesis, Univ. of Heidelberg.

Epstein, S., 1956. Variations in the $^{18}O/^{16}O$ ratios of freshwater and ice. Natnl. Acad. Sc. Nucl. Science Series Report 19: 20-28.

Epstein, S., Sharp, R. and Gow, A.J., 1965. Six year record of oxygen and hydrogen isotope variations in South Pole firm. J. Geophys. Res. 70: 1809.

Eriksson, E., 1966. Major pulses of tritium in the atmosphere. Tellus 17: 118-130.

Eriksson, E., 1967. Isotopes in hydro-meteorology. In: Isotopes in Hydrology, IAEA, Vienna: 21-33.

Etheridge, D.M., Steele, L.P., Langenfelds, R.L., Francey, R.J., Barnola, J.-M., and Morgan, V.I., 1996. Natural and anthropogenic changes in atmospheric CO_2 over the last 1000 years from air in Antarctic ice and firn. J.Geophys. Res. D 101: 4115-4128.

Facy, L., Merlivat, L., Nief, G. and Roth, E., 1963. The study of the formation of a hailstone by means of isotopic analysis. J. Geophys. Res. 63: 3841-3848.

Farquhar, G.D., Lloyd, J., Taylor, J.A., Flanagan, L.B., Syvertsen, P., Hubick, K.T., Wong, S.C. and Ehleringer, J.R., 1993. Vegetation effects on the isotope composition of oxygen in atmospheric CO_2. Nature 363: 439-443.

Ferronski, V.I. and Brezgunov, V.S., 1989. Stable isotopes and ocean mixing. In: Handbook of Environmental Isotope Geochemistry (P. Fritz and J.Ch. Fontes, eds), Vol. 3. Elsevier: 1-28.

Fontes, J.C. and Olivry, J.C., 1977. Gradient isotopique entre 0 en 4000m dans les precipitations du Mount Cameroun. Comptes Rendus Reunion Annuelle Sciences de la Terre, Soc. Geol. Francaise Paris: 171.

Fontes, J.Ch., 1981. Paleowaters. In: Stable Isotope Hydrology (Gat and Gonfiantini, eds.), IAEA Techn. Report no. 210, Chapt 12: 273-302.

Francey, R.J. and Tans, P.P., 1987. Latitudinal variation in oxygen-18 of atmospheric CO_2. Nature 327: 495-497.

Francey, R.J., Tans, P.P., Allison, C.E., Enting, I.G., White, J.W.C. and Troller, M., 1995. Changes in oceanic and terrestrial carbon uptake since 1982. Nature 373: 326-330.

Fricke, H.C. and O'Neil, J.R.O., 1999. The correlation between $^{18}O/^{16}O$ ratios of meteoric water and surface temperature; its use in investigating terrestrial climate change over geologic time. Earth Planet. Sc. Lett. 170: 181-196.

Friedman, I., 1953. Deuterium content of natural waters and other substances. Geochim. Cosmochim. Acta 4: 89-103.

Friedman, I., Machta, L. and Soller, R., 1962. Water vapour exchange between a water droplet and its environment. J. Geophys. Res. 67: 2761-2766.

Friedman, I., Redfields, A.C., Schoen, B. and Harris, J., 1964. The variation of deuterium content of natural waters in the hydrologic cycle. Rev. Geophys. 2: 177-224.

Gat, J.R., Karfunkel, U. and Nir, A., 1962. Tritium content of rainwater from the Eastern Mediterranean area. In: Use of Tritium in the Physical and Biological Sciences, IAEA, Vienna: 41-54.

Gat, J.R. and Tzur, Y., 1967. Modification of the isotope composition of rainwater by processes which occur before groundwater recharge. Proc. IAEA Symp. on Isotopes in Hydrology, Vienna: 49-60.

Gat, J.R. and Carmi, I., 1970. Evolution of the isotopic composition of atmospheric waters in the Mediterranean Sea area. J. Geophys. Res. 75: 3039-3048.

Gat, J.R. and Dansgaard, W., 1972. Stable isotope survey of the freshwater occurrences in Israel and the Jordan Rift Valley. J. Hydrol. 16: 177-211.

Gat, J.R., 1980. The isotopes of hydrogen and oxygen in precipitation. In: Handbook of Environmental Isotope Geochemistry (P. Fritz and J.Ch. Fontes, eds.), Vol. 1: 22-48.

Gat, J.R., 1983. Precipitation, groundwater and surface waters: Control of climate parameters and their utilization as palaeoclimatic tools. In: Palaeoclimates and Palaeowaters: a Collection of Environmental Isotope Studies, IAEA, Vienna: 3-12.

Gat, J.R. and Carmi, I., 1987. Effect of climate changes on the precipitation patterns and isotope composition of water in a climate transition zone - case of the eastern Mediterranean Sea area. In: The Influence of Climate Change and Climate Variability on the Hydrologic Regime and Water Resources. IAHS 168: 513-523.

Gat, J.R. and Matsui, E., 1991. Atmospheric water balance in the Amazon basin: an isotopic evapotranspiration model. J. Geophys. Res. 96: 13179-13188.

Gat, J.R., Bowser, C. and Kendall, C., 1994. The contribution of evaporation from the Great Lakes to the continental atmosphere: estimate based on stable isotope data. Geophys. Res. Lett. 21: 557-560.

Gat, J.R., 1995. Stable isotopes of fresh and saline lakes. In: Physics and Chemistry of Lakes (A. Lerman, D. Imboden and J. Gat, eds.), New York, Springer-Verlag: 139-166.

Gat, J.R. and Lister, G.S., 1995. The "catchment effect" on the isotopic composition of lake waters: its importance in paleo-limnological interpretations. In: Problems of Stable Isotopes in Tree-Rings, Lake Sediments and Peat-bogs as Climatic Evidence for the

Holocene (B. Frengel, B. Stauffer and M. Weiss (eds.), Paleoclimate Res. vol. 15, G. Fisher: 1-15.

Gat, J.R., 1996. Oxygen and hydrogen isotopes in the hydrologic cycle. In: Annual Rev. Earth Planet. Sc. 24: 225-262.

Gat, J.R., Shemesh, A., Tziperman, E., Hecht, A., Georgopoulos, D. and Ozden, B., 1996. The stable isotope composition of water of the eastern Mediterranean Sea. J. Geophys. Res. 101: 6441-6451.

Gat, J.R., 1998. Modification of the isotopic composition of meteoric waters at the land-biosphere-atmosphere interface. In: Isotope Techniques in the Study of Environmental Change, IAEA, Vienna: 153-163.

Gedzelman, S.D., Rosenbaum, J.H. and Lawrence, J.R., 1989. The megalopitan snowstorm of 11-12 February 1983: isotopic composition of the snow. J. Atmosph. Sc. 46: 1637-1649.

Groeneveld, D.T., 1977. Tritium analysis of environmental water. PhD Thesis, Groningen University: pp.131.

Hagemann, R., Nief, G. and Roth, E. 1970. Absolute isotopic scale for deuterium analysis of natural waters. Absolute D/H ratio for SMOW. Tellus 22: 712-715.

Horita, J., 1988. Hydrogen isotope analysis of natural waters using a H_2–water equilibration method: a special implication to brines. Chem. Geol. (Isot. Geosc. Sect.) 72: 89-94.

Horita, Y. and Gat, J.R., 1989. Deuterium in the Dead Sea: re-measurement and implications for the isotope activity correction in brines. Geochim. Cosmochim. Acta 53: 131-133.

IPCC 2001. Intergovernmental Panel on Climate Change. The Scientific Basis, Report Working Group I to IPCC Third Assessment Report (TAR) (eds. Houghton J., Yihui, D.) Cambridge University Press (in press).

Jacob, H., and Sonntag, Ch., 1991. An 8-year record of the seasonal variation of ^{2}H and ^{18}O in atmospheric water vapour and precipitation at Heidelberg, Germany. Tellus 43B: 291-300.

Jouzel, J., Merlivat, L. and Roth, E., 1975. Isotopic study of hail. J. Geophys. Res. 80: 5015-5030.

Jouzel, J. and Merlivat, L., 1984. Deuterium and oxygen-18 in precipitation: modelling of the isotopic effects during snow formation. J. Geophys. Res. 89: 11749-11757.

Jouzel, J., Koster, R.D., Suozzo, R.J., and Russell, G.L., 1994. Stable water isotope behaviour during the last glacial maximum: a general circulation model analysis. Journal of Geophysical Research D 99: 25,791-25,801.

Junge, Ch.E., 1963. Air Chemistry and Radioactivity. Academic Press.

Kaufman, S. and Libby, W.F., 1954. The natural distribution of tritium. Phys. Rev. 93: 1337-1344.

Keeling, C.D., 1958. The concentration and isotopic abundances of atmospheric carbon dioxide in rural areas. Geochim. Cosmochim. Acta 13: 322-334.

Keeling, C.D., Bacastow, R.B., Carter, A.F., Piper, S.C., Whorf, T.P., Heimann, M., Mook, W.G. and Rocloffzen, H., 1989. A three-dimensional model of atmospheric CO_2 transport based on observed winds: 1. Analysis of observational data. Geophysical Monograph 55: 165-236.

Keeling, C.D., Piper, S.C. and Heimann, M., 1989. A three-dimensional model of atmospheric CO_2 transport based on observed winds: 4. Mean annual gradients and interannual variations. Geophysical Monograph 55: 305-363.

Keeling, C.D., Whorf, T.P., Whalen, M. and van der Plicht, J., 1995. Interannual extremes in the rate of rise of atmospheric carbon dioxide since 1980. Nature 375: 666-670.

Keeling, R.F.,1988. Measuring correlations between atmospheric oxygen and carbon dioxide mole fractions: a preliminary study in urban air. J. Atm. Chem. 7: 153-176.

Keeling,R.F. and Shertz, S.R.,1992. Seasonal and interannual variations in atmospheric oxygen and implication for the global carbon cycle. Nature 358: 723-727.

Keeling, R.F., Stephens, B.B., Najjar, R.G., Doney, S.C., Archer, D., and Heimann, M., 1998. Seasonal variations in the atmospheric O2/N2 ratio in relation to the kinetics of air-sea gas exchange. Glob. Biogeochem. Cycles 12: 141-163.

Kirschenbaum, I., 1951. Physical properties and analysis of heavy water. Natl. Nuclear Energy Series, Div. III 4A.

Krankowsky, D., and Mauersberger, K., 1996. Heavy Ozone - A Difficult Puzzle to Solve. Science 274: 1324-1325.

Kroopnick, P. and Craig, H., 1972. Atmospheric Oxygen: isotopic composition and solubility fractionation. Science 175: 54-55.

Kukla, G.J. and Kukla, H.J., 1974. Increased surface albedo in the northern hemisphere. Science 183: 709-714.

Leguy, C., Rindsberger, M., Zangwil, A., Issar, A. and Gat, J.R., 1983. The relation between the oxygen-18 and deuterium contents of rainwater in the Negev Desert and air mass trajectories. Isotope Geosciences 1: 205-218.

Levin, I., Graul, R. and Trivet, N.B.A., 1995. Long term observations of atmospheric CO_2 and carbon isotopes at continental sites in Germany. Tellus 47B: 23-34.

Libby, W.F., 1965. Radiocarbon Dating (2nd Ed.). Univ. of Chicago Press, Phoenix Books, Chicago, London: 175 pp.

Lipps, F.B. and Helmer, R.S., 1992. On the downward transfer of tritium to the ocean by a cloud model. J. Geophys. Res. 97: 12889-12900.

Lucas, L.L. and Unterweger, M.P., 2000. Comprehensive review and critical evaluation of the half-life of tritium. J. Res. Natl. Stand. Technol. 105 (4): 541-549.

Luz, B., Barkan, E., Bender, M.L., Thiemens, M.H., and Boering, K.A., 1999. Triple-isotope composition of atmospheric oxygen as a tracer of biosphere productivity. Nature 400: 547-550.

Luz, B., and Barkan, E., 2000. Assessment of Oceanic Productivity with the Triple-Isotope Composition of Dissolved Oxygen. Science 288: 2028-2031.

Macklin, W.C., Merlivat, L. and Stevenson, C.M., 1970. The analysis of hailstone. Quart. J. Royal Meteor. Soc. 96: 472-486.

Majoube, M., 1971. Fractionnement en oxygène-18 et en deuterium entre l'eau et sa vapeur. J. Chim. Phys. 10: 1423-1436.

Malaize, B., Paillar, D., Jouzel, J., and Raynaud, D., 1999. The Dole effect over the last two glacial-interglacial cycles. J. Geophys. Res. 104: 14,199-14,208.

Manning, M.R., Lowe, D.C., Melhuish, W.H., Sparks, R.J., Wallace, G., Brenninkmeijer, C.A.M., and McGill, R.C., 1990. The use of radiocarbon measurements in atmospheric studies. Radiocarbon 32: 37-58.

Mason, A.S., Hut, G. and Telegades, KI., 1982. Stratospheric HTO and ^{95}Zr residence times. Tellus 34: 369-375.

Matsui, E., Salati, E., Ribéiro, M., Reis, C.M., Tancredi, A. and Gat, J.R., 1983. Precipitation in the Central Amazon Basin: the isotopic composition of rain and atmospheric moisture at Belem and Manaus. Acta Amazonica 13: 307-369.

Matsuo, S. and Friedman, I., 1967. Deuterium content of fractionally collected rainwater. J. Geophys. Res. 72: 6374-6376.

Mauersberger, K., 1981. Measurement of heavy ozone in the stratosphere. Geophys. Res. Lett.. 8: 935-937.

McDonnel, J.J., Bonell, M., Stewart, M.K. and Pearce, A.J., 1990. Deuterium variations in storm rainfall: Implications for stream hydrograph separation. Water Resources Res. 26: 455-458.

Meijer, H.A.J., van der Plicht, J., Gislefoss, J.S. and Nydal, R., 1995. Comparing long-term atmospheric ^{14}C and ^{3}H records near Groningen, The Netherlands with Fruholmen, Norway and Izana, Canary Islands ^{14}C stations. Radiocarbon 37(1): 39-50.

Meijer, H.A.J., and Li, W.J., 1998. The use of electrolysis for accurate $\delta^{17}O$ and $\delta^{18}O$ isotope measurements in water. Isot. Environ. Health Stud. 34: 349-369.

Melander, L., 1960. Isotope Effects on Reaction Rates. Roland Press, New York.

Merlivat, L. and Contiac, M., 1975. Study of mass transfer at the air-water interface by an isotopic method. J. Geophys. Res. 80: 3455-3464.

Merlivat, L., 1978. Molecular diffusivities of $H_2{}^{16}O$, $HD^{16}O$ and $H_2{}^{18}O$ in gases. J. Chim. Phys. 69: 2864-2871.

Merlivat, L. and Jouzel, J., 1979. Global climatic interpretation of the deuterium-oxygen 18 relationship for precipitation. J. Geophys. Res. 84: 5029-5033.

Molion, L.C.B., 1987. Micro-meteorology of an Amazonian rainforest. In: R.E. Dickinson (Editor), The Geophysiology of Amazona. Wiley, New York.

Mook, W.G., and Grootes, P.M., 1973. The measuring procedure and corrections for the high precision mass-spectrometric analysis of isotopic abundance ratios, especially referring to carbon, oxygen and nitrogen. Int. J. Mass Spectrom. Ion Phys. 12: 273-298.

Mook, W.G., Groeneveld, D.J., Brouwn, A.E. and Van Ganswijk, A.J., 1974. Analysis of a run-off hydrograph by means of natural ^{18}O. Proc. Conf. Isotope Techniques in Ground-Water Hydrology, IAEA, Vienna: 145-153.

Moser, H. and Stichler, W., 1971. Die Verwendung des Deuterium und Sauerstoff-18 Gehalts bei Hydrologischen Untersuchungen.Geol. Bavarica 64: 7-35.

Moser et al., 1972. In: Jahresbericht 1971/1972. Inst. f. Radiohydrometrie der Gesellschaft f. Strahlen- und Umweltforschung mbH, München: 99-103.

Moser et al., 1978. In: Jahresbericht 1978. Inst. f. Radiohydrometrie der Gesellschaft f. Strahlen- und Umweltforschung mbH, München: 55-60.

Newell, R.S., 1963. Transfer through the tropopause and within the stratosphere. Quarterly Journal Royal Meteorol. Soc. 89: 167-204.

Nir, A., Kruger, S.T., Lingenfelter, R.E. and Flamm, E.J., 1966. Natural Tritium. Reviews of Geophysics 4: 441-456.

Nydal, R. and Lovseth, K., 1983. Tracing bomb ^{14}C in the atmosphere 1962-1980. Journal of Geophysical Research C 88: 3621-3642.

Östlund, H.G., 1967. Hussicane tritium I: Preliminary results on Hilda 1964 and Betsy 1965. In: Isotope Techniques in the Hydrologic Cycle. Am. Geoph. Union Monogr. 11: 58.

Östlund, H.G. and Fine, R.A., 1978. Oceanic distribution and transport of tritium. Proc. IAEA. Conf. on the Behaviour of Tritium in the Environment, San Fransisco: 303-312.

Payne, B.R. and Yurtsever, Y., 1974. Environmental isotopes as a hydrogeological tool in Nicaragua. Conf. Isotope Techniques in Ground-Water Hydrology, IAEA, Vienna: 193-200.

Pierre, C., Vergnaud-Grazzini, C., Thunron, D. and Saliege, J.F., 1986. Composition isotopiques de l'oxygene et du carbon des masses d'eau en Mediterranée. Mem. Soc. Geol. Ital. 36: 165-174.

Pionke, H.B. and Dewalle, D.R., 1992. Intra and inter-storm ^{18}O trends for selected rainstorms in Pennsylvania. J. Hydrol. 138: 131-143.

Prentice, I.C., et al., 2001. The carbon cycle and atmospheric CO_2. Chapter 3 in Climate Change: The Scientific Basis, the contribution of WGI of the IPCC to the IPCC Third Assessment Report (TAR) (eds. Houghton J., Yihui, D.) Cambridge University Press (in press).

Rindsberger, M. and Magaritz, M., 1983. The relation between air-mass trajectories and the water isotope composition of rain in the Mediterranean Sea area. Geophys. Res. Lett. 10: 43-46.

Rindsberger, M., Jaffe, M., Rahamim, S. and Gat, J.R., 1990. Patterns of the isotopic composition of precipitation in time and space: data from the Israeli storm water collection program. Tellus 42B: 263-271.

Roeloffzen, J.C., Mook, W.G. and Keeling, C.D., 1991. Trends and variations in stable carbon isotopes of atmospheric carbon dioxide. Pro. IAEA Symp. on Stable Isotopes in Plant Nutrition, Soil Fertility and Environmental Studies. IAEA, Vienna, 1991: 601-618.

Roether, W., 1967. Estimating the tritium input to ground water from wine samples: ground-water and direct run-off contribution to central European surface waters. Proc. IAEA Conf. on Isotopes in Hydrology, IAEA, Vienna: 73-90.

Rozanski, K., Sonntag, Ch. and Munnich, K.O., 1982. Factors controlling stable isotope composition of modern European precipitation. Tellus 34: 142-150.

Rozanski, K., Gonfiantini, R. and Araguas-Araguas, L., 1991. Tritium in the Global Atmosphere: distribution patterns and recent trends. J. Physics G: Nuclear Particle Physics 17: 5523-5536.

Rozanski, K., Araguas-Araguas, L. and Gonfiantini, R., 1993. Isotopic patterns in modern global precipitation. In: Climate Change in Continental Isotopic Record (P.K. Swart, K.L. Lohman, J.A. McKenzie and S. Savin, edc.). Geophys. Monogr. 78: 1-37.

Salati, E., Dall'ollio, A., Matsui, E. and Gat, J.R., 1979. Recycling of water in the Amazon Basin, an isotopic study. Water Resources Res. 15: 1250-1258.

Siegenthaler, U. and Oeschger, H., 1980. Correlation of ^{18}O in precipitation with temperature and altitude. Nature 285: 314.

Sofer, Z. and Gat, J.R., 1972. The isotopic composition of evaporating brines: effect of isotopic activity ratio in saline solutions. Earth Planet. Sc. Lett. 26: 179-186.

Sonntag, Ch., Munnich, K.O., Jacob, H. and Rozanski, K., 1983. Variation of Deuterium and Oxygen 18 in continental precipitation and groundwater, and their causes. In: Variation in the Global Water Budget (Street-Perrot et al., (eds.). Reidel Publ.: 107-124.

Stahl, W., Aust, H. and Dounas, A., 1974. Origin of Artesian and thermal waters determined by oxygen, hydrogen and carbon isotope analysis of water samples from the Sperkhios Valley, Grees. Conf. Isotope Techniques in Ground-Water Hydrology Vol. I, IAEA, Vienna: 317-339.

Stephens, B.B., Keeling, R.F., Heimann, M., Six, K.D., Murnane, R., and Caldeira, K.C., 1998. Testing global ocean carbon cycle models using measurements of atmospheric O_2 and CO_2 concentration. Global Biogeochemical Cycles 12: 213-230.

Stuiver, M. and Quay, P.D., 1981. Atmospheric ^{14}C changes resulting from fossil fuel CO_2 release and cosmic ray flux variability. Earth Planet. Sci. Lett. 53: 349-362.

Suess, H., 1955. Radiocarbon concentration in modem wood. Science 122: 415.

Sverdrup, H.U., 1951. Evaporation from the oceans. In: Compendium of Meteorology Amer. Meteor. Soc (T. Malone, ed.): 1071-1081.

Tans, P.P., De Jong, A.F.M. and Mook, W.G., 1979. Natural atmospheric ^{14}C variation and the Suess effect. Nature 280: 826-828.

Tans, P.P., Fung, I.Y. and Takahashi, T., 1990. Observational constraints on the global atmospheric CO_2 budget. Science 247: 1431-1438.

Taylor, A.B., 1972. The vertical variations of the isotopic concentrations of tropospheric water vapour over continental Europe and their relationship to tropospheric structure. NZ Inst. Nucl. Sci. Rep. INS-R-107: pp 45.

Thiemens, M.H., Jackson,T., Mauersberger,K., Schueler, B., and Morton, J., 1991. Oxygen isotope fractionation in stratospheric CO_2. Geophys. Res. Lett. 18: 669-672.

Thiemens, M.H., Jackson, T., Zipf, E.C., Erdman P.W., and van Egmond C., 1995. Carbon Dioxide and Oxygen Isotope Anomalies in the Mesosphere and Stratosphere. Science 270: 969-971.

Tse, R.S., Wong S.C. and Yuen, C.P., 1980. Determination of deuterium/hydrogen ratios in natural waters by Fourier transform nuclear magnetic resonance spectrometry. Anal.Chem. 52: 2445.

Tzur, Y., 1971. Isotopic composition of water vapour. Ph.D. thesis, Feinberg Graduate School at the Weizmann Institute of Science, Rehovot, Israel.

Vogel, J.C., Lerman, J.C. and Mook, W.G., 1975. Natural isotopes in surface and groundwater from Argentina. Hydrol. Sciences Bull. XX (2): 203-221.

Weiss, W., Roether, W. and Dreisigacker, E., 1979. Tritium in the North Atlantic Ocean. Proc. IAEA Conf. on The Behaviour of Tritium in the Environment, San Francisco (1978): 303-312.

White, J.W.D. and Gedzelman, D., 1984. The isotopic composition of atmospheric water vapour and the concurrent meteorological conditions. J. Geophys. Res. 89: 4937-4939.

WMO, World Meteorological Organization, Global Atmosphere Watch program. Several reports available, e.g. WMO-GAW-No. 132 Report of the 9th WMO Meeting of Experts on Carbon Dioxide Concentration and Related Tracer Measurement Techniques, Aspendale, Australia, 1997.(WMO TD-952). See also web page of WMO: http:l/www.wmo.ch/.

Woodcock, A.H. and Friedman, I., 1963. The deuterium content of raindrops. J. Geophys. Res. 68: 4477.

Yurtsever, Y., 1975. Worldwide survey of isotopes in precipitation. IAEA report, Vienna.

LITERATURE

H.Moser **W.Rauert**	**Isotopenmethoden in der Hydrologie** (1980) (in German language) ISBN 3-443-01012-1	Gebr. Borntraeger Berlin, Stuttgart
P.Fritz **J.Ch.Fontes**	**Handbook of Environmental Isotope Geochemistry** ISBN 0-444-41781-8 Vol.1. The Terrestrial Environment A (1980) Vol.2. The Terrestrial Environment B (1986) Vol.3. The Marine Environment A (1989)	Elsevier SciencePubl. Amsterdam, Oxford New York, Tokyo ISBN 0-444-41780-X ISBN 0-444-42225-0 ISBN 0-444-42764-3
F.J.Pearson **e.a.**	**Applied Isotope Hydrogeology**, a case study in Northern Switzerland (1991) ISBN 0-444-88983-3	Elsevier Science Publ. Amsterdam, Oxford, New York, Tokyo
I.Clark **P.Fritz**	**Environmental Isotopes in Hydrogeology** (1997) ISBN 1-56670-249-6	Lewis Publishers Boca Raton, New York
F.Gasse **Ch.Causse**	**Hydrology and Isotope Geochemistry** ISBN 2-7099-1377-1	Editions de l'Orstom Paris
W.Kaess	**Tracing in Hydrogeology** (1998) ISBN 3-443-01013-X	Balkema
C.Kendall **J.J.McDonnell**	**Isotopes in Catchment Hydrology** (1998) ISBN 0-444-50155-X	Elsevier/North Holland Publ.Comp. Amsterdam

E.Mazor	**Chemical and Isotopic Groundwater Hydrology – The applied approach** (1998) ISBN 0-8247-9803-1	Marcel Dekker Inc.
P.G.Cook **A.L.Herczeg** **(ed.)**	**Environmental Tracers in Subsurface Hydrology** (2000) ISBN 0-7923-7707-9	Kluwer Acad. Publ.
G.Friedlander **J.W.Kennedy** **E.S.Macias** **J.M.Miller**	**Nuclear and Radiochemistry** (1981) ISBN 0-471-86255-X	John Wiley & Sons New York, Chichester, Brisbane, Toronto
G.Faure	**Principles of Isotope Geology** (1986)	John Wiley & Sons

IAEA PUBLICATIONS

IAEA CONFERENCE PROCEEDINGS

1963 **Radioisotopes in Hydrology**, Tokyo, 5-9 March 1963, IAEA, Vienna, 459 pp. (STI/PUB/71) (out of print)

1967 **Isotopes in Hydrology**, Vienna, 14-18 November 1966, IAEA, Vienna, (in co-operation with IUGG), 740 pp. (STI/PUB/141) (out of print)

1970 **Isotope Hydrology**, Vienna, 6-13 March 1970, IAEA, Vienna, (in co-operation with UNESCO), 918 pp. (STI/PUB/255) (out of print)

1974 **Isotope Techniques in Groundwater Hydrology**, Vienna, 11-15 March 1974, IAEA, Vienna, 2 volumes: 504 and 500 pp. (STI/PUB/373) (out of print)

1979 **Isotope Hydrology** (in 2 volumes), Neuherberg, Germany, 19-23 June 1978, IAEA, Vienna, (in co-operation with UNESCO), 2 volumes of 984 pp. (STI/PUB/493) ISBN 92-0-040079-5 and ISBN 92-0-040179-1

1983 **Isotope Hydrology**, Vienna, 12-16 September 1983, IAEA, Vienna, (in co-operation with UNESCO), 873 pp. (STI/PUB/650) ISBN 92-0-040084-1

1987 **Isotope Techniques in Water Resources Development**, Vienna, 30 March-3 April 1987, IAEA, Vienna, (in co-operation with UNESCO), 815 pp. (STI/PUB/757) ISBN 92-0-040087-6

1992 **Isotope Techniques in Water Resources Development**, Vienna, 11-15 March 1991, IAEA, Vienna, (in co-operation with UNESCO), 790 pp.(STI/PUB/875) ISBN 92-0-000192-0

1993 **Isotope Techniques in the Study of Past and Current Environmental Changes in the Hydrosphere and the Atmosphere,** Vienna, 19-23 April 1993, IAEA, Vienna, 624 pp. (STI/PUB/908) ISBN 92-0-103293-5

1995 **Isotopes in Water Resources Management** (in 2 volumes), IAEA, Vienna, 20-24 March 1995, IAEA, Vienna, 2 volumes: 530 and 463 pp. (STI/PUB/970) ISBN 92-0-105595-1 and 92-0-100796-5

1998 **Isotope Techniques in the Study of Environmental Change**, Vienna, 14-18 April 1997, IAEA, Vienna, 932 pp. (STI/PUB/1024) ISBN 92-0-100598-9

1999 **Isotope Techniques in Water Resources Development and Management**, 10-14 May 1999, IAEA, Vienna, CDRom (IAEA-CSP-2/C) ISSN 1562-4153

SPECIAL IAEA SYMPOSIA

1967 **Radioactive Dating and Methods in Low-Level Counting,** Monaco, 2-10 March 1967, IAEA, Vienna, 744 pp. (STI/PUB/152) (out of print)

1979 **Behaviour of Tritium in the Environment,** San Fransisco, USA, 16-20 October 1978, 711 pp. (STI/PUB/498) ISBN 92-0-020079-6

1981 **Methods of Low-Level Counting and Spectrometry,** Berlin, Germany, 6-10 April 1981, IAEA, Vienna, 558 pp. (STI/PUB/592) (out of print)

IAEA REPORTS AND TECHNICAL DOCUMENTS (TECDOCS)

Environmental Isotope Data no.1 – no.10: World Survey of Isotope Concentration in Precipitation, Data from network of IAEA and WMO over period 1953-1991, published 1969-1994.

Interpretation of Environmental Isotope and Hydrochemical Data in Groundwater Hydrology, Proc. Adv. Group Meeting, Vienna, 27-31 January 1975, IAEA, Vienna, 1976, 230 pp. (STI/PUB/429) ISBN 92-0-141076-X

Isotopes in Lake Studies, Proc. Adv. Group Meeting, Vienna, 29 August-2 September 1977, IAEA, Vienna, 1979, 290 pp. ISBN 92-0-141179-0 (out of print)

Arid Zone Hydrology: Investigations with Isotope Techniques, Proc. Adv. Group Meeting, Vienna, 6-9 November 1978, IAEA, Vienna, 1980, 265 pp. (STI/PUB/547) ISBN 92-0-141180-4

Stable Isotope Standards and Intercalibration on Hydrology and Geochemistry, (R. Gonfiantini ed.), Report on Consultants' Meeting, Vienna, 8-10 September 1976, IAEA, Vienna, 1977.

Stable Isotope Hydrology Deuterium and Oxygen-18 in the Water Cycle, (J.R.Gat and R.Gonfiantini eds.), Monograph by Working Group, IAEA, Vienna, 1981, 340 pp. (STI/DOC/10/210)

Palaeoclimates and Palaeowaters: A Collection of Environmental Isotope Studies, Proc. Adv. Group Meeting, Vienna, 25-28 November 1980, IAEA, Vienna, 1981, 207 pp. (STI/PUB/621) ISBN 92-0-141083-2

Guidebook on Nuclear Techniques in Hydrology, by Working Group IAEA, Vienna, 1983, 439 pp. (STI/DOC/10/91/2)

Stable Isotope Reference Samples for Geochemical and Hydrological Investigations, (R. Gonfiantini ed.), Report by Advisory Group's Meeting, Vienna, 19-21 September 1983, IAEA, Vienna, 1984.

Stable and Radioactive Isotopes in the Study of the Unsaturated Soil Zone, Proc. Meeting on IAEA/GSF Progr., Vienna, 10-14 September 1984, IAEA, Vienna,1985, 184 pp. (TECDOC-357)

Isotope Techniques in the Study of the Hydrology of Fractured and Fissured Rocks, Proc. Adv. Group Meeting, Vienna, 17-21 November 1986, IAEA, Vienna, 1989, 306 pp. (STI/PUB/790)

Stable Isotope Reference Samples for Geochemical and Hydrological Investigations, Report on Consultants' Meeting, Vienna, 16-18 September 1985, edited by G. Hut, IAEA, Vienna, 1987.

Use of Artificial Tracers in Hydrology, Proc. Adv. Group Meeting, Vienna, 19-22 March 1990, IAEA, Vienna, 1990, 230 pp. (TECDOC-601)

C-14 Reference Materials for Radiocarbon Laboratories, (K. Rozanski, ed), Report on Consultants' Meeting, Vienna, 18-20 February 1981, IAEA, Vienna 1991.

Guidelines for Isotope Hydrology, Manuel for Operation of an Isotope Hydrology Laboratory IAEA, Vienna, 1999 (in prep.)

Isotopes of Noble Gases as Tracers in Environmental Studies, Report by Consultants' Meeting, Vienna, 29 May-2 June, 1989, IAEA, Vienna, 305 pp. (STU/PUB/859) (out of print) ISBN 92-0-100592-X

Statistical Treatment of Data on Environmental Isotopes in Precipitation, IAEA, Vienna, 1992, 781 pp. (STI/DOC/10/331)

Isotope and Geochemical Techniques applied to Geothermal Investigations, Proc. Res. Coord. Meeting, Vienna, 12-15 October 1993, IAEA, Vienna, 1995, 258 pp. (TECDOC-788)

Reference and Intercomparison Materials for Stable Isotopes of Light Elements, Proc. Cons. Meeting, Vienna, 1-3 December 1993, IAEA, Vienna, 1995. (TECDOC-825)

Manual on Mathematical Models in Hydrogeology, IAEA, Vienna, 1996, 107 pp. (TECDOC-910)

SYMBOLS AND ABBREVIATIONS

Bq	Becquerel (= one disintegration per sec.)
CDIAC	Carbon Dioxide Information Center, Oak Ridge, TN
CSIRO	Commonwealth Science Research Organization, Australia
d	Deuterium-excess: $d = {}^{2}\delta - 8\,{}^{18}\delta$
D_m	Molecular diffusion constant
DXS	Deuterium excess or d-excess
E	Evaporation
E/P	Ratio of evaporation to precipitation rates
EL	Evaporation Line: change of the isotopic composition of surface waters undergoing evaporation
GMWL	Global Meteoric Water Line: MWL with d = 10‰
GNIP	Global Network of Isotopes in Precipitation
h	Relative humidity
h_N	Relative humidity normalised to the temperature of a lake surface
IAEA	International Atomic Energy Agency
IPCC	Intergovernmental Panel on Climate Change
ITF	Isotope Transfer Function: change of isotopic composition of water by the passage from precipitation to the hydrologic systems
ITCZ	Inter-Tropical Convergence Zone
K_X	Equilibrium constant
LMWL	Local MWL: a best fit for the isotope composition of precipitation at any location - not necessarily with a slope of 8
MWL	Meteoric Water Line: a line in ${}^{2}\delta$ vs. ${}^{18}\delta$ with a slope of $\Delta^{2}\delta/\Delta^{18}\delta = 8$
NOAA	National Oceanic and Atmospheric Agency (USA)
pcpt	Precipitation
P_{CO_2}	Atmospheric CO_2 concentration (in ppm $=10^{-6}$)
R_x	Isotopic (abundance) ratio
S_E	Slope of EL in ${}^{2}\delta$ vs. ${}^{18}\delta$ space
S_E^*	Slope of EL when δ_L and δ_a are in isotopic equilibrium
SMOW	Standard Mean Ocean Water
VSMOW	Vienna Standard Mean Ocean Water, deposited at the IAEA, Vienna
TU	Tritium Unit: 1 TU equals the concentration of ${}^{3}H$ when ${}^{3}H/{}^{1}H = 10^{-18}$
α	Isotope fractionation factor
δ	Isotopic "content" $= R_x/R_{standard} - 1$
Δ	Relative ${}^{14}C$ activity (see for accurate definition Vol.I, Sect.11.5.3)
ε	Isotope fractionation $= \alpha - 1$

CONSTANTS

a	year = 3.1558×10^{7} s
amu	atomic mass unit = $1.660\ 54\times10^{-27}$ kg
c	velocity of light (in vacuum) = $2.997\ 925\times10^{8}$ m·s^{-1}
cal	calorie = 4.184 J
e	elementary/electron/proton charge = $1.602\ 18\times10^{-19}$ C
eV	electronvolt = $1.602\ 18\times10^{-19}$ J
g	acceleration of free fall = 9.806 65 m·s^{-2}
h	Planck constant = $6.626\ 08\times10^{-34}$ J·s
J	Joule = 0.2390 cal
k	Boltzmann constant = $1.380\ 54\times10^{-23}$ J/K
m_e	electron mass = $9.109\ 39\times10^{-31}$ kg
m_n	neutron mass = $1.674\ 93\times10^{-27}$ kg
m_p	proton mass = $1.672\ 62\times10^{-27}$ kg
M/E eq.	mass/energy equivalence: 1 amu ≡ 931.5 MeV
N_A	Avogadro constant = $6.022\ 14\times10^{23}$ mol^{-1}
π	= 3.141 592 6535
R	gas constant = 8.314 51 J·K^{-1}·mol^{-1}
T	thermodynamic temperature = t (^{0}C) + 273.15 K
V_m	molar volume (= 22.41 L·mole^{-1} at STP)

Subject Index

k

l

m

n

o

p

r

s

t

v

W